# Steel Truss Optimisation and Segmentation Strategies for Large Spans

A Case Study on The Pier Redevelopment in Scheveningen



(Page intentionally left blank)

# Steel Truss Optimisation and Segmentation Strategies for Large Spans

A case study of The Pier Redevelopment in Scheveningen

by

Apsara Shyna Baiju 6054595

In partial fulfilment of the requirements for the degree of

Master of Science in Civil Engineering at the

Delft University of Technology



In collaboration with **Haskoning** 

An electronic version of this thesis is available at http://repository.tudelft.nl/.





# Colophon

Author Apsara Shyna Baiju

MSc. Civil Engineering

Faculty of Civil Engineering and Geosciences

Delft University of Technology

#### **GRADUATION COMMITTEE**

Chair & Main Supervisor Dr. F. Kavoura

**Associate Professor** 

Department of Engineering Structures

Faculty of Civil Engineering and Geosciences

Delft University of Technology

Secondary Supervisor Ir. T. R. (Tom) van Woudenberg

Lecturer

Department of Materials, Mechanics, Management and Design

Faculty of Civil Engineering and Geosciences

Delft University of Technology

Company Supervisor Ir. E. Holla

Senior Consulting Engineer

Department of Industry and Buildings

Haskoning

(Page intentionaly left blank)

## Acknowledgement

I would like to sincerely thank everyone who supported me throughout this thesis journey.

First, I am deeply grateful to Dr. Florentia Kavoura and Ir. Tom van Woudenberg from TU Delft, as well as Ir. Eddy Holla from Haskoning, for their encouragement, constructive input, and continuous guidance during my research. Their willingness to make time for discussions, read through my work thoroughly, and provide thoughtful feedback despite their busy schedules was something I truly appreciated. Their support played an essential role in shaping the direction and quality of this work.

Also, I would like to pay special regards to my colleagues at Haskoning for an inspiring work environment, their valuable input, practical perspectives, and everyday support, which made this process more productive and meaningful.

Finally, I want to thank my friends and family for standing by me through every stage of this project. Your patience, support, and belief in me have meant the world.

Apsara Shyna Baiju August 2025

## **Abstract**

This thesis presents a material-efficient steel roof truss design for the redevelopment of The Pier in Scheveningen. A parametric workflow integrating Rhino-Grasshopper, Karamba3D structural analysis, and OptiCroSec cross-section optimisation is developed to minimise total structural steel weight. Four architecturally compatible truss alternatives are explored, resulting in the selection of a Pratt truss with a total steel mass of 31 tonnes. This configuration corresponds to approximately 48 tonnes of embodied carbon (CO2-eq, lifecycle stages A1-A3) and achieves a 27% mass reduction compared to the heaviest considered alternative. Insights from four Haskoning case studies informed a practical two-segment truss segmentation strategy, with splice plates strategically located in the shear-dominant zones. This segmentation approach limits individual segment weights to 11.3 tonnes, complying with Dutch transport restrictions (maximum dimensions of 23 m × 3.5 m × 2 m x 32 t).

Validation of the optimisation and segmentation methodology was performed using RFEM analysis and Eurocode-based hand calculations, demonstrating deviations below 1% for mass and deflection criteria. Interviews conducted with Dutch steel fabricators underscored steel member self-weight as the primary driver of fabrication costs, reinforcing the validity of the weight-focused optimisation objective.

The study demonstrates the effectiveness of integrating parametric geometry optimisation, cross-sectional sizing, and transport-driven segmentation strategies. The resulting design approach achieves substantial reductions in material use and embodied carbon emissions while ensuring practical constructability and compliance with structural codes.

# **Contents**

1	Intr	oduction 1
	1.1	Research objectives
	1.2	Research scope
	1.3	Methodology
		1.3.1 Part 1
		1.3.2 Part 2
		1.3.3 Part 3
2	Lite	rature
	2.1	Introduction
	2.2	Steel Truss
	2.3	Constructability
	2.4	Steel Connections
	2.5	Optimisation approaches for steel trusses
		2.5.1 Topology and Geometry optimisation
		2.5.2 Genetic algorithm
		2.5.3 Weight optimisation- Galapagos
3	Vali	dation of Workflow
	3.1	Validation of Workflow with a Simply Supported Beam
	3.2	Validation of workflow with a Warren truss with verticals
		3.2.1 Parametric Design and Structural analysis using Grasshopper
		3.2.2 Structural Analysis using RFEM
		3.2.3 Structural Analysis as per EN 1993-1-1
		3.2.4 Cross-Section Optimisation
		3.2.5 Weight Optimisation
4	Segr	mentation of Trusses 23
	4.1	Introduction
	4.2	Member Level Segmentation
	4.3	Nodal Level Segmentation
	4.4	Case study: Omnisport Apeldoorn
	4.5	Case study: Adam Tower
	4.6	Case Study: X
	4.7	Case study: Y
5	Cost	t Optimisation 37
	5.1	Introduction
	5.2	Direct and Indirect cost
	5.3	Breakdown of Direct costs

		5.3.1	Material cost	38
		5.3.2	Fabrication cost	38
		5.3.3	Connection cost	39
		5.3.4	Transportation Cost	39
	5.4	Concl	sion	40
6	Case	study	The Pier	41
	6.1	Introd	ection	41
	6.2	Load o	n Truss	43
	6.3	Floor	ayout and load distribution	45
		6.3.1	Beam Design for floor layout 1	47
		6.3.2	Truss to Floor connection	50
	6.4	Truss	opology alternatives	50
		6.4.1	Truss topology 1	50
		6.4.2	Results	53
		6.4.3	Truss topology 2	54
		6.4.4	Results	56
		6.4.5	Truss topology 3	58
		6.4.6	Results	59
		6.4.7	Truss topology 4	61
		6.4.8	Results	65
	6.5		ntation and Connection	66
7	Find	ings		70
′	7.1	_	sation workflow	70
	7.1	_	iss design	70
	7.3		ntation strategies for large span	72
	7.3 7.4	_	otimisation	72
	7.5			73
8	Con	clucion	and Recommendations	74
O		Conch		7 <b>-</b>
				76
۸ -	a d	: A C	nagahannan Carinta	οn
Aļ	-		rasshopper Scripts	<b>80</b>
	A.1		supported beam	
	A.2		rd truss	81
	A.3		or the Pier- Model 1	82
	A.4		or the Pier- Model 2	85
	A.5		or the Pier- Model 3	86
	A.6	Truss	for the Pier- Model 4	87
Αį			tandard Truss- Utilisation checks	89
	B.1	Exam	le Calculation	89
Aį	pend	ix C I	ist of Cross-Sections	91
Aį	pend	ix D I	ollowcore Slab Calculation	93
Αį	pend	ix E (	ost data and Assumptions	96
•	-		stimation Interview Summaries	97

Appendi	ix F	Case Study: Interview summary	99
F.1	Case	study 1: Omnisport Apeldoorn	99
F.2	Case	Study 2- Adam Tower	100
F.3	Case	study 3: X	101
F.4	Case	Study 4: Y	102
Append	ix G	Box Beam Design	103
Appendi	ix H	<b>Detailed Result of Case Study Option 1</b>	105
H.1	Opti	on A	105
		Connection Design	107
I.1	Con	nection on Top chord	107
I.2	Con	nection on Bottom Chord	111

# **List of Figures**

Parametric Trusses [2]	1
The Pier [4]	2
Methodology Workflow	3
Steps for truss design for The Pier	4
	6
	7
	7
	7
	8
	10
<u>*</u>	11
<u>*</u>	11
Solution space[30]	12
Worldon	12
	13
	14
	14
	16
	16
	17
	21
	22
Optimised truss design	22
Truss spliced at midspan of members	24
	24
	25
<u> •</u>	25
	26
	27
	27
	27
	28
	28
	29
	29
	30
<u>.                                     </u>	30
	31
	31

	Elevation highlighting the K bracing
	Erection
	Adam Tower: Connection Detail
	Case Study X: Section Drawing
4.21	Case Study X: Connection Detail
4.22	Case Study Y
4.23	Case Study Y: Segmentation plan
5.1	Direct Costs
5.2	Maximum transport dimensions for road transport with a standard permit in the Neth-
	erlands
6.1	The Pier
6.2	Island 3
6.3	Forces on truss
6.4	
6.5	Detailing
6.6	
	<b>r</b>
6.7	.6.
6.8	
6.9	Floor plan 2
6.10	Truss to floor connection
6.11	Truss topology 1
	Parametric model of Topology 1
	Loads- Model 1
	Grouping members
	Cross section- Model 1
	Cross section- Model 1
	Shear force diagram (kN)
	Moment diagram (kNm)
	Deformation
	Truss topology 2
6.21	Parametric model of Topology 2
	Loads- Model 2
6.23	Cross section- Model 2
6.24	Cross section- Model 2
6.25	Shear force diagram (kN)
6.26	Moment diagram (kNm)
	Deformation
	Truss topology 3
	Model 3
	Loads- Model 3
	Cross section- Model 3
	Cross section- Model 3
	Shear force diagram(kN)
	Moment diagram (kNm)
	Deformation
	Truss Topology 4
	Topology 4
	Option D
	Grasshopper model of beam
7	A HOMENTONIA HIVARA VI INACIII

	Loads- Model 4									
	Truss topology 4									
6.42	Typical welded connection		 	 		 				64
	Cross section- Model 4									
6.44	Cross section- Model 4		 	 		 				65
	Shear force diagram $(kN)$									
6.46	Moment diagram (kNm)		 	 		 				65
	Deformation									
6.48	Member Numbers		 	 		 				67
6.49	Segmentation point									
6.50	Splice connection for compression member		 	 		 				68
	Splice connection for tension member									
7.1	Option D -lightest design									
8.1	Final Truss Design		 	 		 				74
A.1	Grasshopper script for Beam Model		 	 		 				80
A.2	Grasshopper script for Truss Model-1									
A.3	Grasshopper script for Truss Model-2									
A.4	Grasshopper script for Truss Model-3									
A.5	Grid									
A.6	Variables									
A.7	Creating model									
A.8	Cross section optimisaiton									
A.9	Results									
	Variables for model 2									
	Creating model 2									
	Cross-section optimisation and results									
	Variables for model 3									
	Creating model 3									
	Cross-section optimisation and results									
A.16	Variables for model 4		 	 		 				87
	Creating model 4									88
	Cross-section optimisation and results									88
	_									
D.1	VBI-1									94
D.2	VBI-3		 	 	•	 				95
H.1	Option A		 	 		 				105
I.1	Connection for splice on top chord		 	 		 				107
I.2	Check for plate									
I.3	Design data									
I.4	Check for Bolt									
I.5	Splice connection for tension member									
I.6	Check for plate									
I.7	Design data									
I.8	Check for bolts									

# **List of Tables**

3.1	Results-Beam	14
3.2	Vertical displacement of the truss using virtual-work ( $E = 21000 \text{kN/cm}^2$ )	17
3.3	Axial stresses in truss members	17
3.4	Results - Truss	18
3.5	Input parameters used for cross-section optimisation	18
5.1	Examples of Direct and Indirect costs	38
6.1	Loads acting on the truss	43
6.2	Roof load breakdown	44
6.3	First floor load breakdown	44
6.4	Ferris-wheel vertical support reactions	45
6.5	Ferris-wheel horizontal support reactions	45
6.6	Line loads applied to beams and trusses	46
6.7	Design line loads	47
6.8	Design data for moment verification (edge beam)	48
6.9	Design data for shear verification (edge beam)	48
6.10	Design data for moment verification (interior beam)	49
6.11	Design data for shear verification (interior beam)	49
6.12	Design line loads	50
	Results 1	54
	Results 2	58
	Design line loads for beam	62
	Design line loads for top chord	63
	Design line loads for bottom chord	63
	Self-weight for hollow-section redesign	66
	Axial forces in selected members	67
7.1	Weight comparison	70
7.1	Embodied carbon results per design option (Dutch NMD factors)	71
1.2	Embodica carbon results per design option (Duten NVID factors)	/ 1
B.1	Values exported from Karamba®	89
C.1	List of Cross- Sections	92
D.1 D.2	Hollow-core slab verification (A200, 6400 mm × 1200 mm)	93 94
D.2	vermeation summary for nonow-core stab tayout 3 (A200, 0.40 III × 1.20 III)	クコ
E.1 E.2	Welding productivity and labour cost (labour rate = 72€/h)	96 96
G.1	Design data – bending (ULS)	103

G.2	Design data – shear (ULS)	103
G.3	Serviceability data – total load	104
H.1	Values exported from Karamba®	106
I.1	Cross-sections present in the splice	107
I.2	Bolt data used in the design	107
I.3	Member-end forces applied to the splice	107
I.4	Cross-section present in the splice	111
I.5	Bolt properties adopted in the design	111
I.6	Member-end forces applied to the splice (equilibrium check)	111

# **Chapter 1**

## Introduction

Steel trusses have long been in use to support structures like halls, bridges, railway stations, terminals, hangers, etc. Design of a truss in the traditional way begins with a preferred topology, member profiles, and iterate until code checks pass. The engineering industry is continuously seeking better ways of design where alternate layouts and joint positions can be checked and lighter, cheaper, lower carbon solutions can be generated. The concept of advanced parametric design has risen in prominence since early 21st century [1]. Parametric modelling, or parametric design, involves developing models guided by pre-programmed rules or algorithms, commonly referred to as "parameters." [1]. The use of internal logic arguments in parametric design software paved the way for a lot of flexible design options in the early design stage, rather than by being manually manipulated, which resulted in design speed increasing significantly.

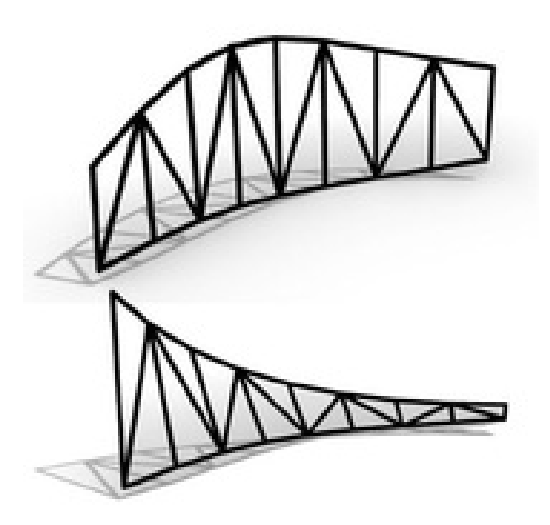


Figure 1.1: Parametric Trusses [2]

This research examines truss design through the lens of parametric design and optimisation to obtain lighter and cheaper designs. When designing large span trusses, considerations such as segmentation for ease of transport and on-site handling become essential. This thesis investigates the parametrisation of a single span truss using a case study, conducted in collaboration with Haskoning, supports this research.

Creating large, visually striking indoor open spaces has become essential to attract the public, enhance experiences, and increase commercial opportunities in buildings. Large indoor open spaces can be adapted for various types of events, and this flexibility makes them valuable to attract visitors year-round. This is particularly relevant in the redevelopment of De Pier in Scheveningen, Netherlands,

where ReBorn Real Estate, co-owner of the project, plans to replace the ageing structure with a new one that meets the demands for year-round use and enhanced visitor experiences [3]. Haskoning, as engineering consultants for the new design, aims to achieve material and cost-efficient trusses that balance structural performance and environmental impact and simplify construction logistics. Meeting these challenges requires systematic optimisation techniques, which will be addressed in this research.

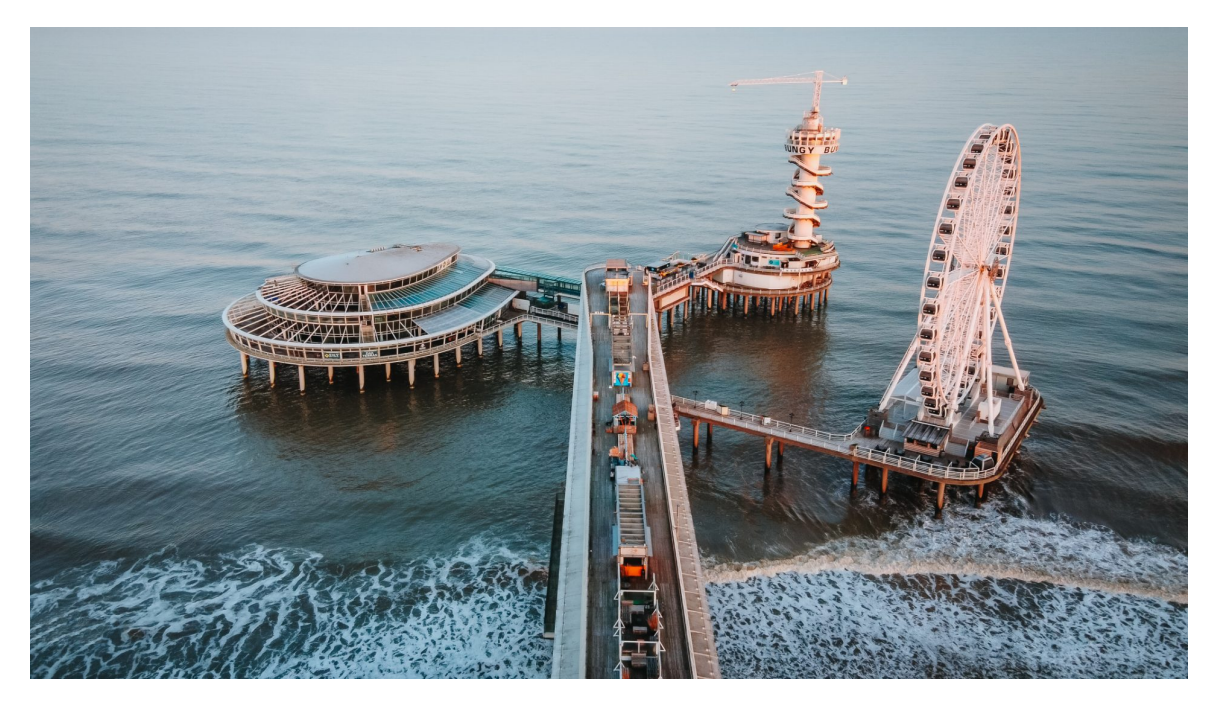


Figure 1.2: The Pier [4]

## 1.1 Research objectives

This research aims to optimise the design of steel trusses for large-span, column-free structures by balancing key objectives such as material, cost efficiency and practical implementation requirements, including segmentation strategies. This thesis is structured around three main objectives and they are;

#### **Objective 1:**

Determine a material-efficient design for a large-span steel truss for The Pier Redevelopment project. Supporting sub questions:

- 1. How to optimise the weight of the truss for the Pier using parametric design tools?
- 2. How much embodied carbon can be reduced through structural optimisation of steel trusses for The Pier?
- 3. Determine the best segmentation strategy for truss in The Pier and design connection for the same.

#### Objective 2

Study segmentation strategies and connection methods for steel trusses to balance constructability, and transportation requirements.

#### Supporting sub questions:

1. Identify different segmentation strategies and connection designs used for real projects and how they satisfy constructability and transportation requirements.

#### **Objective 3**

To integrate direct cost modelling into parametric truss design for improved decision-making on trade-offs between weight and total cost.

#### Supporting sub question:

1. What are the direct costs in steel truss construction, and how can they be integrated into a parametric cost model to assess trade-offs between weight and total cost?

## 1.2 Research scope

This study focuses on optimising the design of steel trusses specifically for large-span, column-free structures, with multiple objectives including material efficiency and cost efficiency. Maximum deflection and utilisation are constrained in the design process. The primary material considered is S355 hot-rolled steel sections; other materials or hybrid solutions are not included in the scope. The research incorporates practical aspects such as segmentation for on-site assembly, as well as connection details to allow easy disassembly and potential reuse of the trusses. This integrated approach ensures alignment with both academic goals and real-world implementation needs.

However, aspects related to corrosion resistance and long-term durability of the trusses for The Pier are excluded from this research in order to keep the project manageable within the set timeframe. While the effects of galvanising are acknowledged, they are not analysed in detail. For connection detailing, only conventional bolted plate connections are considered to prioritise future reuse; friction-grip, post-tensioned, or slip-critical joints fall outside the scope of this study.

## 1.3 Methodology

To achieve the research objectives, the project is structured into different parts. This section outlines the research methods and tools used to achieve the thesis objectives within the given time frame. The methodology integrates parametric modelling, optimisation and structural analysis within a case study to explore optimal steel truss designs. The validation of methodology is also addressed in this section along with practical considerations such as segmentation, connections for disassembly.

#### 1.3.1 Part 1

The first part focuses on building a strong foundation for the research through literature review, parametric modeling, preliminary structural analysis and cross-section and weight optimisation for a standard truss. This is to validate the methodology used to answer research objective one. The results from the analysis will be checked against other method to confirm this methodology works accurately.

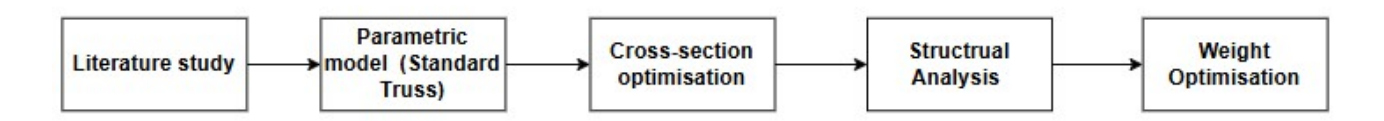


Figure 1.3: Methodology Workflow

#### **Literature Review:**

A comprehensive literature study is conducted to understand the current state-of-the-art in steel truss optimisation and segmentation strategies. This includes an investigation of constructability and sus-

tainability aspects, along with existing methods in optimisation. The findings of this study are presented in Chapter 2.

#### **Parametric Model Development:**

In chapter 3, a parametric truss model is developed using Grasshopper, a plugin for Rhino 8. The initial geometry, boundary conditions, load cases and cross section and material to the truss elements are assigned. A key step in this process is determining which truss design parameters will be variables and which will remain fixed, ensuring an effective optimisation strategy.

#### **Preliminary Structural Analysis:**

Once the initial geometry is established, structural analysis is performed using the Karamba3D plugin in Grasshopper. This analysis helps in understanding the behaviour of the truss under various load combinations, setting the foundation for optimisation later. The standard truss model will also be analysed using RFEM to ensure the model works properly. A comparison of the values obtained for max axial force, max deflection, stress in critical members, etc is done for each method.

#### **Cross-section and weight optimisation:**

Cross-section optimisation will be done using Karamba3D by selecting the most efficient cross-section from the given list of cross-sections for each element within Grasshopper. To minimize the structural weight of the truss, the Galapagos plugin in Grasshopper is used. Galapagos evaluates each design based on its fitness by selectively breeding and mutating better performing solutions until it converges on an optimal or near-optimal configuration.

Rhino 8, Grasshopper and all plugins needed for this thesis are made available using the professional license from Haskoning.

#### 1.3.2 Part 2

In the second part the focus will shift towards the case study which is presented in chapter 6.

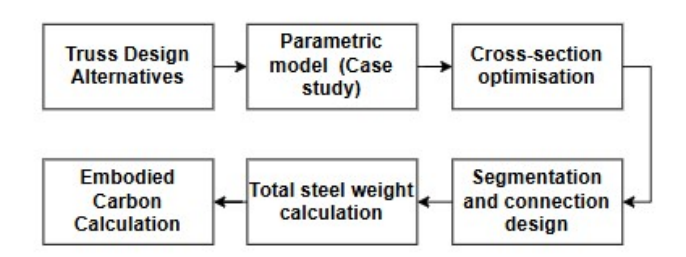


Figure 1.4: Steps for truss design for The Pier

#### Truss design alternatives

A set of concept-level roof-truss layouts will first be drafted, exploring different directions of span, topology, truss spacing and beam arrangements. Each concept will be checked for basic structural demand and practical buildability. Line-loads and Ferris-wheel reactions are estimated, and the resulting hollow-core slab spans are verified against supplier limits with the VBI tool. VBI tool is available online through the website of the supplier VBI. Concepts that push past manufacturability, clearance or code constraints, such as schemes needing slab lengths that the supplier cannot provide are discarded at this stage. Only the options that remain feasible are carried forward for the detailed parametric modelling that follows.

#### **Parametric Modelling and Cross-section Optimisation:**

Parametric models of feasible design alternatives will be developed in Grasshopper using the bound-

ary conditions and load case from the case study. Structural analysis is done using Karamba 3D once the geometry is established within cross-section optimisation as described in Part 1. The methodology explained in part 1 is replicated except for using Galapagos. Galapagos plugin is not necessary for the case study.

#### **Calculating Total Steel Weight and Embodied Carbon Saving:**

The total steel weight including the trusses and beams in the configuration, is calculated. Embodied carbon for each option is assessed by calculating the Global Warming Potential (GWP) from cradle-to-gate, i.e., covering production stages A1-A3 as defined by EN 15804 [5]. The calculation uses emission factors from the Dutch National Environmental Database (NMD). Different designs will be compared using GWP values to find the alternative with minimal environmental impact. The results are analysed to determine the most efficient truss design. The final selection is based on material efficiency and embodied carbon savings. The research concludes with the recommendation of an optimal or near optimal truss configuration

#### **Segmentation and Connection Design**

Location for the segmentation for a design option will be done and connection is designed and verified using IDEA StatiCa. The software is available through Haskoning's professional license.

#### 1.3.3 Part 3

Part 3 is focused on qualitative research on the different practical implications of a project. This qualitative research is done mainly based on interviews with experts and literature.

#### **Segmentation of Truss**

To understand how a large span truss can be transported, erected and taken apart for future reuse, a dedicated segmentation study will be performed in chapter 4. Two complementary strategies will be explored:

- Member-level segmentation
- Node-level segmentation

Projects done by Haskoning which has critical truss segmentation, are treated as case studies to understand complex real world situations and how they were dealt with.

#### **Cost optimisation**

Chapter 5 explores the costs involved in steel truss construction, including material, fabrication, connection, and transportation costs through expert interviews.

This structured methodology ensures a logical workflow, progressing from theoretical study to practical implementation and optimisation, ultimately delivering an efficient steel truss design.

# **Chapter 2**

## Literature

## 2.1 Introduction

This chapter reviews the existing body of knowledge relevant to the optimisation of large-span steel trusses and practical considerations. It examines key structural principles, different optimisation strategies, circular design principles etc. The chapter begins by explaining fundamental truss concepts and then explores various optimisation approaches, and other topics which are made use of in the thesis later on. This establishes the theoretical foundation for the methodology and model development in later chapters.

#### 2.2 Steel Truss

In mechanics, a truss can be considered as a structure with two force (either tension or compression) members who are forming triangular units[6]. They are arranged in triangular formations, and the forces are applied only at both the end points. In a truss structure, adjacent members are connected at joints known as connections. These joints are assumed to transfer only axial forces, meaning that bending and torsional moments are typically neglected, as the joints are considered to have no rotational freedom [6]. The chord members include the top (or upper) chord and the bottom (or lower) chord. They function similarly to the flanges of a beam, resisting the tensile and compressive forces that result from bending moments[7]. The web members, consisting of diagonal and vertical elements, serve distinct roles: diagonals primarily carry shear forces within the truss, while verticals contribute both to shear resistance and to supporting loads, effectively shortening the span of the chord members. The figure below shows the different truss elements in a standard Howe truss.

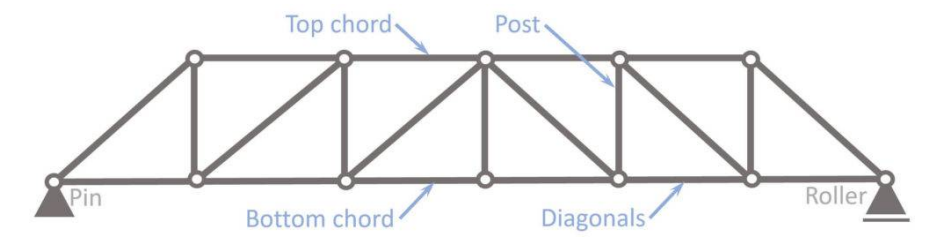


Figure 2.1: Truss Elements [8]

There are different types of trusses, Warren truss, Pratt truss, and Howe truss are some of the common ones. Figure below shows different truss topologies.

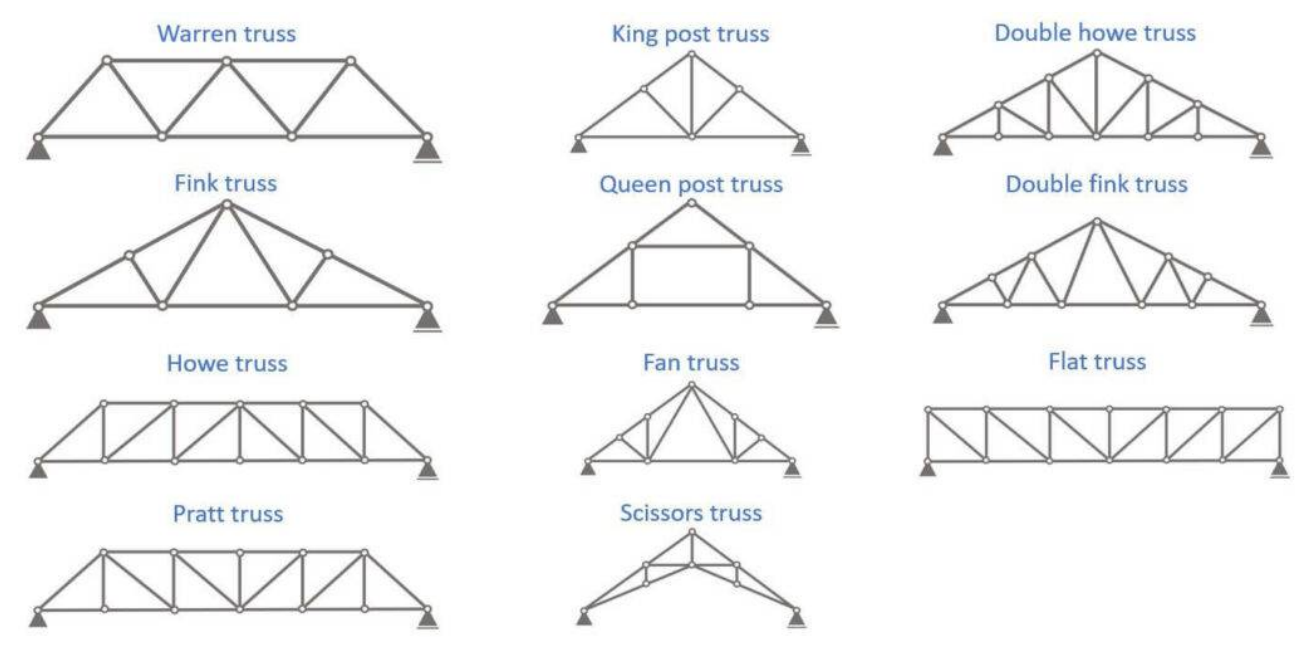


Figure 2.2: Different Truss Topologies [8]

## 2.3 Constructability

In this context, constructability refers to the processes involved in producing, transporting, and installing the trusses used in the case study project. The consistency in the size and shape of truss elements directly affects production complexity by minimizing the need for custom fabrication and assembly [9]. Pasquire et al. [10] define standardisation as "the extensive use of components, methods or processes with regularity, repetition and a successful history." Wong et al. [11], [12] further explain that standardisation can be reflected in the repeated use of grids, component sizes, and connection details. To reduce the high variety of profiles in truss design, grouping strategies are often applied [13], [14]. Elements are grouped based on similar mechanical properties and comparable stress levels, as illustrated in the figure below. Among the various grouping methods—such as neural networks, fully stressed design, cardinality constraints, and direct adaptation of the objective function using penalty terms [9], the method based on cardinality constraints typically yields the lightest solution. However, this approach involves solving a large-scale optimisation problem, which increases computational cost and can introduce greater variability in the results [15].



Figure 2.3: Grouping based on similar mechanical properties [9]

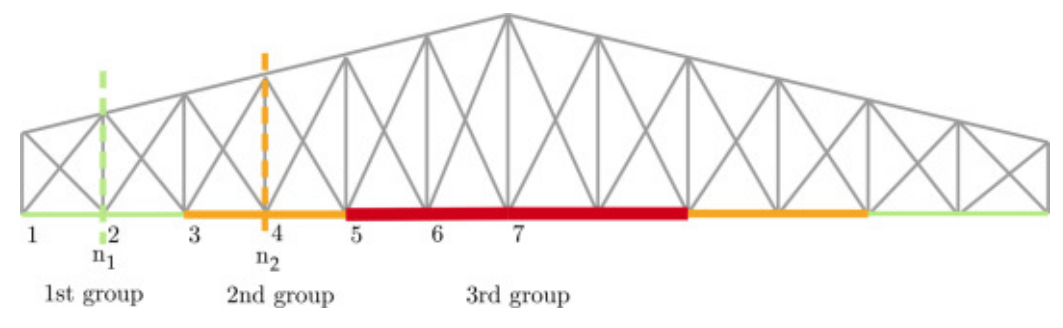


Figure 2.4: Grouping based on similar stress levels [9]

The truss installation considers the assembly of the truss, which is influenced by member size and the method of connecting the members. Transporting the members to the site is also a challenge, depending on truck size, availability, and cost. To minimize transportation emissions, the required transport movements should be reduced. As sustainability is a key interest of this project, ensuring easy disassembly is important for the potential reuse of truss members in the future. Reusing structural elements is more sustainable than recycling them[16]. Considering these practical concerns, truss elements need to be segmented as efficiently as possible.

#### 2.4 Steel Connections

The performance of joints plays a critical role in ensuring the safety, stability and durability of a structure. The behaviour of structural joints is typically characterised by three main properties:

- **Stiffness:** The resistance of the joint to deformation under load. Higher stiffness means the joint deforms less under a given force.
- **Strength:** The maximum load the joint can carry before failure.
- **Ductility:** The ability of the joint to undergo significant deformation before failure. This property is crucial for absorbing energy and avoiding brittle failure.

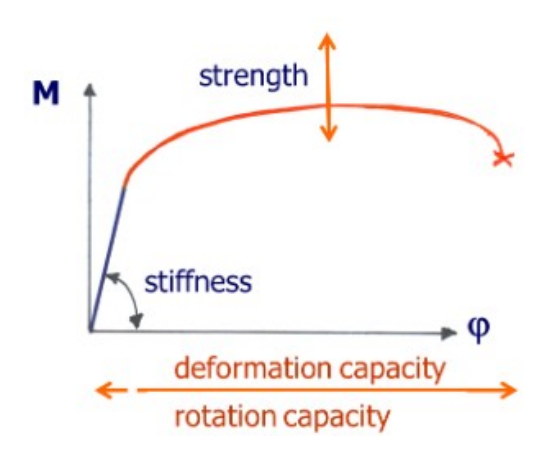


Figure 2.5: Joint behavior[17]

For the design of joints in steel truss, there are pinned connections which allow rotation without resisting moments but can effectively transfer axial forces. Rigid connections resist both moments and forces. Semi-rigid connections which provide partial moment resistance and allow limited rotation[18]. Typically, trusses are designed based on the assumption that members carry only axial forces and therefore have pinned connections.

- 1. Welded Connections
- 2. Bolted Connections
- 3. Hybrid Connections Factory-welded components assembled with bolts on-site.

Welded joints allow connections at various angles but have drawbacks like high welding effort, alignment difficulties, residual stresses, and the inability to disassemble [18]. Bolted connections, primarily resist axial tension or compression. The design of bolted connections is following specific guidelines for bolt spacing, edge distances, and allowable hole sizes from Eurocode to ensure safety and performance. However, errors in assembly or accidental damage can introduce bending moments, potentially leading to bolt failure[18]. Design errors can lead to higher material usage, construction challenges, and inefficient performance. To ensure structural safety, the load-bearing capacity of node

connections must exceed that of the most stressed member in tension. This creates a reserve capacity, allowing stress redistribution in case of an element failure, preventing catastrophic collapse. If a node is weaker than its most stressed member, excessive steel usage occurs without improving safety[18].

## 2.5 Optimisation approaches for steel trusses

Since the optimisation of steel truss designs for large-span, column-free structures involves iterative evaluations of numerous design alternatives, it can be computationally demanding. Single-objective optimization methods focuse on minimising or maximising a single criterion such as weight or cost which often overlooked critical performance metrics like stability and deflection[19]. From the study by [20], multi-objective optimization approaches, such as Genetic Algorithms (GA), allow for the simultaneous consideration of these conflicting objectives and constraints, providing a set of optimal solutions known as the Pareto front. Each solution on the Pareto front represents a trade-off among the objectives, offering comprehensive and practical solutions[20]. While parametric modelling tools like Grasshopper and its plugins facilitate streamlining the optimization workflows, achieving convergence to globally optimal solutions remain a challenge due to the computational intensity of complex load scenarios and the constraints imposed by environmental and architectural requirements[21].

In the context of this thesis, single objective optimisation is used, where the goal is to minimize the volume of materials used while still maintaining structural equilibrium and strength. This can be accomplished by adjusting material properties, member sizes, or the geometry of the truss. Truss optimization can generally be categorized into three types: size, shape, and topology optimization [22]. Size optimization involves modifying the cross-sectional areas of the members. Shape optimization refers to adjusting the coordinates of the nodes to improve performance. Topology optimization changes the configuration of how members are connected to the nodes, potentially altering the overall layout of the structure [23].

## 2.5.1 Topology and Geometry optimisation

In structural optimization, topology and geometry are two key aspects that define the efficiency and performance of a truss.

- 1. Topology Optimization: Determines which members should exist in the truss and how they are connected[24]. It involved the addition and removal or elements and nodes. There are several methods in topology optimisation. One example is ground structure method [25]. It starts with an initial dense ground structure and removes unnecessary elements while maintaining structural performance. Thereby eliminating redundant members to minimize material use and ensuring the best load path for force transmission[25]. Constraints considered in this approach are maximum stress and strain limits, deflection limitations, load-carrying capacity and stability[25].
- 2. Geometry Optimization: Focuses on the placement of nodes (joints) in the structure to minimize forces, displacements, and material use[24].

Simultaneous optimization of both geometry and topology, as discussed in, can lead to more efficient and lightweight designs compared to optimizing them separately[26]. If topology is fixed before adjusting geometry, the structure might be over-constrained and inefficient. If geometry is optimized first, the topology may still contain redundant members.

#### 2.5.2 Genetic algorithm

According to [27], Genetic Algorithm (GA) is an evolutionary optimisation technique inspired by natural selection, widely used for solving complex and non-linear problems. It begins by gener-

ating a population of potential solutions, represented as chromosomes encoding candidate designs. These individuals are evaluated using a fitness function that measures their performance against the optimization objectives. Superior solutions are more likely to propagate to subsequent generations through selection methods like the roulette wheel ensuring that advantageous traits are prioritized. New solutions (offspring) are generated using crossover, which recombines genetic material from parent solutions, and mutation, which introduces random changes to maintain diversity and avoid premature convergence[20]. Elitist strategies ensure the best-performing individuals survive in the next generation, retaining optimal traits[27]. This iterative process continues until stopping criteria, such as a maximum number of generations or achieving a satisfactory fitness level, are met.

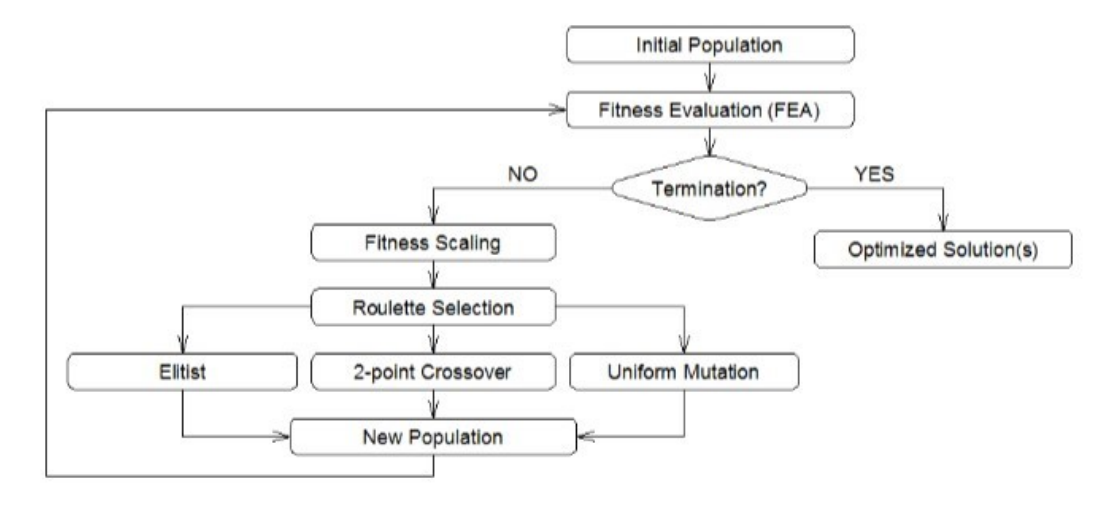


Figure 2.6: GA workflow[27]

#### 2.5.3 Weight optimisation- Galapagos

To minimize the structural weight of the truss, the Galapagos plugin in Grasshopper[28] is used to perform genetic algorithm-based optimization. Galapagos is an evolutionary solver[29] and Evolutionary Solvers are a class of optimization algorithms inspired by the principles of natural evolution and genetics. These solvers operate through mechanisms such as selection, mutation, and crossover to evolve a population of potential solutions over successive generations. Rather than attempting to solve a problem in a single step, evolutionary solvers iteratively refine solutions, making them particularly effective for tackling complex, ill-defined, or highly nonlinear problems[30].

The core of an Evolutionary Solver's operation can be understood through the concept of a Fitness Landscape, a visual and conceptual model used to represent how different combinations of variables (or genes) affect the performance (or fitness) of a solution.

In the simplified example illustrated below, the model uses two genes, Gene A and Gene B, which represent two independent variables that can change. As these genes are varied, the overall fitness of the solution changes, and this change is represented by the height on the 3D surface: the higher the point, the better the solution. The job of the Evolutionary Solver is to explore this landscape and find the highest peak, which corresponds to the optimal or best solution.

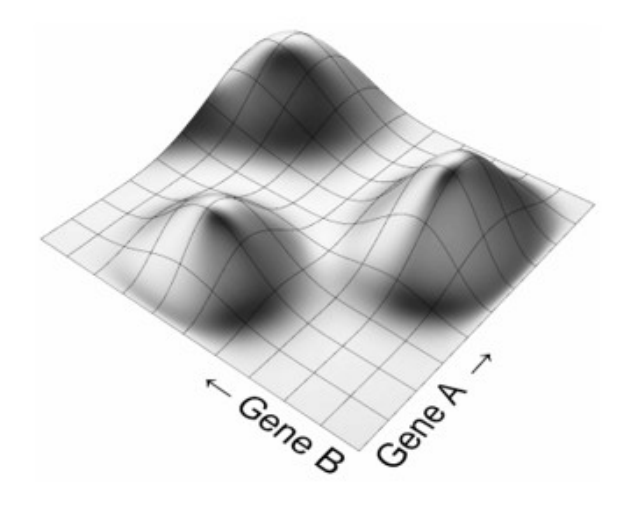


Figure 2.7: Solution space[30]

Each unique combination of Gene A and Gene B corresponds to a specific location on this landscape. For more complex problems involving many genes (e.g., 12 or more), the fitness landscape exists in a high-dimensional space that is difficult to visualize but follows the same conceptual structure.

The Evolutionary Solver begins without any prior knowledge of the shape or peaks of this landscape. It starts by generating an initial population of random solutions, referred to as genomes, each containing values for all genes. These genomes are then evaluated for fitness, and through iterative processes of selection, mutation, and recombination, the solver evolves the population toward better solutions over time.

After the initial population of random genomes is generated and evaluated, each genome's fitness is measured based on its position on the fitness landscape (as indicated by the red dots in the image below). The higher the position (i.e., elevation), the better the fitness. Using these fitness values, the solver ranks the genomes from best to worst. The poorly performing genomes (those in the low-lying areas) are discarded, while the better-performing genomes are retained for the next step. However, selecting only the best genome is not enough, since it's unlikely that any individual from the first random generation has already found the optimal solution. Instead, the solver breeds the better-performing genomes with each other. This recombination of genes creates a new generation of genomes, each potentially exploring new areas of the fitness landscape.

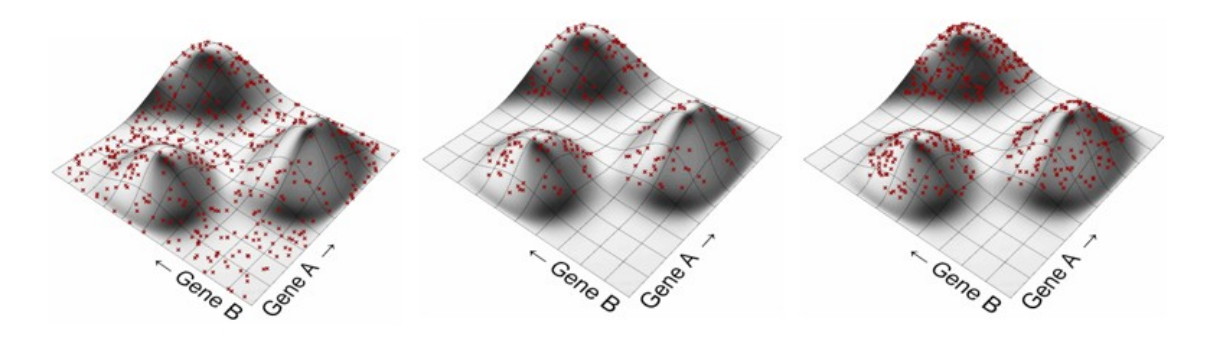


Figure 2.8: Solution space[30]

This breeding process allows the solver to explore intermediate spaces between high-performing regions, leading to potentially better solutions over time. As generations progress, the population shifts toward higher fitness regions, ideally converging at or near the global optimum.

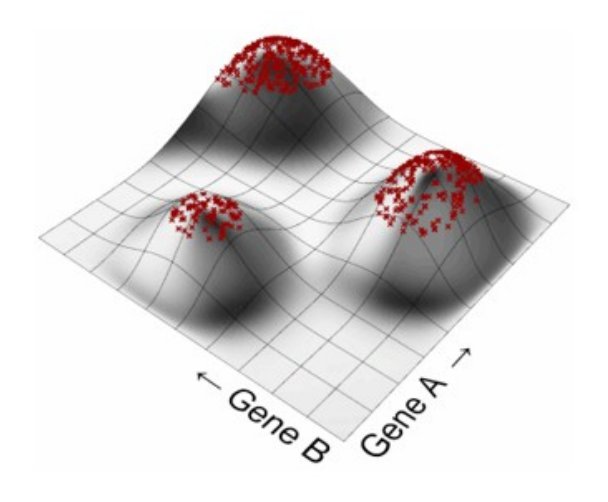


Figure 2.9: Solution space[30]

# **Chapter 3**

## Validation of Workflow

This chapter explains the workflow between parametric design, structural analysis, and optimisation using Grasshopper. To explain the process, a simply supported beam and warren truss with verticals is used and details about the structural analysis and optimisation are provided in the following sections.

## 3.1 Validation of Workflow with a Simply Supported Beam

A simply supported beam is used to validate the workflow mentioned in the methodology. This involved:

- 1. Defining a simply supported beam geometry and load case.
- 2. Conducting structural analysis using three different methods:
  - Grasshopper with Karamba3D, a parametric structural analysis plugin.
  - RFEM, a widely used structural analysis software in industry.
  - Hand calculation as per EN 1993-1-1.

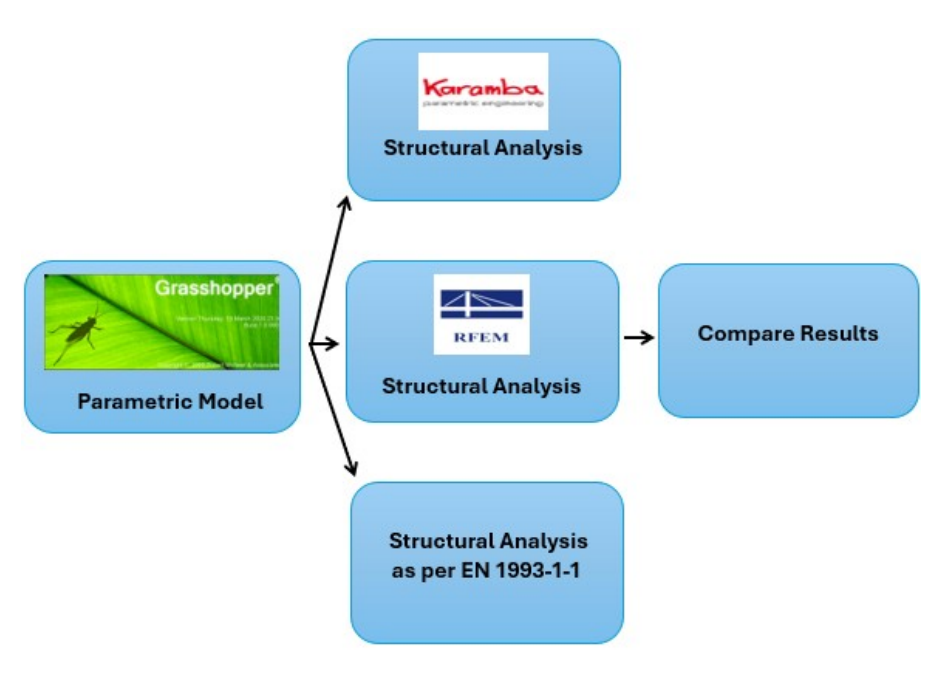


Figure 3.1: Workflow

The beam is modelled as an IPE100 section made of steel S355 in Grasshopper. It is simply supported

with a pinned bearing at x = 0 and a roller bearing at x = 5 allowing longitudinal movement. A 2 kN downward point load is applied at mid-span. Self weight is neglected. Structural analysis of the beam is done using the 'analyse' component of Karamba3D. This component gives the reactions, axial forces, bending moment, shear force, max deflection, mass, and stress values of the beam. A screenshot of the beam geometry is shown in figure 3.2, and values of each output are discussed in table 5.1.

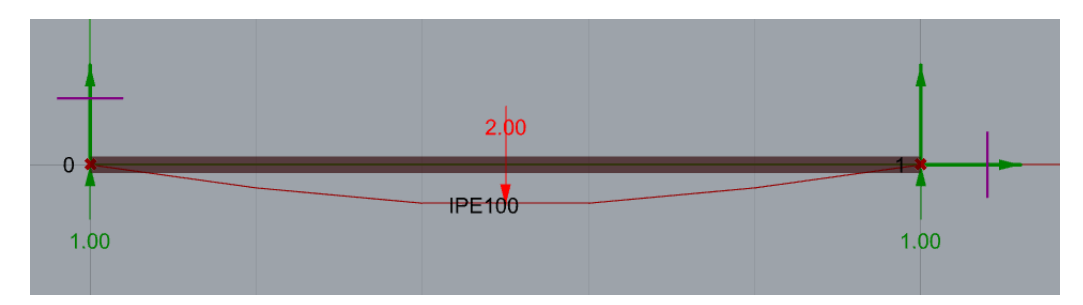


Figure 3.2: Karamba3D Model

An identical model was created in RFEM with similar support and loading conditions and structural analysis was performed. The results obtained are discussed in the following sections. The figure 3.3 below shows the beam model in RFEM.

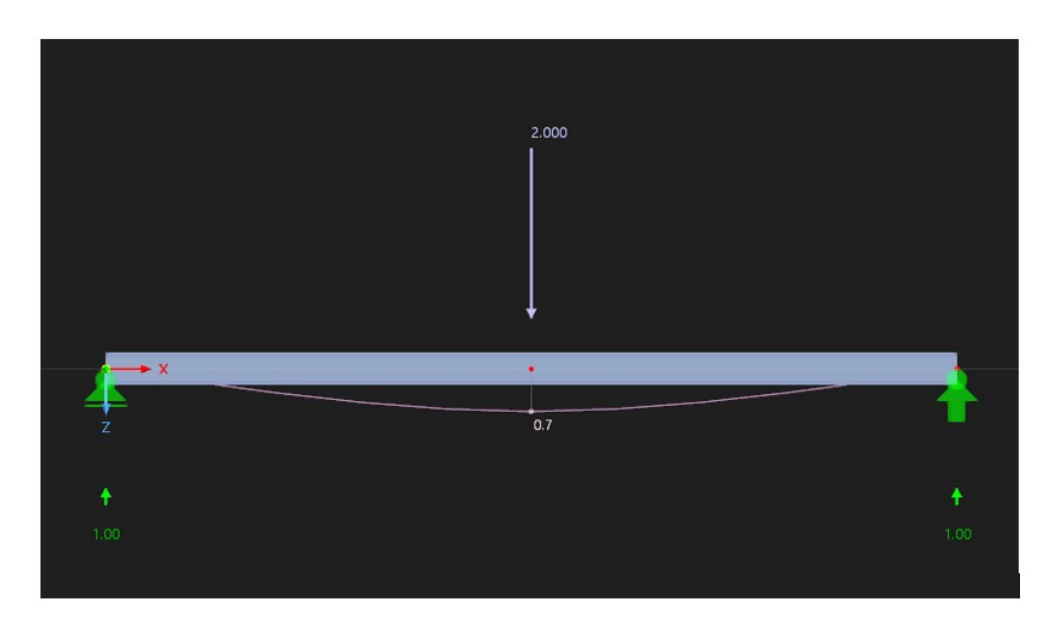


Figure 3.3: RFEM Model

#### **Results**

Parameter	Karamba3D	RFEM	Hand Calculation
Max. Axial Force	0	0	0
Max. Bending moment	2	2.5	2.5
Shear force	1	1	1
Max Deflection (mm)	13	14.5	15
Material usage kg	40.5	40	40
Max stress N/mm^2	73.1	73.1	73.5

Table 3.1: Results-Beam

Table 5.1 shows the comparison of results after doing analysis in the three methods and it shows a high level of agreement between Karamba3D, RFEM, and hand calculation results. Key parameters such as axial force, shear force, material usage, and maximum stress show negligible differences,

confirming the accuracy and validity of the Grasshopper-Karamba3D model. Minor deviations in bending moment and deflection are expected due to differences in mesh refinement, tolerance setting, interpolation functions, solver precision and assumptions[31][32]. The formulas used for hand calculations are based on Euler-Bernoulli beam theory, which assumes small deformations, neglects shear deformation, and idealises supports as perfectly pinned or fixed. It also assumes uniform, linearly elastic material properties throughout the beam[33]. Karamaba3D uses Timoshenko beam theory which allows the beam to rotate due to shear and allow a bending curve[31][28]. 1–2 mm difference in deflection or 0.5 kNm in bending moment is not significant in practical design.

This comparative approach helped ensure a correct understanding of structural theory application and provided baseline validation, confirming that results obtained from Grasshopper/Karamba3D, RFEM, and hand calculations align closely.

#### 3.2 Validation of workflow with a Warren truss with verticals

#### 3.2.1 Parametric Design and Structural analysis using Grasshopper

Once the analysis methodology was validated using the beam model. A standard truss geometry was defined in Grasshopper, enabling easy adjustments to its form and dimensions through simple parametric changes. For a truss, the most important parameters are truss span, height, depth, number of panels, truss topology, and member sizes [34]. According to the specific needs of the project some of these parameters are kept fixed or variable. To demonstrate the workflow for structural analysis, weight and cost optimisation, in this research the span and topology of the truss is kept fixed.

The varying parameters will be height and depth of the truss, number of panels and member sizes[35]. These parameters are adjusted to minimise weight and cost while controlling deflection and ensuring stability. Member sizes are a key variable as optimizing member cross-sectional areas directly reduces structural weight by eliminating excess material, as each member is sized just enough to carry its forces. The truss height (depth) is another key variable: a deeper truss generally increases stiffness, which lowers deflections for a given load, allowing the use of smaller member sections (hence weight savings) up to an optimal point[23]. Height ratio H is defined in grasshopper using

$$H = \frac{\text{Length of the truss curve}}{\text{Height of the truss}}$$

The number of panels is defined as width ratio D

$$D = \frac{\text{Length of a single truss}}{\text{Height of the truss}}$$

Within Grasshopper, various loading scenarios were applied, and boundary conditions were clearly defined. Using Karamba3D, a structural analysis was performed directly within the parametric model. Grasshopper script that shows the loading and support conditions are provided in the Appendix A.

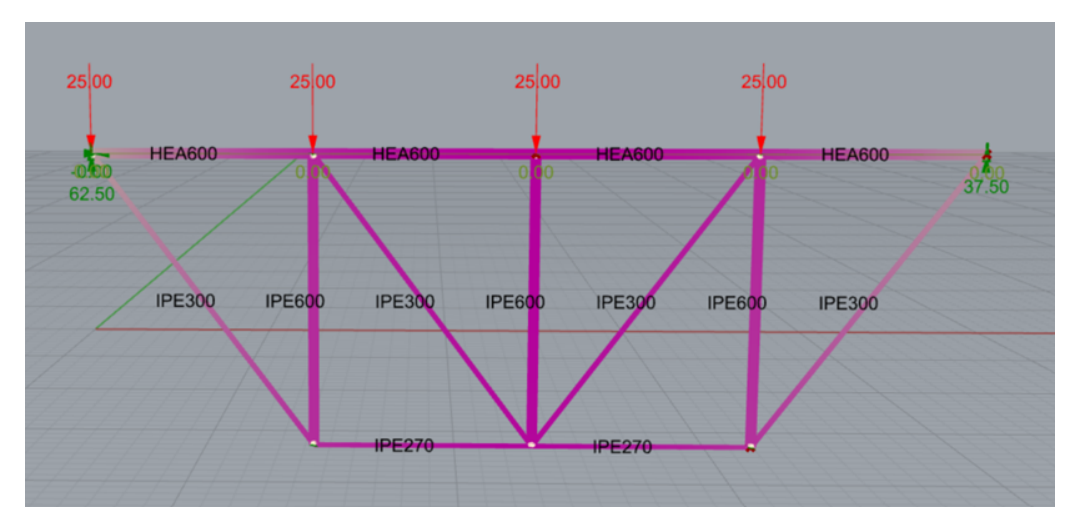


Figure 3.4: Truss model in Karamba3D

Figure 3.4 shows the geometry of the truss which is analysed. Four different profiles were assigned manually to topchord, bottomchord, truss diagonals and verticals.

#### 3.2.2 Structural Analysis using RFEM

To verify the validity and reliability of Karamba3D's analysis, the truss geometry, including loads and boundary conditions, was recreated in RFEM as shown in 3.5. RFEM was chosen as it is widely accepted in industry practice and serves as a reliable benchmark for result verification[32]. Analysing the model in RFEM confirmed the consistency of results between Karamba3D and RFEM, which is discussed in table 3.4.

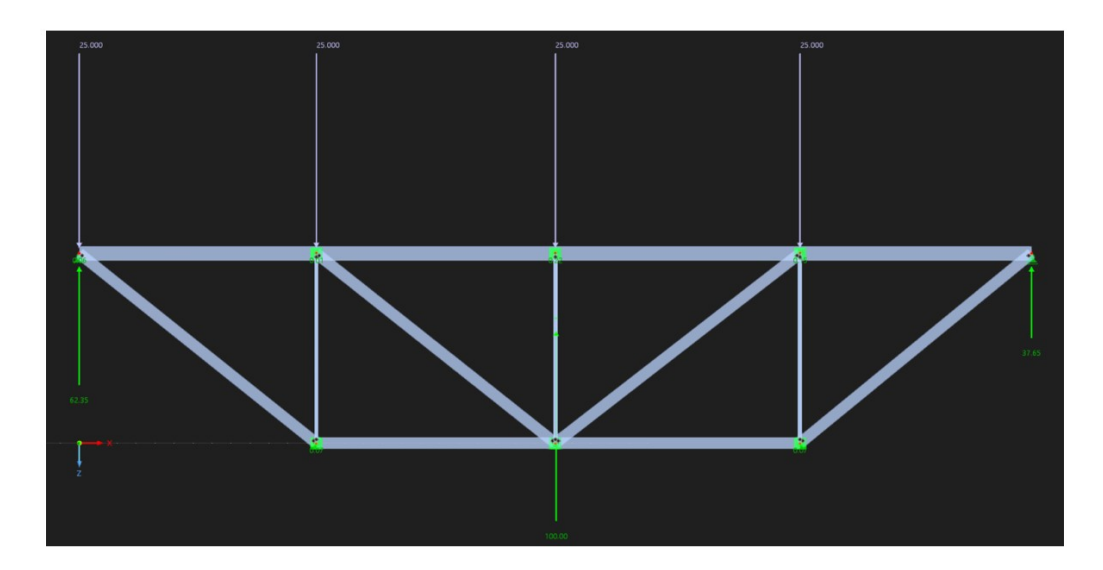


Figure 3.5: RFEM Model

#### 3.2.3 Structural Analysis as per EN 1993-1-1

EN 1993-1-1 provides the design rules for steel structures[36]. Axial forces, stresses, and deflections were determined as shown below.

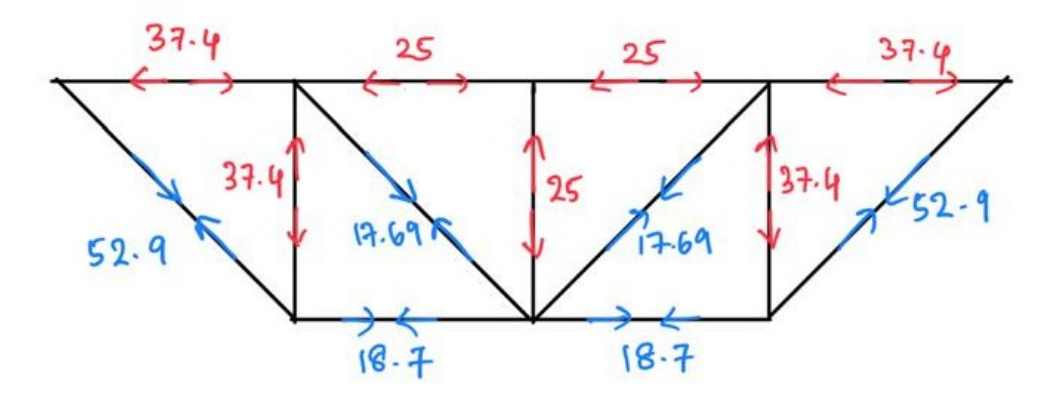


Figure 3.6: Internal Force

#### **Maximum Displacement calculation**

Member	Count	N ( <b>kN</b> )	n (unit 1kN)	L (m)	$A$ (cm $^2$ )	$\frac{N  n  L}{E  A}$ (m)
Top chord outer	2	-37.4	-0.25	12.5	178	0.0000328
Top chord inner	2	-25.0	-0.50	12.5	178	0.0000881
Vertical outer	2	-37.4	-0.50	12.5	156	0.0000713
Vertical middle	1	-25.0	-0.50	12.5	156	0.0000478
Bottom chord	3	18.7	0.50	12.5	62.6	0.0003030
Outer diagonals	2	52.9	0.25	17.68	72.7	0.0002540
Inner diagonals	2	17.69	-0.25	17.68	72.7	-0.000107
				$\Sigma$ (all 1	nembers)	0.00249m = $0.249$ cm

Table 3.2: Vertical displacement of the truss using virtual-work ( $E = 21000 kN/cm^2$ ).

Member group	N (kN)	$A  (\mathrm{cm}^2)$	$\sigma$ (kN cm <sup>-2</sup> )	Nature
Top-chord outer	-37.4	178	-0.210	C
Top-chord inner	-25.0	178	-0.140	C
Vertical outer	-37.4	156	-0.240	C
Vertical middle	-25.0	156	-0.160	C
Bottom chord	18.7	62.6	0.299	T
Outer diagonals	52.9	72.7	0.728	T
Inner diagonals	17.69	72.7	0.243	T

Table 3.3: Axial stresses in truss members

#### **Results**

The table 3.4 shows a comparison of structural analysis results for the truss, obtained using Karamba3D, RFEM, and hand calculation. The near-identical values across all three methods demonstrate the reliability and accuracy of the Karamba3D model, confirming its effectiveness for structural analysis of the truss system.

Parameter	Karamba3D	RFEM	Hand Calculation
Mass (kg)	17370.5	17310	17370
MaxDisp (cm)	0.23	0.25	0.25
Max stress (kN/cm <sup>2</sup> )	0.728	0.728	0.728
Max Bending moment	-1.21	-1.3	-
Max axial force (kN)	52.9	53	52.9
Shear force	0	0	0

Table 3.4: Results - Truss

#### 3.2.4 Cross-Section Optimisation

Cross-section optimisation is a type of size optimisation and it only changes the size of the cross-section of each structural member. This is implemented in Grasshopper using a Karamba3D component called 'OptiCroSec' (OCS), which aims to find the optimal cross-section of each structural member within a given range[28]. The input parameters for this component are specified in the table below.

Parameter	Value	Description
MaxUtil	0.7	Maximum utilization ratio
MaxDisp	h/250	Maximum displacement (cm)
ULSIter	5	Maximum number of iterations for ULS calculation
DispIter	5	Maximum number of iterations for displacement
nSamples	3	Number of sample points for cross-section design
Elast	True	Elastic cross-section design
$\gamma_{M0}$	1	Material safety factor
$\gamma_{M1}$	1	Material safety factor for buckling

Table 3.5: Input parameters used for cross-section optimisation

Utilisation is defined as the unity check of steel members and the calculation done using the procedure described in EN 1993-1-1. The check is performed in ULS, whereas the deformation check is performed in SLS[28]. The maximum deformation is set to h/250 [36].

The cross-section family from which selections can be made is defined by specifying a range of cross-sections. Karamba3D offers a useful tool for this: the Cross Section Range Selector. This component allows for selecting cross-sections based on shape and maximum dimensions. Alternatively, it is possible to input a custom list of cross-sections, ideally sorted by their efficiency[37]. To conserve material, it is best to sort the list by cross-section weight. When a specific family of profiles is selected (e.g., I-shaped profiles), this sorting, usually from smallest to largest height, is done automatically [28]. The list of cross sections used is shown in the Appendix C.

#### **Optimisation Procedure**

Firstly the initial geometry with given sections is analysed. This outputs the section forces in all elements. Subsequently, the smallest cross-section within a cross-section family, which satisfies the boundary condition for utilisation, is chosen for each member. This process is an iterative process which stops when the cross-sections do not change anymore or when the maximum number of iterations has been reached. This component always tries to satisfy the utilisation boundary condition first. It is not possible within this component to consider the displacement condition first[28],[37].

To calculate the Utilisation, Karamba3D runs finite element analysis with the sections to get N, Vy, Vz, Mt, My, Mz at n sample points along every member. At each sample point, method 2 of Annex B Eurocode 3 is implemented including buckling, LTB, interaction factors, kyy, kzz etc [36].

The internal calculations inside Karamba's OCS component utilises the interaction equation of axial compression and biaxial bending from Eurocode 3[36].

Verification is done according to the following interaction equation (Eurocode 3, Clause 6.3.3, Method 1, Equation 6.61)[36]:

$$\eta = \frac{N_{\rm Ed}}{\chi_y N_{pl,\rm Rd}} + k_{yy} \frac{M_{y,\rm Ed}}{\chi_{LT} M_{y,\rm Rd}} + k_{zz} \frac{M_{z,\rm Ed}}{M_{z,\rm Rd}} \le 1.0$$
 (3.1)

Here:

- $N_{\rm Ed}$  is the design axial force,
- $M_{y,Ed}$ ,  $M_{z,Ed}$  are design moments about the major and minor axes,
- $\chi_y, \chi_{LT}$  are buckling reduction factors for axial and lateral-torsional instability,
- $k_{yy}, k_{zz}$  are interaction factors (amplifying bending effect under compression),
- $N_{vl.Rd}$ ,  $M_{u.Rd}$ ,  $M_{z.Rd}$  are the plastic resistances of the section.

This equation is applied to all elements that may experience a combination of compression and bending. In an ideal truss, the moment terms simply evaluate to zero, making the axial term dominant.

The following equations are utilised to verify cross-sections in Karamba3D.

1. Cross-Section Capacities: Using section properties, the plastic resistances are computed:

$$N_{pl,\mathrm{Rd}} = \frac{A f_y}{\gamma_{M0}}, \quad M_{y,\mathrm{Rd}} = \frac{W_{pl,y} f_y}{\gamma_{M0}}, \quad M_{z,\mathrm{Rd}} = \frac{W_{pl,z} f_y}{\gamma_{M0}}$$

- 2. **Buckling Parameters:** Euler critical loads  $N_{cr,y}$ ,  $N_{cr,z}$  and critical moment  $M_{cr}$  for lateral-torsional buckling are calculated based on geometry and effective lengths
- 3. Non-Dimensional Slenderness:

$$\bar{\lambda}_y = \sqrt{\frac{N_{pl,\text{Rk}}}{N_{cr,y}}}, \quad \bar{\lambda}_z = \sqrt{\frac{N_{pl,\text{Rk}}}{N_{cr,z}}}, \quad \bar{\lambda}_{LT} = \sqrt{\frac{M_{pl,\text{Rk}}}{M_{cr}}}$$

4. Buckling Reduction Factors:

$$\phi = \frac{1}{2} \left[ 1 + \alpha (\bar{\lambda} - 0.2) + \bar{\lambda}^2 \right], \quad \chi = \frac{1}{\phi + \sqrt{\phi^2 - \bar{\lambda}^2}}$$

The imperfection factor  $\alpha$  depends on the buckling curve (a, b, c, or d) and is taken from EC3 Table 6.1[36]. Karamba3D caps all moment gradient coefficients  $C_{my}, C_{mz}, C_{mLT} \leq 0.9$  by default for conservative design.

5. Interaction Factors:

$$k_{yy} = k_{zz} = 1 + \beta \left( \frac{N_{\text{Ed}}}{N_{pl,\text{Rd}}} - n_0 \right)$$

where  $\beta$  and  $n_0$  are coefficients depending on cross-section type, taken from EC3 Annex B, Table B.3 [36].

6. Utilisation Evaluation: The utilisation  $\eta$  is calculated at each sample point on each member using the interaction equation. The maximum utilisation along the element defines  $U_{\text{max}}$ .

- 7. **Section Upgrade:** If  $U_{\text{max}} > \text{MaxUtil}$ , the constraint given, the element is assigned the next larger cross-section from its family list.
- 8. Convergence: The iteration stops when all elements satisfy  $U_{\rm max} \leq {\tt MaxUtil}$ , or if the section list is exhausted, or a maximum iteration count is reached. In the example Warren Truss optimisation according to table 3.5 convergence was reached within 5 iterations. Final section assignments, utilizations, and details are then output.

The "Details" output in Karamba3D includes cross-section capacities, buckling parameters, and EC3 factors but not the actual design forces  $N_{\rm Ed}$ ,  $M_{y,\rm Ed}$ ,  $M_{z,\rm Ed}$ . These design actions are computed live within each loop iteration based on the current FE results. An example calculation with section properties, reduction factors, and interaction parameter extracted from Karamba3D and design forces assumed are shown in Appendix B.

#### 3.2.5 Weight Optimisation

To minimize the structural weight of the truss, the Galapagos plugin in Grasshopper is used.

**Genomes (Design variables):** These are the input parameters that Galapagos will modify to find an optimal solution. Here the genomes are;

- Truss height ratio (h)
- Truss width ratio (d)

The Fitness (objective function): This is the value that needs to be minimised: total weight of the structure (W).

#### **Problem Statement in Galapagos**

Given a truss whose geometry parameters,

$$\mathbf{g} = (h, d)$$

are variables and whose members must be selected from a discrete catalogue, galapagos find the geometry that produces the global minimum self-weight.

Galapagos supplies the stochastic search on g while Karamba's Optimize Cross Section (OCS) is executed inside every Galapagos evaluation to deterministically choose the lightest feasible profile for each element-group.

The nested loop explaining how OCS is integrated with Galapagos is shown in the flow chart 3.7. The optimisation process starts with an initial geometry with an initial height and width ratio, which is assigned with adequate steel profiles that satisfy the design checks and constraints. The total mass of this model is then minimised by varying the height and depth ratio using Galapagos, and the loop is exited when the best fitness value is attained.

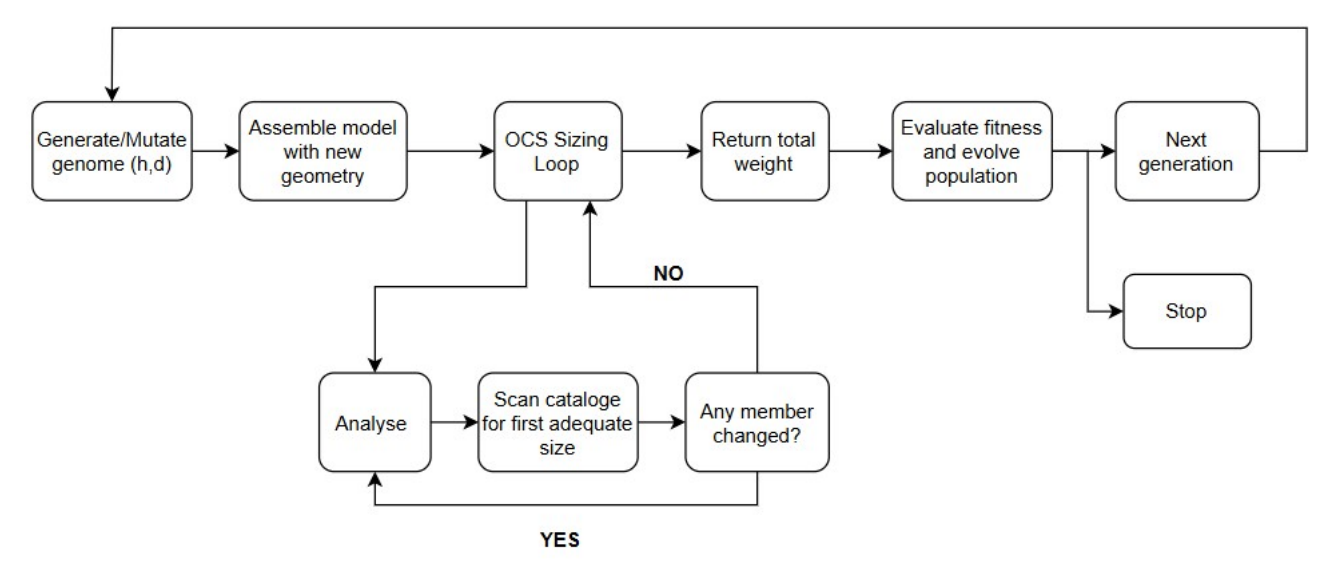


Figure 3.7: Optimisation loop

#### Variables inside Galapagos

$\mathbf{g}$	Geometry (genes): $\mathbf{g} = (h, d)$	
$\mathbf{X}(\mathbf{g})$	Nodal coordinates generated from g	
$L_e(\mathbf{g})$	Length of element $e$ for geometry $\mathbf{g}$	
$A_e(\mathbf{g})$	Lightest catalogue area chosen by OCS for element $e$ under	
	geometry g	
ho	Material density	

#### **Objective function**

$$MinW(\mathbf{g}) = \sum_{e=1}^{E} \rho A_e(\mathbf{g}) L_e(\mathbf{g})$$
 (1)

Equation (1) turns the full optimisation problem into the search for the two geometric genes g = (h, d). Because the OCS component deterministically upgrades any overstressed member before the weight is measured, every candidate that reaches the Galapagos solver is already ULS and SLS compliant. The fitness landscape seen by the genetic algorithm is therefore continuous, low dimensional, and penalty free. The nested loop with OCS and weight optimisation thus delivers a geometry–section combination that is globally minimum within the chosen catalogue and design space.

**Solver Result:** When the solver is started, Galapagos will generate an initial population of solutions and evaluate their fitness. After selecting the best ones, it combines their "genes" (design variables), mutates them slightly, and create a new generation. This is repeated until it finds the best solution or reaches a stopping point. Galapagos stores the best solution it found and updates the Grasshopper sliders accordingly. The resulting chart from Galapagos solver is given in figure 3.8.

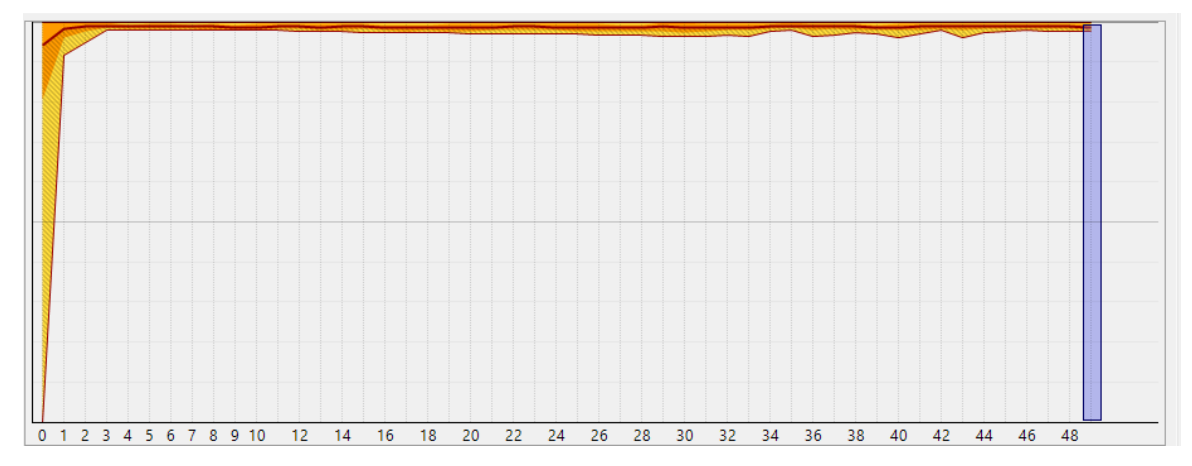


Figure 3.8: Solver result

The Galapagos optimisation run shown above illustrates the evolutionary progress in minimizing the total structural weight of the truss. The chart shows the fitness evolution over generations with the number of generations in the x- axis and fitness value (truss weight in kg) in the y-axis. Over 50 generations, the algorithm explored a broad range of input combinations (genomes), gradually improving fitness values. The chart reveals a convergence trend, where the best solution stabilises around a minimum fitness value of 16842.7.

The figure 3.9 shows the optimisation result with updated profiles, height ratio and width ratio.

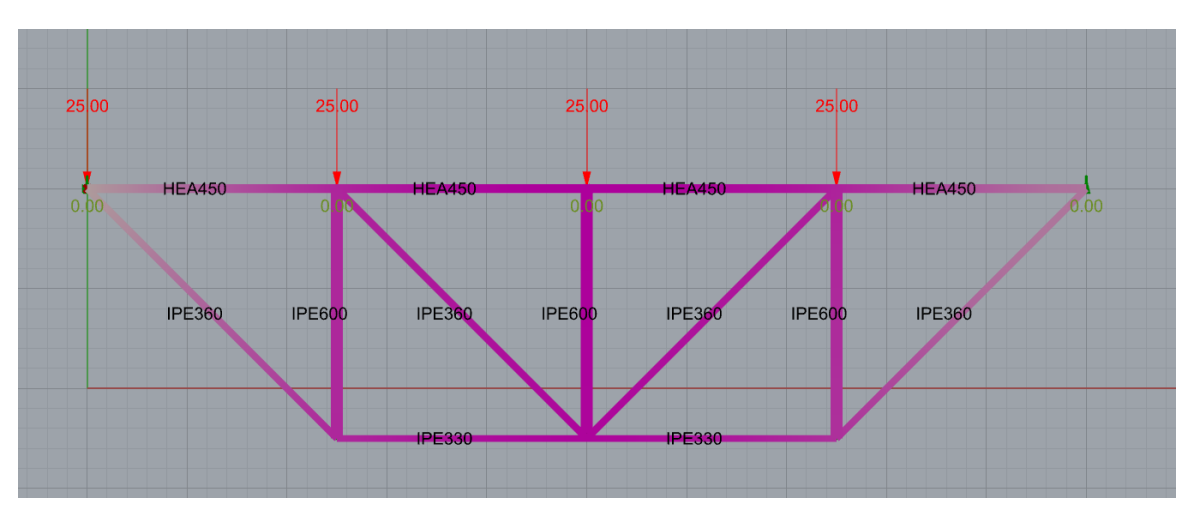


Figure 3.9: Optimised truss design

# **Chapter 4**

# **Segmentation of Trusses**

### 4.1 Introduction

Large-span steel trusses often need to be segmented into smaller modules for practical reasons such as transportation, on-site erection, handling, and potential future reuse. Segmentation refers to dividing a truss into smaller sections or members that are connected during erection. This section discusses segmentation strategies for steel trusses, comparing member-level segmentation (splicing within members), node-level segmentation (splitting the truss at joints) and case studies where some of these segmentation strategies are used. Key considerations include structural performance of each strategy, the types of connections used, and the practical benefits and limitations.

For very large trusses, a common practice is to fabricate partial assemblies (modules) in the shop which are then connected on site. Modern steel construction practice favors bolted site splices over field welding for connecting these truss segments, due to speed and reliability of bolting. Welded splices on site are less common (used mainly if exposed bolted connection is not preferred for architectural reasons) because they require more on-site work and inspection. Bolted splices, however, must be designed to carry significant forces. In section 4.2 a standard Warren truss with verticals is used as an example to explain common segmentation strategies.

Two fundamental strategies can be identified for how the truss is broken into segments:

- Member-level segmentation, where individual members (chords or web members) are cut and spliced within their length.
- Node-level segmentation, where the break occurs through the nodes (joints), dividing the truss into modules that connect at those node interfaces.

Each approach has distinct structural implications and connection requirements.

## 4.2 Member Level Segmentation

Cutting a major truss member, such as a top or bottom chord into shorter segments introduces splices at locations that were originally continuous. Structurally, these splices become critical sections, as they must safely transfer the axial forces present in the member. If a splice is introduced in a region with high internal force, it must be designed with sufficient strength and stiffness, and may even govern the overall design of the member.

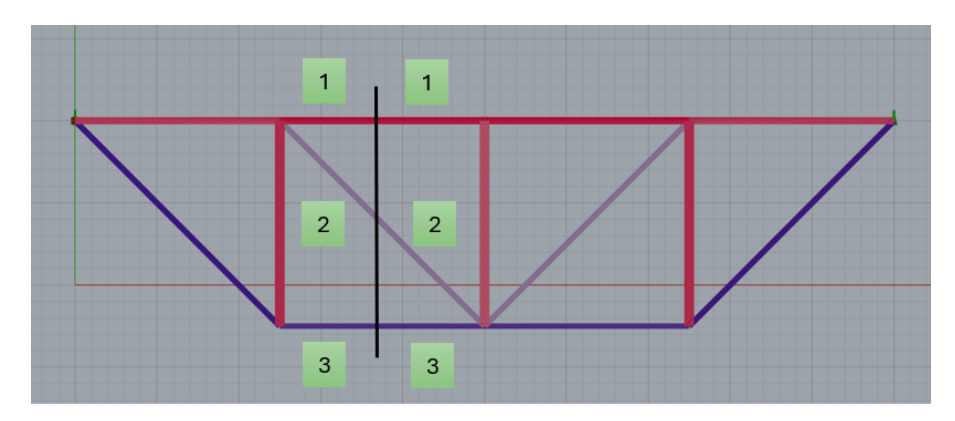


Figure 4.1: Truss spliced at midspan of members

For example, in a simply supported roof truss subjected to uniform loading, splicing the bottom chord at mid-span places the splice at the location of maximum tension force. Similarly, a splice in the top chord near mid-span would be subject to high compressive forces assuming no lateral loads are present.

If the chord is an open section (like an I-beam or channel), plates can be bolted on either side to connect the two pieces. Design of the splice itself follows standard connection design rules. For bolted splices, the Eurocode (EN 1993-1-8) provides formulas for bolt shear, bolt bearing, and plate tension resistance and other relevant design checks[38].

In the case of a tension member, the net section and the strength of the connectors must meet or exceed the design axial force  $N_{Ed}$  (factored axial force). For a tension member, when plates are added to the bolt, the tension forces are pulling the plates away. So the plates needs to be thicker for the force flow to go through the bolts. Tension splices often use cover plates on either side of the member or flanges, with enough bolts to ensure the splice's capacity exceeds the member's design force.

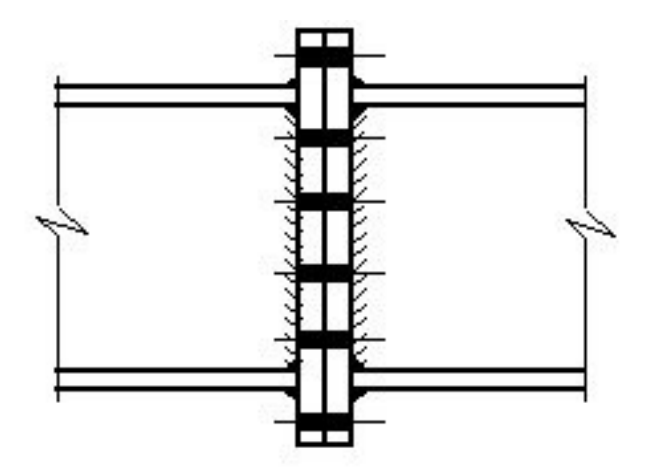


Figure 4.2: Connection for tension members

In compression members, there is an advantage in the members pushing the plates but this could also result in buckling of the members. Therefore, additional considerations such as alignment and buckling must be addressed. Eurocode 3 [36] specifies that the bracing system must be capable of resisting a lateral force at the splice equal to approximately 1% of the compression force, to account for initial imperfections. This is quantified as:

$$F_{\perp} = \frac{a_m N_{Ed}}{100}$$

where  $a_m$  is the imperfection factor (typically taken as 0.5), resulting in a lateral bracing force re-

quirement of approximately 0.5% of  $N_{Ed}$ .

Compression splices may use milled flat ends in bearing or preloaded bolts to ensure continuity. The structural implication of a mid-member splice, if properly designed and executed, is minimal reduction in strength but a possible small increase in deformation if slip occurs. If ordinary (non-slip-critical) bolts are used, the truss may experience a one-time slip at each splice under initial loading, which can increase deflections.

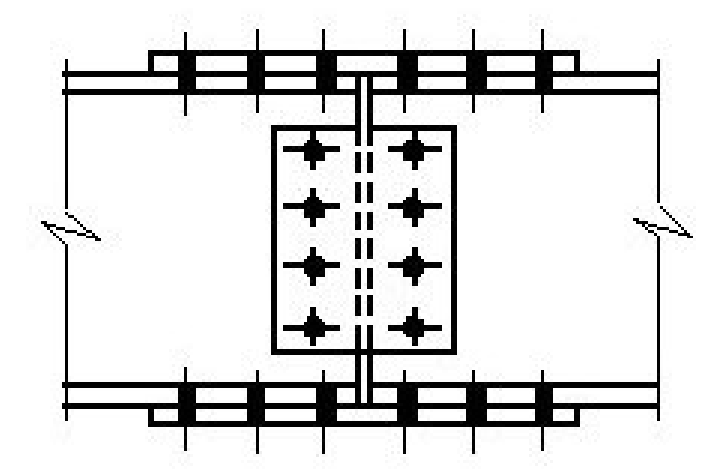


Figure 4.3: Connection for compression members

In some cases spliced members are also welded together on-site. For round hollow section, a full-penetration butt weld splice might be used at mid-member. However, welded splices are not demountable and is not suitable when segmentation is done for future reuse.

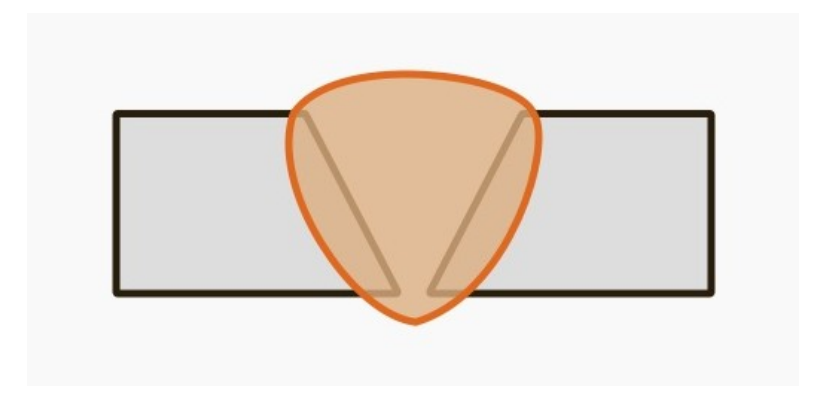


Figure 4.4: Full penetration butt weld connection

Beyond internal forces, other practical aspects influence the decision to splice a member. Segmenting members is only feasible if other joints along the truss are also bolted in certain situations.

For instance, trusses used in outdoor or harsh environments are typically hot-dip galvanized (HDG) to protect against corrosion and extend durability. In such cases, temperature effects during galvanizing can lead to deformation and internal stresses. If a splice is placed at mid-span while other joints are welded, the cantilevering portion of the cut member can deflect significantly due to the temperature effects and change in stresses introduced during galvanizing. This deflection can make it very difficult to properly install the connection. The length of the cantilevered portion plays a critical role in this behaviour. As a result, structural engineers must carefully consider the thermal and mechanical effects of the galvanizing process when determining where to segment the truss. In addition to this, during transport, trusses segmented at mid-span require special handling. Temporary vertical bracing must be provided to stabilize the cantilevering portion and prevent bending or damage. If the cantilevered

segment is relatively short, this can be managed effectively with added vertical support, making the installation of a bolted connection at mid-span more practical. An example of this is shown in figure 4.5.

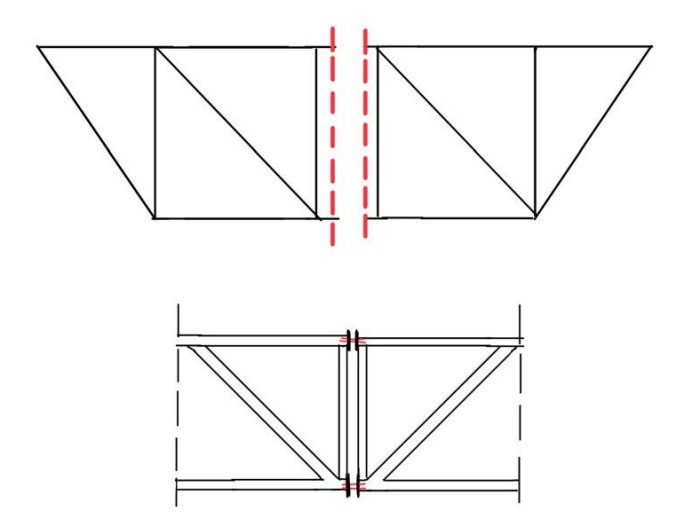


Figure 4.5: Hot dipped galavanised truss spliced through member

Here, the cut is made close to the adjacent joint so that the length of the cantilevering part is minimum and an end plate connection is made at the cut. The rest of the joints can be welded in this case. A case study utilising this method is discussed in the following section.

For trusses that are installed indoors, where environmental exposure is minimal, HDG is not done and either welded or bolted connections may be used, depending on project needs. However, even in such cases, transportation and handling must be carefully planned.

Cutting members at the midspan with higher internal force and axial stress are more crucial because it demands more joint strength. This will require more plates, bolts, and complex configurations at the joint. Segmenting members with less internal forces will be usually a more robust design. The decision must be tailored to the specific project requirements, site conditions, and the available lifting and handling equipment.

# **4.3** Nodal Level Segmentation

In this section, nodal level segmentation is discussed. When segmented at the nodes, each module of the truss is essentially an assembly of members that ends at a node. Structurally, this means the global geometry of the truss is divided, but each module may be a stable sub-truss on its own (especially if it includes at least one complete triangle of the web system for stiffness). When the modules are connected at the node, the forces transfer from one module to the other where each segment remains, similar to a monolithic truss. One structural advantage here is that all members remain intact from node to node, with their full section capacity.

Node-level segmentation, therefore, can maintain the original force path more directly, but it concentrates multiple member forces into one joint region, which must be designed to transfer all those forces between modules.

Figure 4.6 and 4.7 shows two node-level segmentation strategies for a truss structure.

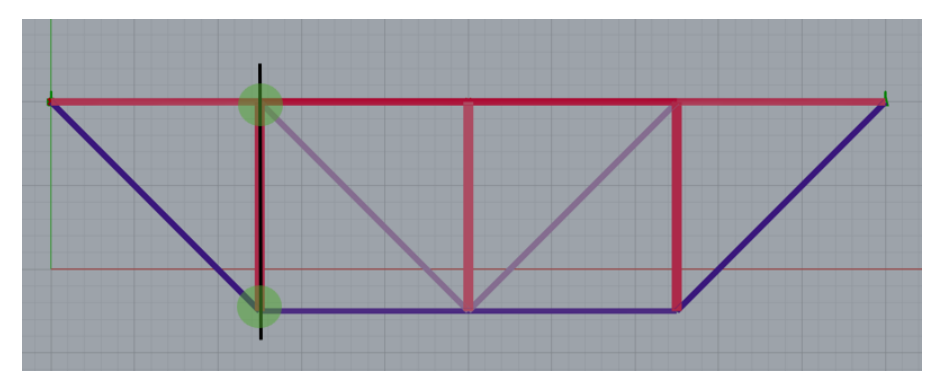


Figure 4.6: Nodal-level segmentation of truss 1

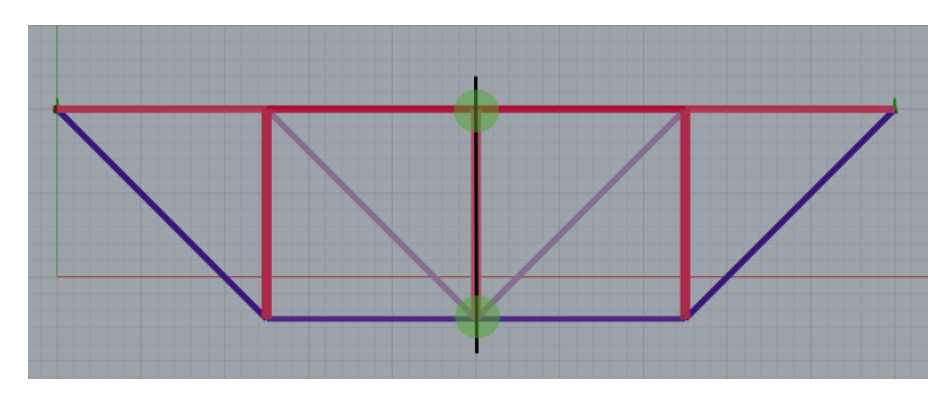


Figure 4.7: Nodal-level segmentation of truss 2

When a truss is segmented at a node, the node itself must be reconstituted with bolts or other connectors. A typical approach is to use gusset plates or cover plates that overlap the interface. For instance, if the top chord is split at a node, a cover plate can span across the two chord ends, bolting to each, effectively creating a moment-resisting splice at that location. Similarly, the diagonal and vertical web members that frame into the node can be bolted to a shared gusset plate so that when two halves of the truss are brought together, the gusset ties them together. If the original truss design assumed pin-jointed connections, the node splice can be designed as a pin as well. Figure 4.8 shows an example nodal connection.

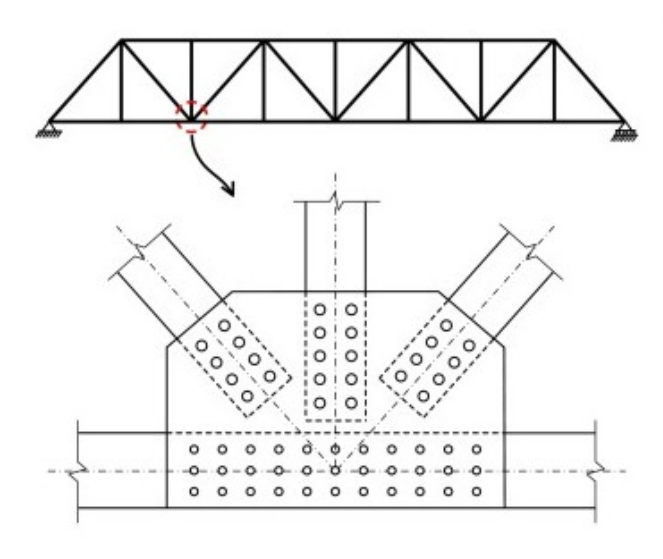


Figure 4.8: Gusset plate connection

## 4.4 Case study: Omnisport Apeldoorn

This section discusses a case study which utilises one of the above mentioned segmentation strategies. Omnisport Apeldoorn is a multifunctional sports facility designed by Haskoning that houses primarily a cycling track, an athletic track and top sports hall. In addition to this, conferences, public events, meetings and other business events are also held at this large open space. The roof structure is made of steel trusses. All information in this section is obtained from interviewing structural engineers at Haskoning who was part of this project. The images and drawings are from the web and Haskoning project archives. The figure 4.9 shows the sports facility in the completed stage in 2007.

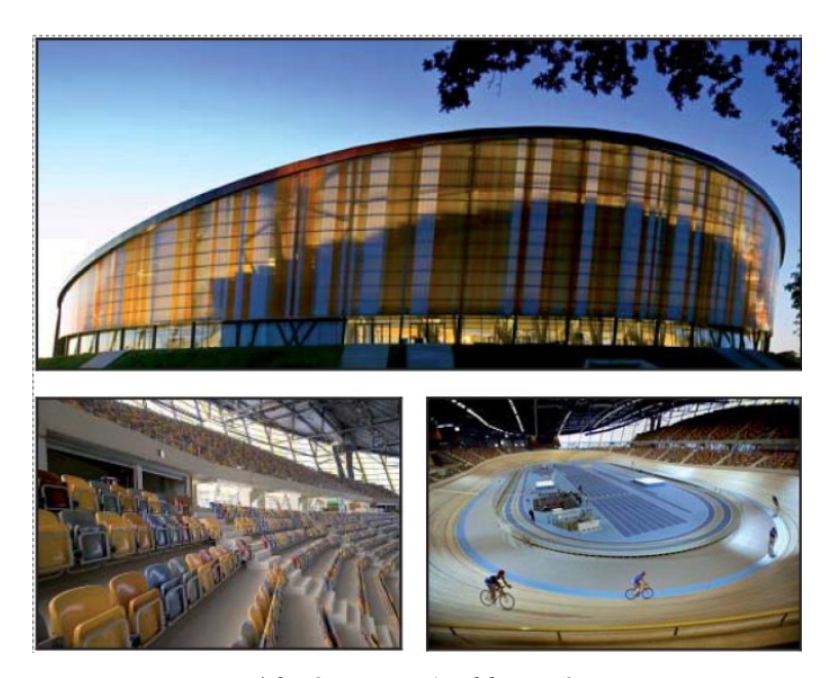


Figure 4.9: Omnipost Apeldoorn Overview

In the figure 4.10, trusses of different lengths are visible. The longest truss is 105 meter long and the depth of all the trusses are 5 meters.

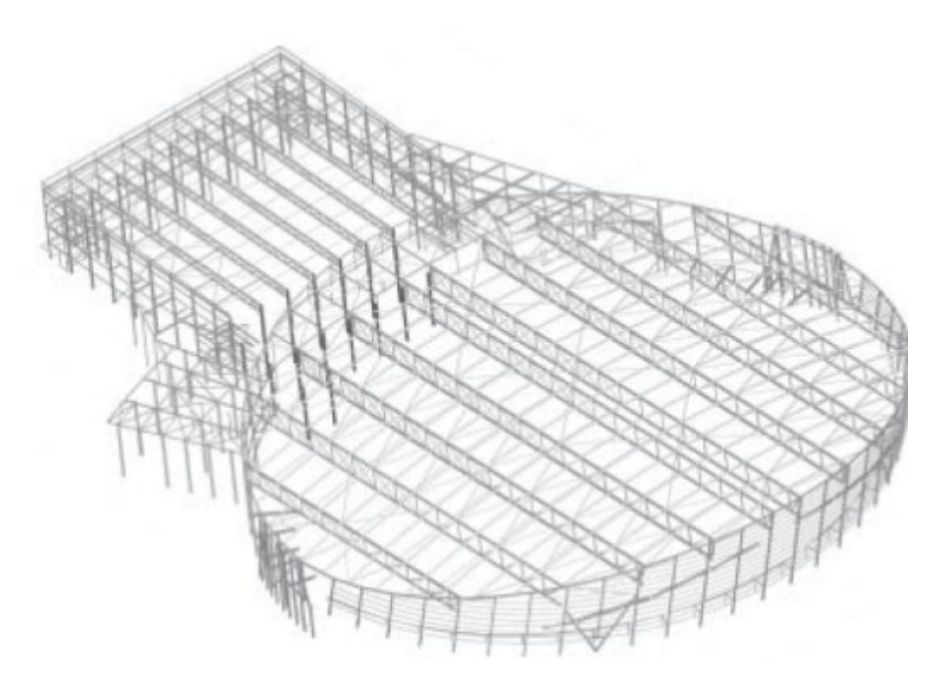


Figure 4.10: Omnipost Apeldoorn: Structure

The longest truss is used here as an example to explain the segmentation process.

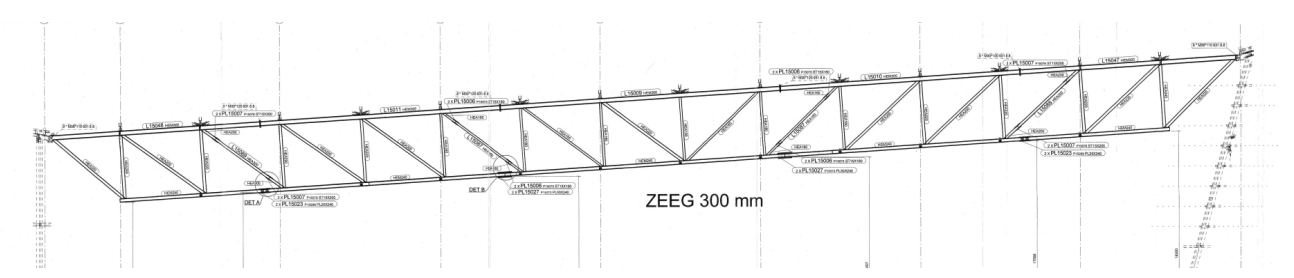


Figure 4.11: Omnipost Apeldoorn: Longest truss

The transportation of these large span trusses were difficult using standard or special use trucks. Trucks have limitations on the height of the truss as well. The height of the truss under discussion is 5m, which makes it difficult to transport vertically or horizontally. In such cases the trusses are kept at an angle to have clearance over bridges or viaducts. Special supports are required to transport a truss diagonally in a truck.

Due to transportation limitations, these trusses has to be cut at one or more places to achieve the transportable length. These trusses were cut at 3 points along the length of the truss and they were bolted at these locations. The rest of the connections are all welded connections which gives a cleaner connection because this avoids force transfer through plates and bolts. This made the onsite handling and hoisting easier.

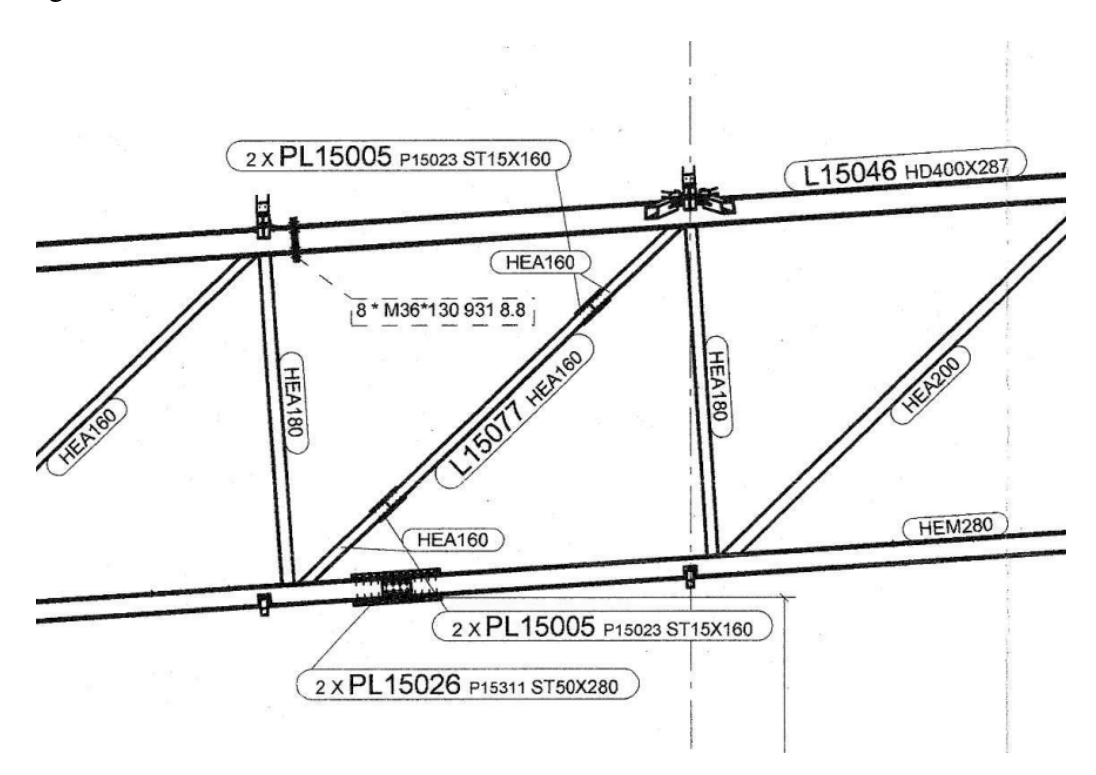


Figure 4.12: Omnisport Apeldoorn: Segmentation zone

In the figure 4.12 it is clear that the cut made in the top chord, is not in the middle, but closer to a node. This is done to reduce the length of the overhanging part of the member on both sides. Bottom chord is also spliced in a similar manner. The diagonal is slender compared to other members, so to avoid the risk of damage to the diagonal member it is transported separately and bolted on site as seen in the figure 4.12.

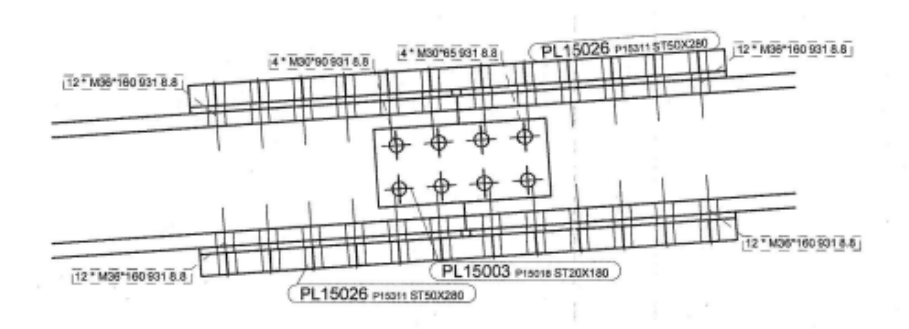




Figure 4.14: Splice detail (close-up)

The connection made at the cut is shown in the figure 4.14. The two separate members are connected using additional plates and bolts. The top chord is in compression, which means the sections can be connected using plates between them and bolted together. For tension members, the connection has to be stronger as the members are pulling away from each other. Thick additional plates of 30 mm are used on the top, and bottom flanges as well as on the web and bolted. For this truss, open sections are used.

## 4.5 Case study: Adam Tower

Segmentation of truss is not always done because of transport constraints. The case study discussed in this section have constraints regarding erection. The Adam Tower in Amsterdam is a well known attraction with a revolving structure at the top. The existing structure was modified and 3 more stories were added on top as a new crown with a sky deck. Haskoning was the structural engineering consultant for the project and all information regarding the project was collected from Structural engineers at Haskoning who were involved in the project and other information available on the web.

The client required completely column free 360 degree views in the revolving restaurant, and open rectangular bays to avoid obstructing the windows and to have shallow floor depths. This project is a good example of adaptive reuse. The original structure consisted of a 22 storey concrete structure. The challenge at Haskoning's hands was the new steel crown structure on top of the original roof which had to be supported on just four points which were the corners of the existing concrete core and had to be rotated 45 degrees relative to the original tower. Here high-strength steel was used for the trusses (S460) which was critical in keeping the floor depths reasonable.



Figure 4.15: Adam Tower

Conventional trusses with bracing would obstruct the view and would limit the floor space availability, hence the decision to use Vierendeel type of trusses of 29 meters were made. Vierendeel is a square ring of rigid-jointed steel beams without diagonals. This choice resulted in heavier members and stiffer connections. The new crown overhangs the original facade by 1.5 meters and the crown is a 32m x 32m square ring. The load-bearing scheme relies on the four Vierendeel trusses that span from the reinforced concrete core corners to the crown corners and the four perimeter Vierendeel truss on the cantilever part.

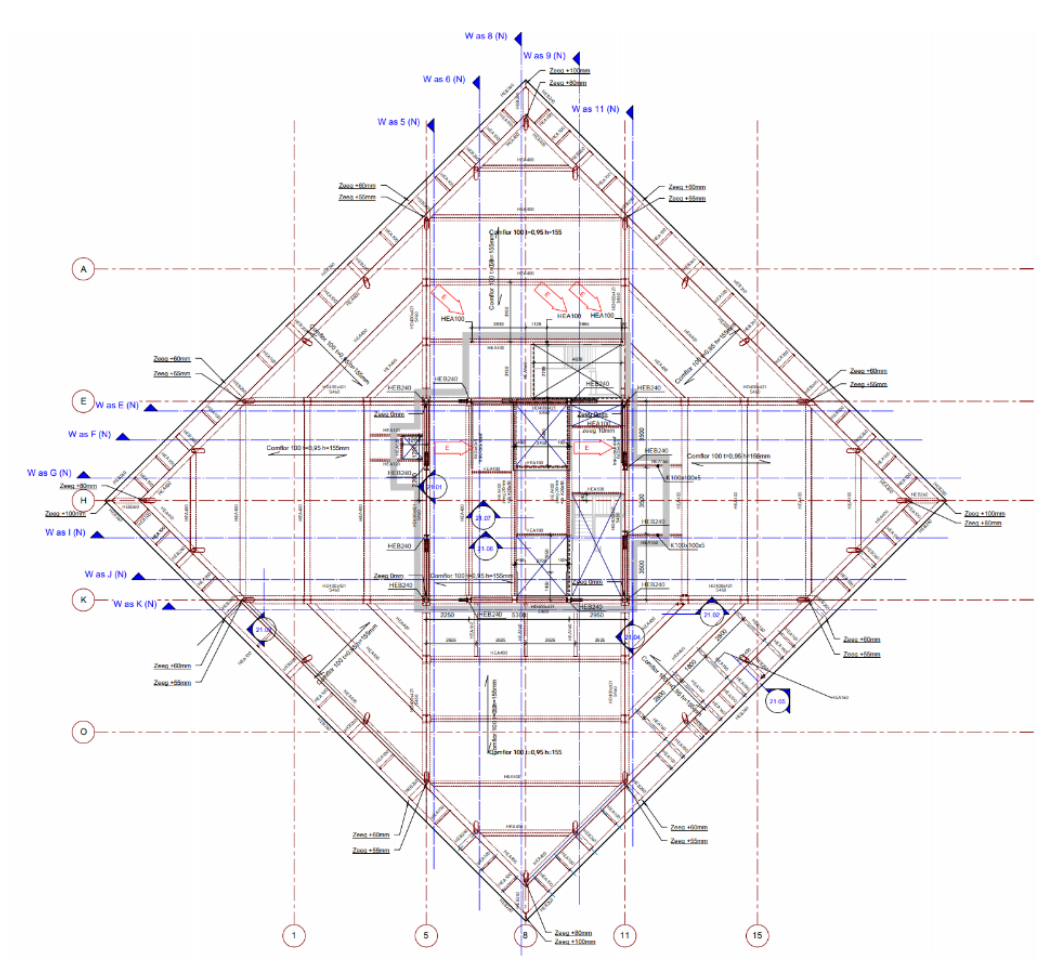


Figure 4.16: Adam Tower: Crown

The ring itself resists some lateral load, but extra K-bracing was placed only inside the small core extension (around lifts/stairs) so that the public floors remain unobstructed. The global frame is therefore "non-sway".

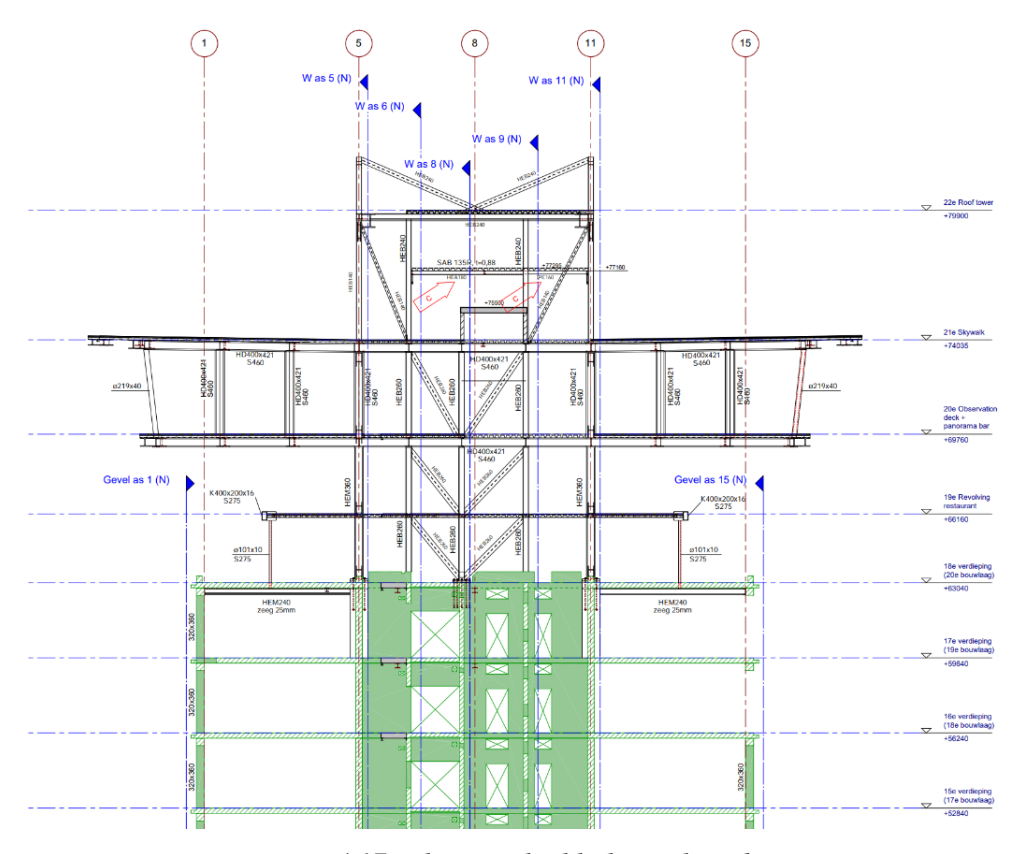


Figure 4.17: Elevation highlighting the K bracing

### **Segmentation of Vierendeel frames:**

For ease of fabrication, erection and on-site assembly, the team opted for two sides of the Vierendeel ring to be fabricated as continuous beams, while the remaining two sides were segmented into several bolted pieces. This segmentation strategy was mainly driven by the need to manage lifting logistics at a 74 meters height. The segmented beams incorporated short erection columns and featured splice connections, designed as simple compression-and-tension couples at the bottom and top chords respectively. This detail ensured the site connections were straightforward and could be executed safely and efficiently at height.

#### **Erection Strategy:**

As quoted by structural engineer at Haskoning, "Constructing the crown at 74 meters above ground level posed significant logistical challenges, particularly given that only one crane in Europe at the time was capable of making lifts at that height." To minimize hoist movements and reduce the risk and duration of work, pre-assembling large modules at ground level was done. Each module combined a central segment with two side segments, and came complete with metal-deck floors, edge scaffolds, and safety nets. This modular strategy meant that instead of lifting and assembling hundreds of small members piece-by-piece at height, the crown could be erected using just a few large, pre-decked picks. Additional field splices were introduced at low-moment points to further facilitate this process, making the connections both manageable and safe.





Figure 4.18: Erection



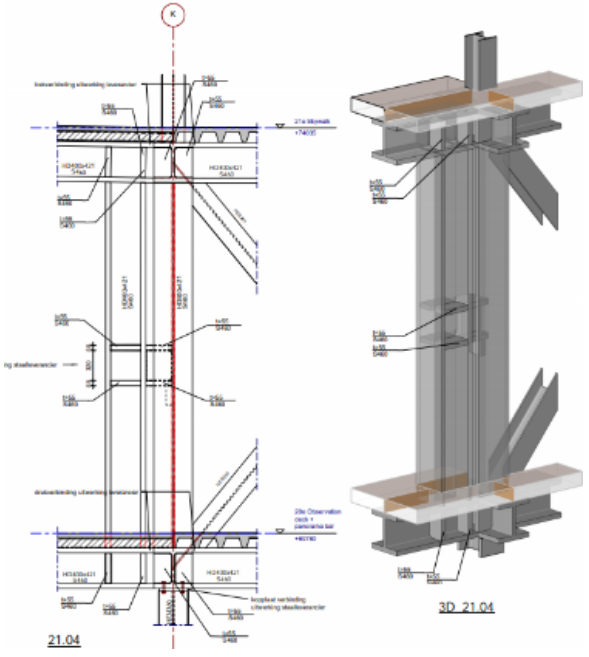


Figure 4.19: Adam Tower: Connection Detail

The Adam Tower crown shows how structural design can meet demanding architectural and logistical requirements simultaneously. The segmentation of the Vierendeel frames, the splice detailing, and the modular erection strategy collectively ensured that the new addition could be safely and efficiently installed on top of the existing structure, despite height and crane limitations.

## 4.6 Case Study: X

Case study X is a project with a truss design and segmentation strategy that is different from the ones discussed earlier. The project is still in the early design stage, therefore, different alternatives are also discussed. Due to confidentiality agreements with Haskoning, this project is presented here anonymously. All technical information has been sourced from a structural engineer at Haskoning.

The structure under discussion features a truss with a span of 46 meters and a height of 4 meters. It serves as a roof over a column free space. The truss system accommodates a low roof connected to the bottom chord and a high roof connected to the top chord. Figure ?? shows the drawing of the truss.

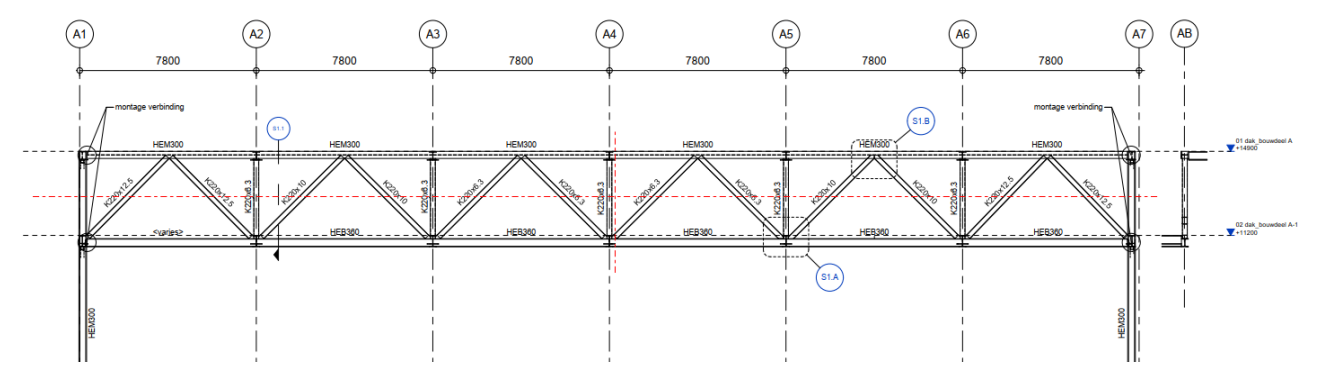


Figure 4.20: Case Study X: Section Drawing

Due to its dimensions, the transportation of the truss using standard permit trucks is not feasible, necessitating segmentation both vertically and horizontally. The segmentation line is marked in red in the figure 4.20.

However, segmenting the truss introduces structural complexities, particularly in this case, the diagonals are cut into 3 different pieces. These joints are often difficult to align accurately on site, because of bending of the cantilevering part or damage due to transportation and handling. As the cut is made in the middle of the truss, the section may carry significant internal forces. A simply supported truss design makes mid-span cuts particularly unfavourable due to high bending and shear forces present at those locations.

An alternative strategy proposed involves avoiding cuts in the top or bottom chords and segmenting at the nodes. However, this option is not preferred because the vertical members are hollow sections and bolted connections are difficult to execute along with the transverse beam present which has to be welded on site. The connection design proposed at present is given in figure 4.21 where the transverse beam can be visualised better.

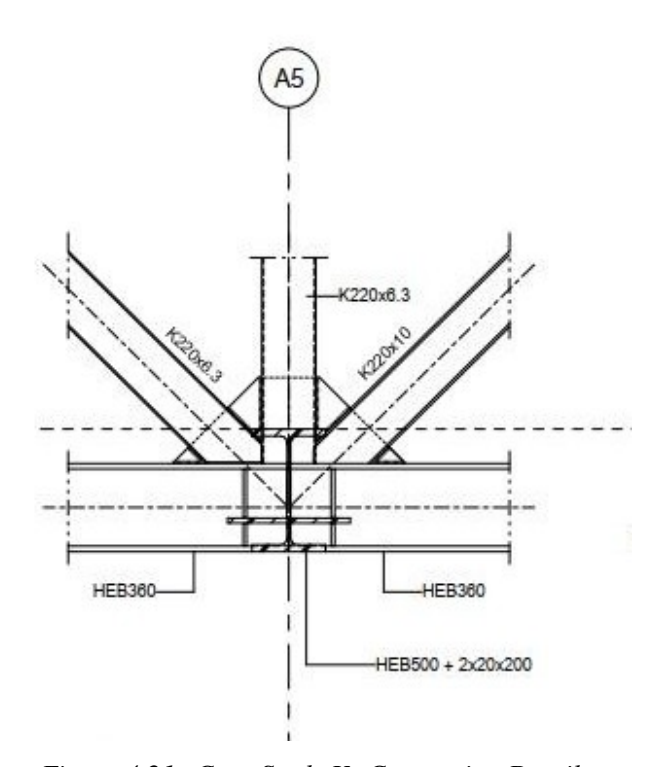


Figure 4.21: Case Study X: Connection Detail

From figure 4.21 it is clear that there is no eccentricity in the line of action of the members at the joint. The design specifically avoids moment connections and eccentricities at joints because these connections are intended to be axial to suit the large span and substantial forces involved.

For the alternatives with no cut horizontally, transportation of the 4m deep truss can be tackled by positioning the truss diagonally on the truck, but this requires precision and a custom truck support system. Therefore, transporting a segment diagonally is often a last resort. In contrast, if a cut is made horizontally, multiple trusses can be stacked and transported together. Trusses may be stacked in small numbers, typically two or three per truck depending on their dimensions and orientation. This method allows for more efficient use of transport resources.

The final decision on segmentation and transport strategy depends heavily on the number of trusses involved. For a single truss, transport and assembly considerations differ from projects involving 20 or more trusses. In projects with higher truss quantities, it becomes critical to evaluate how each truss is transported and what operations are performed at the factory versus on-site. This broader perspective on workflow can lead to optimisation in labor, transport, and construction sequencing.

# 4.7 Case study: Y

Case Study Y involves a unique structural project that required the design and construction of a truss system within a 300 m x 150 m building. This project stands out from previously discussed cases due to the implementation of hot-dip galvanisation (HDG) for fire resistance. Due to confidentiality agreements with Haskoning, this project is presented anonymously. All technical information has been sourced from a structural engineer at Haskoning.

The building features a parking facility on the ground and first floor and a sporting facility on the second floor. The trusses span from the first-floor parking level to the second floor. Due to the requirement for large spans in the parking area with minimal vertical supports, trusses were used to support both the roof and the floor above. The largest truss in this structure is 106.4 meters in length and 4 meters in depth. To meet the fire safety requirements specified by the client, the trusses were designed to provide 90 minutes of fire resistance. As a result, hot-dip galvanisation (HDG) was selected as the protection method to ensure both durability and compliance with fire resistance standards.

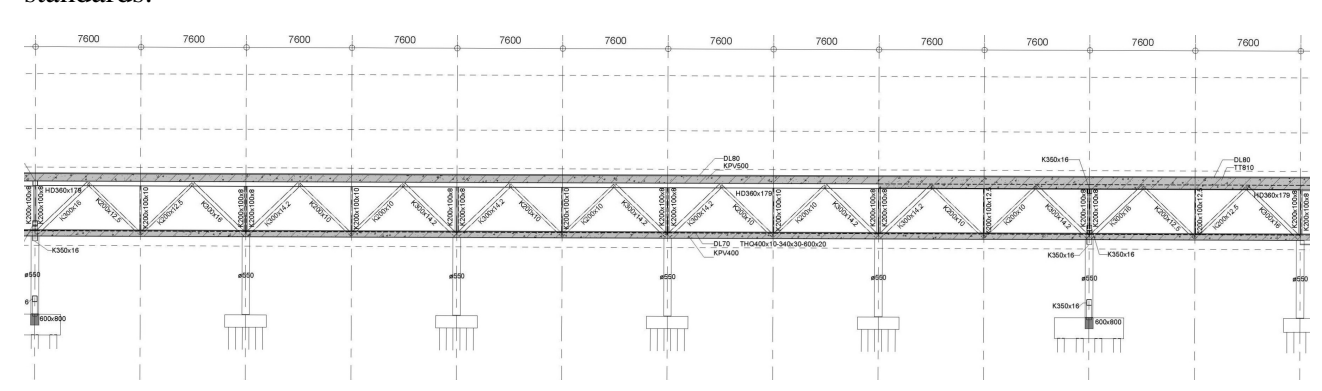


Figure 4.22: Case Study Y

The constraints for realising a 106.4 meter truss for this project were;

### **Galvanising Tub Limitation**

- The steel manufacturer has a galvanising tub of limited size (approx. 25 meters).
- The truss could not be dipped in one piece due to its length (106.4 meters).
- If segmented at the middle of a member, the cantilevering parts deform during HDG process due to temperature effects.
- Maintaining structural integrity and alignment during and after galvanisation was a critical concern.

### **Transport Limitations**

- The 4-meter depth of the truss made it impossible to transport in a horizontal orientation on standard trucks.
- The full-length truss (106.4 meters) exceeded the legal transportation limits and could not be transported as a single unit.

To find a solution for these constraints, the trusses were segmented into lengths of 15.2 meters to fit within the galvanising tub and simplify handling. Cuts were made at the node points of the trusses, allowing for effective reassembly and maintaining structural integrity. A connection similar to figure 4.23 as discussed in the previous section was introduced. End-plate connections were used at both the top and bottom chords to enable secure and precise on-site assembly. Double columns were introduced to stabilise the segmented trusses during both the galvanising process and transportation. The trusses were transported diagonally within the trucks using specially designed support systems to accommodate the 4-meter depth. An innovative support system has to be developed to allow multiple trusses to be transported diagonally within a single truck, improving transportation efficiency and reducing cost.

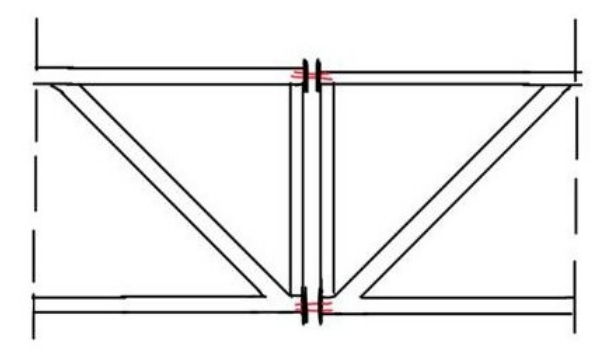


Figure 4.23: Case Study Y: Segmentation plan

# **Chapter 5**

# **Cost Optimisation**

### 5.1 Introduction

The primary goal of structural engineering is to design a structure that complies with the functional demands of the client and has sufficient structural performance. The structure should be sufficiently strong, stiff, stable and safe for the specific situation. When designing structures, safety factors are considered to generate extra safety in the structure. These factors lead to a higher use of material, hence, more cost to provide this level of safety. However, in response to growing environmental and economic concerns, engineers increasingly seek to reduce material usage wherever possible. Optimising the weight of the structure is therefore often pursued not only to improve material efficiency and reduce cost, but also to enhance the sustainability of the design by lowering the embodied carbon and resource consumption.

While structural performance and safety are fundamental, designing large-span steel trusses also requires consideration of cost-effectiveness and constructability. In early stage of engineering, designs are optimised solely for minimum weight, assuming that the lightest structure will be the cheapest. This is often not the case with reality. Minimum-weight designs can require slender members and complex connections with intricate detailing that drive up fabrication and assembly costs. Therefore, optimising only for weight may result in non-economic solutions. A more holistic cost model is required, one that includes connection complexity and material selection to support informed decision making during the early stages of design.

This chapter discusses how different cost components contribute to the total structural cost.

### 5.2 Direct and Indirect cost

Costs of steel truss from production to site can be divided into two categories: direct costs and indirect costs. Direct costs are those which can be clearly attributed to the cost object. Costs which are not directly linked to any one part of the project but are necessary for the overall project execution are called indirect cost. To better understand how this classification applies in the context of steel trusses, interviews were conducted with industry experts. Based on these discussions, the following table was created.

Direct Cost	Indirect Cost
Labour/Fabrication	Engineering
Material	Administration
Connection	Electricity
Transport	Machine maintenance

Table 5.1: Examples of Direct and Indirect costs

In this project, the main focus would be the direct cost. Indirect costs are factored in through defined tariffs or fixed overhead percentages and are not sensitive to changes in structural geometry. Hence Indirect costs are not included in the cost model developed in this study.

### 5.3 Breakdown of Direct costs

The cost of a steel truss can be broken down into several components. The total cost is determined by the engineering, material needed, fabrication, fire protection, transport and construction at site. However, the focus here is on material, fabrication, connection, and transport cost.

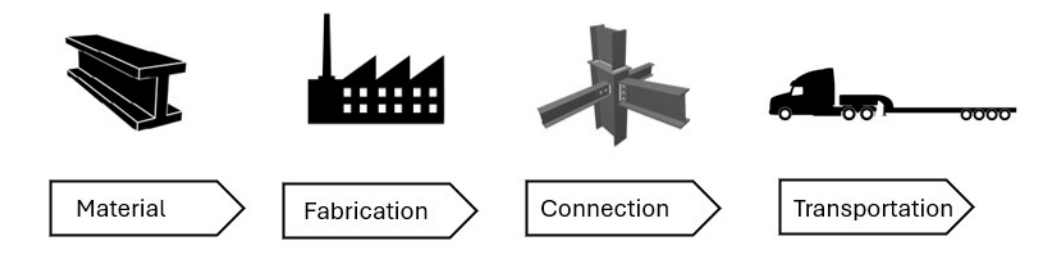


Figure 5.1: Direct Costs

Each component corresponds to a different aspect of project expenditure and is explained in detail below.

#### **5.3.1** Material cost

Material cost represents the most fundamental and influential component in the overall cost of a steel truss. This cost is calculated by multiplying the total weight of the truss by the unit price of steel, expressed in euros per kg. However, this unit price is not a fixed value. It varies significantly depending on the steel grade (e.g.S235 vs S355) and the type of profile used (e.g. I beams, round tubes, rectangular tubes etc.) and the supply source (stock vs mill orders).

In general, higher strength steels such as S355 are more expensive than standard grades like S235 with a typical price difference ranging from 30 to 80 euros per tonne depending on the source. Rectangular hollow sections also tend to cost 5-10% more than round tubes. These variations shows the importance of selecting steel grade and geometry strategically in design.

According to the feedback from cost estimators in the industries, material cost is also the more reliable and widely used cost indicator in practice. Optimizing weight becomes not only structural or environmental but also an economic priority and the experts confirms that material weight is the primary cost driver in steel truss pricing.

### 5.3.2 Fabrication cost

Fabrication cost covers the workshop labour and overhead associated with workshop labour, and operations required to process steel components including cutting, drilling, coating and assembly

preparation. These activities involve both manual labour and machine work, and their complexity can vary widely depending on the number of elements, precision of cuts and welding requirements.

In practice, fabrication cost is typically estimated using an approximate rate per kilogram of steel rather than modelling each process step individually. This simplification reflects industry norms, where a fabrication rate (euro/kg) is used to convert total weight into cost. The rate can change between 1-2 euros per kg, depending on the project type, detail level, and market conditions.

Industry experts suggested that fabrication, primarily consisting of welding and labour, is often approximated as 25–30 percentage of material cost when detailed rates are not available. However a large part of fabrication effort, particularly welding and preparation is often captured within connection related cost estimations and hence not modelled as a separate component in this study.

#### **5.3.3** Connection cost

In steel trusses, there can be bolted or welded connections and they ensure structural continuity and force transfer across elements. Rather than being priced per bolt or gusset plate, connection cost is often estimated as a percentage of the total material cost, due to the difficulty of precisely itemizing each joint. Connection cost can be modelled as a percentage ranging from 3 to 6 of total material cost, depending on the joint complexity.

- **Simple connections:** Pin or hinge joints which involve fewer plates, smaller welds, or simple bolted arrangement. This can be the lower bound of the percentage range(3%)
- Complex connections: Fixed or moment resisting joints which involve multiple gusset plates, intricate welding at various angles, high number of bolts can be near the upper bound (6%), showing higher labour and preparation efforts.

### **5.3.4** Transportation Cost

Transport considerations primarily relate to the segmentation strategy of steel trusses and the ability to transport fabricated segments within standard truck size limits. The figure 5.2 illustrates the maximum standard transport dimensions for road transport with a permit in the Netherlands. These dimensions serve as a critical constraint during the design phase, influencing how the truss is broken down and assembled, but not necessarily impacting the monetary cost significantly.



Figure 5.2: Maximum transport dimensions for road transport with a standard permit in the Netherlands

Although transportation logistics must be considered in structural planning, feedback from expert in-

terviews indicated that the actual cost of transportation, often ranging between 2-5 euro/km depending on distance and logistic requirement, is not a major driver of structural cost. Hence, transportation cost itself is not included in the rest of this study.

## 5.4 Conclusion

Expert interviews and literature consistently highlight that the cost of a steel truss is primarily governed by its weight. Since material weight directly correlates with material cost, optimizing the truss for minimum weight inherently leads to a cost-effective design. Therefore, performing a separate cost optimization is unnecessary and minimizing weight effectively achieves the same goal of reducing cost.

# Chapter 6

# Case study: The Pier

In this chapter, the performed case study is presented. The goal of the case study is to apply parametric design and optimisation techniques to a structure intended to be realised in practice. Additionally, the segmentation strategies discussed in chapter 4 will be applied to the structure. The case study is done in collaboration with Haskoning. Section 6.1 provides the background, highlights key aspects of interest and the specific goals in more detail. The remainder of the chapter focuses on the design of the truss.

## 6.1 Introduction

The case study for this thesis focuses on the redevelopment of **De Pier** in Scheveningen, the Netherlands. The original pier, built in 1961, has reached the end of its service life after decades of corrosion and fatigue damage, making reinforcement no longer economically viable. As a result, the municipality and co-developer, Re:BORN Real Estate plan to redevelop the existing structure into a larger commercial space [3].

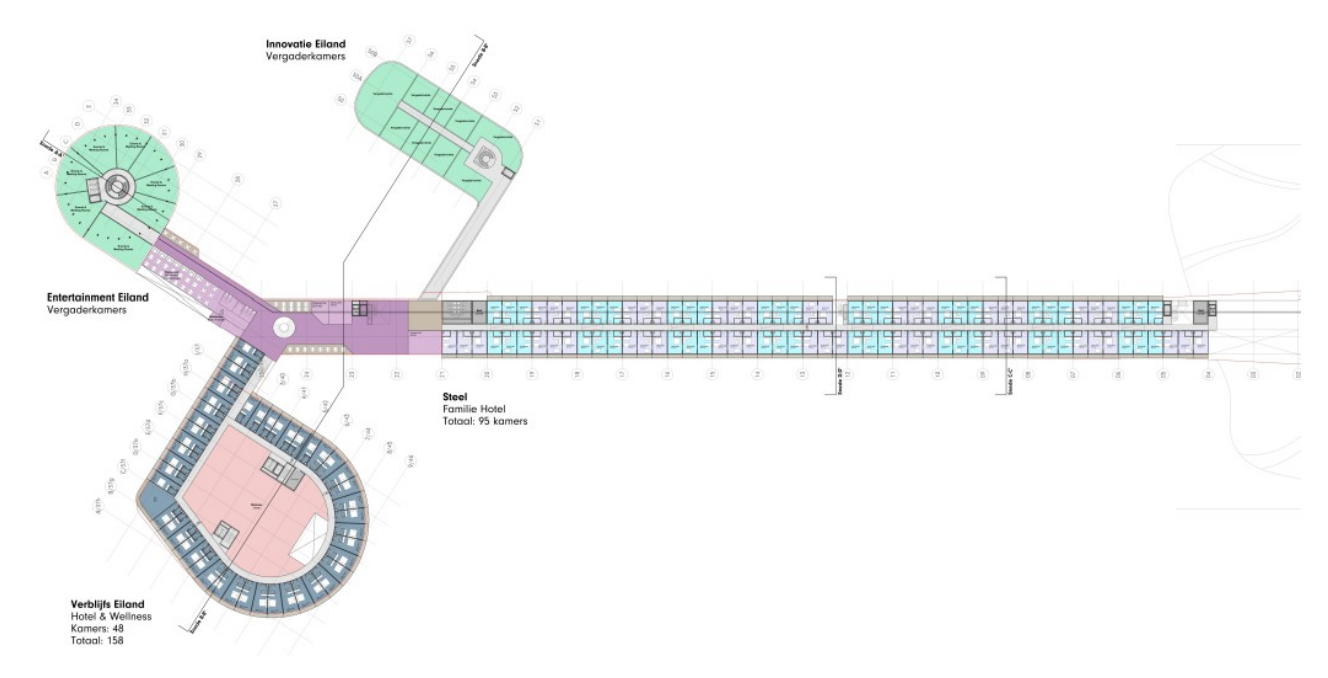


Figure 6.1: The Pier

Figure 6.1 is the master plan for the entire redevelopment project. The design features a long strip extending from the land out into the sea, connecting to three distinct islands. One island will house a

luxury hotel overlooking the sea, another will provide commercial space, and the third will feature an auditorium topped with a rooftop Ferris wheel. The redevelopment of the pier is designed to attract visitors throughout the entire year.

The focus of this study is Island 3, a two-storey steel pavilion that forms a central part of the new development. The structure must fulfil multiple architectural and functional requirements such as:

- Providing a column-free, reconfigurable hall on the ground floor for events such as theatre, exhibitions, etc.
- Meeting rooms and enclosed spaces on the upper level.
- Acting as the primary support frame for the Ferris wheel, transferring both vertical and shear loads.
- Ensuring unobstructed sea view through glass facade.
- Long central corridor connecting the emergency staircase for fire safety.



Figure 6.2: Island 3

Figure 6.2 shows the new architectural rendering of Island 3. To maintain a column-free multipurpose space on the ground floor, a truss system will be used to support the imposed loads from the first-floor meeting rooms and the rooftop Ferris wheel. This thesis specifically focuses on the design of this truss. In line with their circular construction ambitions, Haskoning and Re:BORN Real Estate aim to design truss members and connections which can be reused. This introduces additional structural challenges, including the need for segmentation zones with low stress concentration and bolted joints that allow future dismantling without using destructive methods.

The following sections shows how the proposed optimisation and modelling workflow addresses these complex, real-world constraints. The key objectives are to:

- 1. Map the design space by developing a parametric model using Grasshopper–Karamba3D.
- 2. Optimise truss cross-section using Karamba3D.
- 3. Develop a constructible segmentation strategy by identifying locations for bolted joints. These joints are to be detailed and verified using IDEA Statica.
- 4. Quantify the embodied carbon of the steel structure.
- 5. Recommend a preferred design variant.

## **6.2** Load on Truss

The roof truss in Island 3 is subjected to a combination of permanent and variable loads that come from both conventional building use and special features such as the over-roof Ferris wheel. These loads are transferred through the roof diaphragm, hollow-core slabs, and secondary framing elements into the truss chords and nodes. Table 6.1 lists the loads acting on the truss.

Action
Self-weight of the truss steelwork
Roof dead load
Imposed (live) load on roof
Live load on floor below
Dead Load on the floor below
Ferris-wheel loads

Table 6.1: Loads acting on the truss

Figure 6.3 depicts the uniformly distributed loads and point loads on the truss. Wind load is not considered in the design as the truss is indoors.

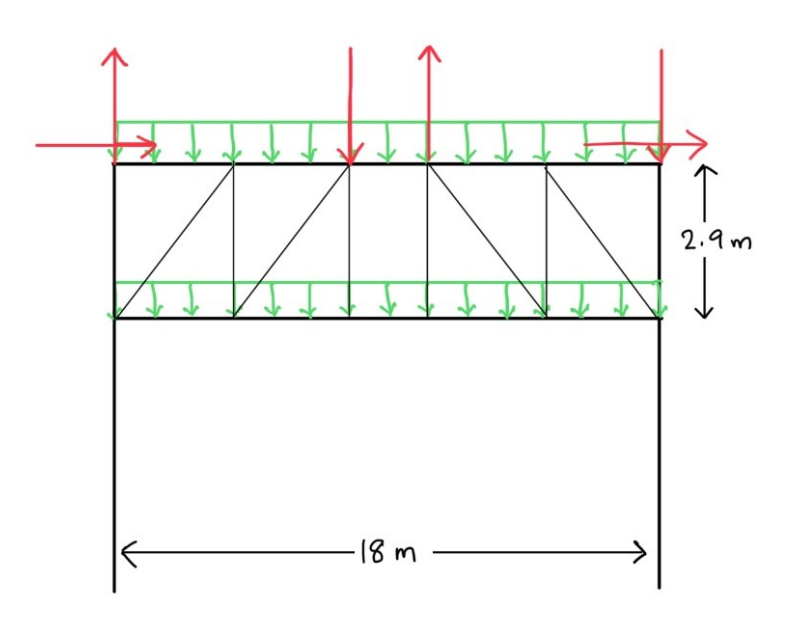


Figure 6.3: Forces on truss

Figure 6.4 shows the components in the roof and floor contributing to the dead load.

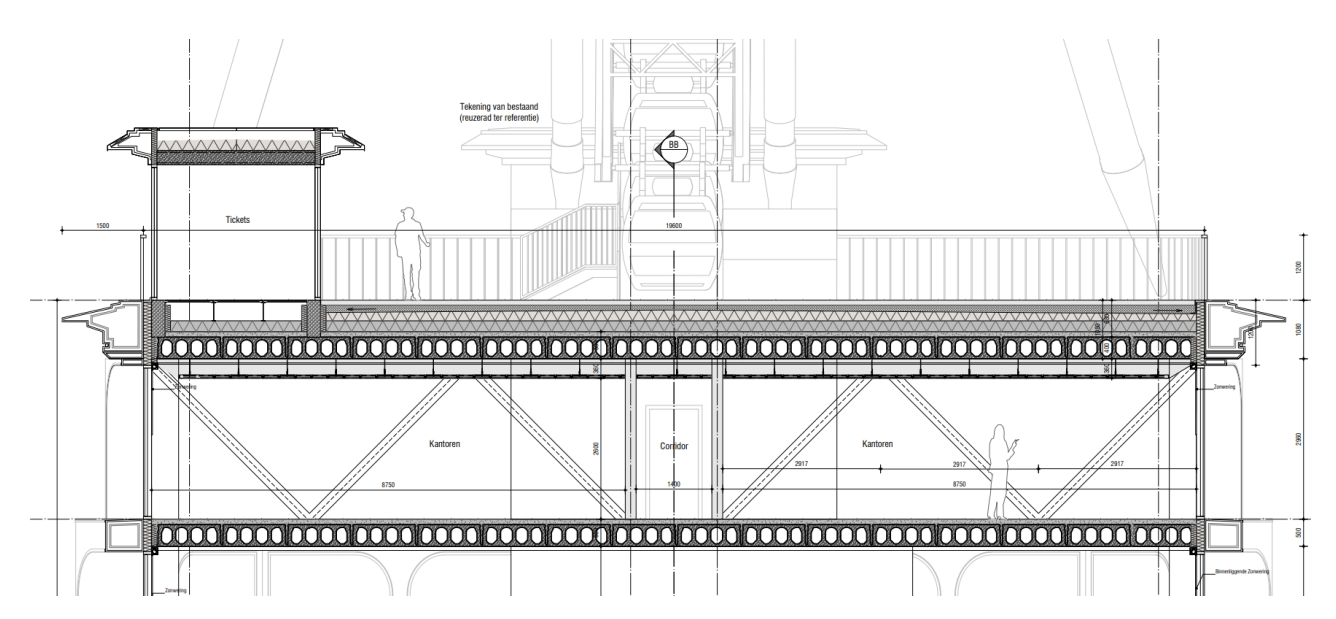


Figure 6.4: Detailing

The following permanent and imposed loads were calculated for the roof and first floor based on standard material densities and usage requirements as given in table 6.2 and table 6.3. Cross-section class of the structure is CC3.

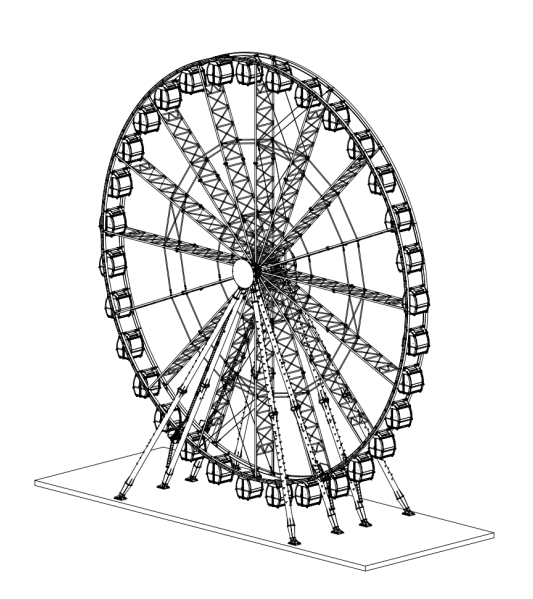
Component	Thickness × Density	Load (kg/m²)	Load (kN/m²)
Cement tiles	$0.05 \text{m} \times 2100 \text{kg/m}^3$	105	1.05
Insulation	0.25m × $25$ kg/m <sup>3</sup>	6.25	0.06
Bitumen layers	_	8	0.08
Compression layer	$0.05 \text{m} \times 2400 \text{kg/m}^3$	120	1.20
Hollow-core slab	d = 200mm	308	3.08
Ceiling & electrical	_	50	0.50
Total Permanent Load (PL)			5.97
Imposed Load (LL)	Use class assumption	_	5.00
<b>Total Roof Load</b>			10.97

Table 6.2: Roof load breakdown

Component	Thickness × Density	Load (kg/m²)	Load (kN/m²)
Compression layer	$0.05 \text{m} \times 2100 \text{kg/m}^3$	105	1.05
Hollow-core slab	d = 200mm	308	3.08
Ceiling & electrical	_	50	0.50
<b>Total Permanent Load (PL)</b>			4.63
Imposed Load (LL)	Use class assumption	_	5.00
<b>Total First Floor Load</b>			9.63

Table 6.3: First floor load breakdown

The Ferris wheel has four supports on each side and it carries vertical and horizontal forces as shown in figure 6.5. The vertical and horizontal loads in SLS and ULS are shown in table 6.4 and table 6.5. All units are in kN.



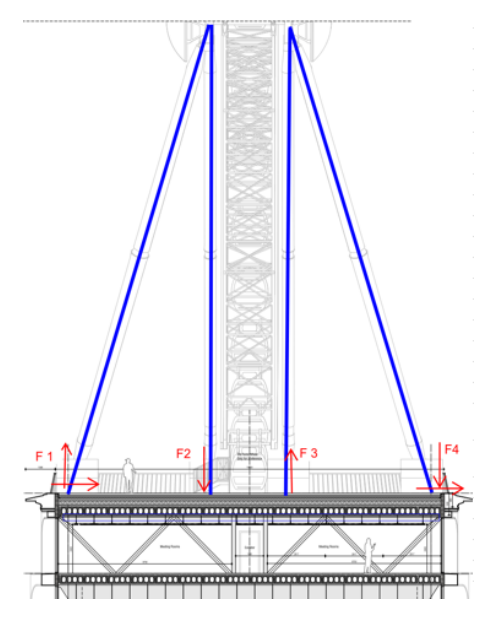


Figure 6.5: Ferris wheel

Vertical load	F1	F2	F3	F4
Own weight $G_k$	20	100	100	20
Live load $Q_k$	10	50	50	10
Wind $W_k$	-360	360	-360	360
SLS total	-330	510	-210	390
ULS total	-553.5	796.5	-391.5	634.5

Table 6.4: Ferris-wheel vertical support reactions

Horizontal load	<b>F</b> 1	F2	F3	F4
Wind $H_k$	100	0	0	100
SLS	100	0	0	100
ULS	165	0	0	165

Table 6.5: Ferris-wheel horizontal support reactions

## 6.3 Floor layout and load distribution

In this section, two floor layout alternatives with different span directions were developed for comparison. The figure 6.6 and figure 6.9 illustrates trusses positioned along the shorter span (18m) of the structure. Based on this truss configuration, two different floor plans were created, each varying in beam placement, span direction, and span length. In this design, hollow-core slabs are used for flooring due to their reduced self-weight, which results from the longitudinal voids cast into the slab; this reduction in weight allows for longer spans and decreased material consumption compared to solid slabs. The feasibility of each plan was evaluated based on the availability of prefabricated hollow core slabs using tools available online by VBI, a supplier of prefabricated floors.

Figures 6.6 and 6.9 shows the two floor layout options discussed in this section. The red lines represent the trusses, green lines indicate the beams, and yellow arrows show the direction of the hollow-core slab spans. The trusses are positioned along the same grid lines as the supports of the Ferris wheel. Each horizontal grid line is spaced 6.4 meters apart. The calculated loads for each floor plan option are given below.

### Floor layout 1

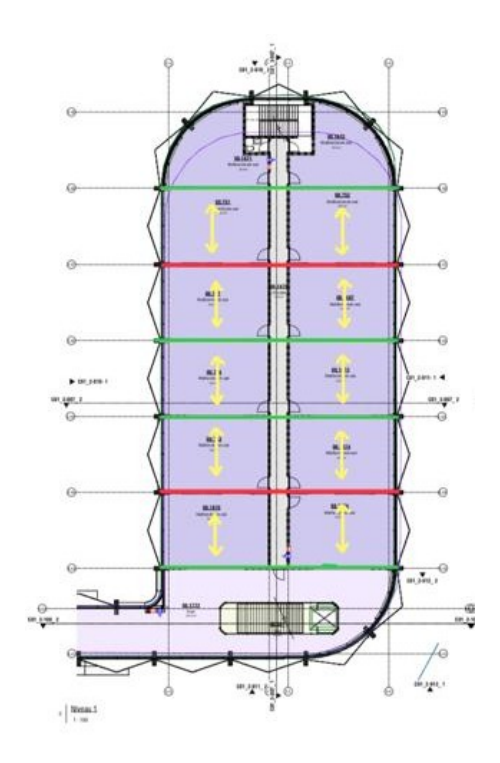


Figure 6.6: Floor plan 1

For calculating characteristic line loads,

Interior spacing s = 6.40 m, Edge half-spacing s/2 = 3.20 m

#### Characteristic line-loads

Support line	<i>b</i> [m]	$G_k b$ [kN/m]	$Q_k b$ [kN/m]
Beam 1 (edge)	3.20	18.8	16.0
Truss 1 (interior)	6.40	37.6	32.0
Beam 2 (interior)	6.40	37.6	32.0
Beam 3 (interior)	6.40	37.6	32.0
Truss 2 (interior)	6.40	37.6	32.0
Beam 4 (edge)	3.20	18.8	16.0

Table 6.6: Line loads applied to beams and trusses.

### Ultimate design line-loads

For ULS, the governing load combination is determined by the following formula [39];

$$w_{Ed} = \gamma_G G_k + \gamma_{Q1} Q_{k1} + \sum \gamma_{Qi} \psi_{0i} Q_{ki}$$

where,  $\gamma_G = 1.35$  (partial safety factor for permanent actions)

 $\gamma_{Q1}$  = 1.5 (partial safety factor for leading variable action)

 $\gamma_{Qi}$  = 1.5 (partial safety factor for accompanying variable actions)

 $\psi_{0i}$  = combination factor for accompanying variable actions

 $G_k$  = characteristic value of permanent action

 $Q_{k1}$  = characteristic value of leading variable action

 $Q_{ki}$  = characteristic value of accompanying variable actions

The table 6.7 shows the uniformly distributed load on the beams and trusses.

Support line	$1.35 G_k b$	$1.50 Q_k b$	$w_{Ed}$ [kN/m]
Beam 1 (edge)	25.4	24.0	49.4
Truss 1	50.8	48.0	98.8
Beam 2	50.8	48.0	98.8
Beam 3	50.8	48.0	98.8
Truss 2	50.8	48.0	98.8
Beam 4 (edge)	25.4	24.0	49.4

Table 6.7: Design line loads

Along with the line loads, the point load from Ferris wheel will be acting on the truss with values as shown in table 6.4 and table 6.5. In this option, the hollow core slab floor spans 6.4 m. The availability of pretensioned hollow core slabs for the required span is checked using VBI's design tool and the result is provided in the Appendix D. Beam positions between the trusses were determined based on the maximum practical prefabrication span, helping to eliminate unfeasible solutions early in the design process.

### **6.3.1** Beam Design for floor layout 1

For the beams marked in green in Figure 6.6, the applied line loads are 49.4 kN/m for edge beams and 98.8 kN/m for internal beams, spanning a length of 18 meters. Standard I- and H-sections were found to be inadequate for this application; therefore, a box beam section was designed to meet the structural demands.

### **6.3.1.1** Edge Beam

Design data used for verification of edge beam in moment and shear is shown in table 6.8 and table 6.9. Detailed calculation is given in the Appendix G.

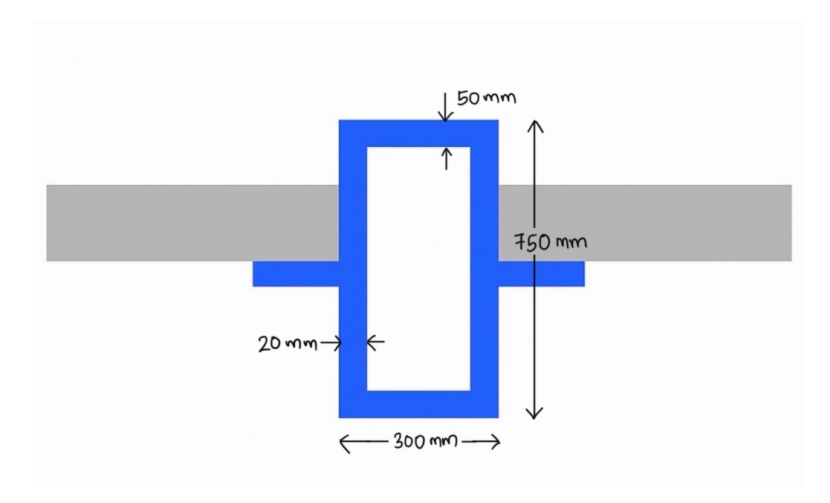


Figure 6.7: Edge Beam

Symbol	Value
$f_y$	$355~\mathrm{Nmm^{-2}}$
$I_y$	$4.59 \times 10^9 \; \mathrm{mm}^4$
$\gamma_{M0}$	1.0
$M_{Ed}$	$2.24 \times 10^9 \; \mathrm{N}  \mathrm{mm}$
$M_{Rd}$	$4.33 \times 10^9 \; \mathrm{N}  \mathrm{mm}$
$\eta = M_{Ed}/M_{Rd}$	0.52

Table 6.8: Design data for moment verification (edge beam)

Symbol	Value
$f_y$	$355~\mathrm{Nmm^{-2}}$
$\gamma_{M0}$	1.0
$V_{Ed}$	484.2 kN
$V_{Rd}$	$6.15 \times 10^3 \text{ kN}$
$A_v$	$3.00 \times 10^4 \; \mathrm{mm^2}$
$\eta = V_{Ed}/V_{Rd}$	0.08

Table 6.9: Design data for shear verification (edge beam)

### **Deflection (SLS)**

The calculated mid-span deflections are

$$\delta_{\text{tot}} = 55.5 \text{ mm}$$
 (total load)  $\delta_{\text{live}} = 22.6 \text{ mm}$  (live load),

which are both within the allowable limits:

$$\delta_{\text{tot}} \le \frac{L}{250} = 72 \text{ mm}, \qquad \delta_{\text{live}} \le \frac{L}{300} = 60 \text{ mm}.$$

Hence the edge beam satisfies the SLS deflection criteria. Detailed calculations are given in Appendix G.

#### 6.3.1.2 Interior beam

Design data used for verification of the interior beam in moment, shear and deflection is shown in the tables below. Detailed calculations are given in the Appendix G.

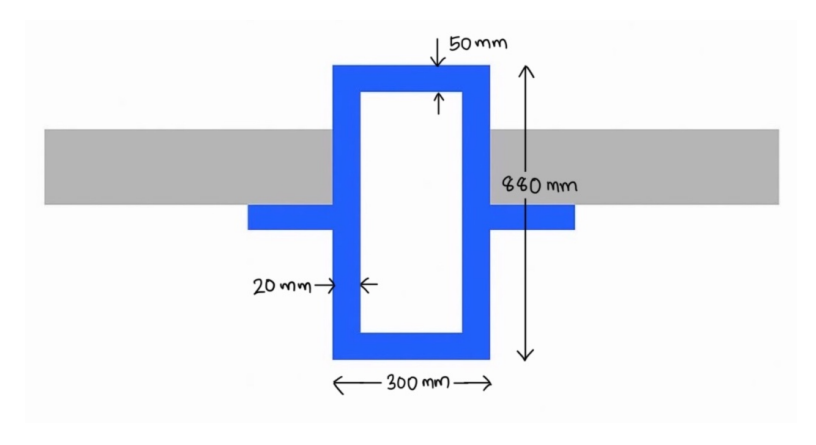


Figure 6.8: Interior beam

Symbol	Value
$I_y$	$6.75 \times 10^9 \; \mathrm{mm}^4$
$f_y$	$355~\mathrm{Nmm^{-2}}$
$\gamma_{M0}$	1.0
$M_{Ed}$	$4.26 \times 10^9 \; \mathrm{N}  \mathrm{mm}$
$M_{Rd}$	$5.78 \times 10^9 \; \mathrm{N}  \mathrm{mm}$
$\eta = M_{Ed}/M_{Rd}$	0.74

Table 6.10: Design data for moment verification (interior beam)

Symbol	Value
$f_y$	$355~\mathrm{Nmm^{-2}}$
$\gamma_{M0}$	1.0
$V_{Ed}$	928.8 kN
$V_{Rd}$	$7.21 \times 10^3 \text{ kN}$
$A_v$	$3.52 \times 10^4 \; \mathrm{mm^2}$
$\eta = V_{Ed}/V_{Rd}$	0.13

Table 6.11: Design data for shear verification (interior beam)

### Deflection (SLS). The calculated mid-span deflections are

$$\delta_{\text{tot}}$$
 = 71.6 mm (total load),  $\delta_{\text{live}}$  = 30.8 mm (live load),

which are both within the allowable limits:

$$\delta_{\rm tot} \le \frac{L}{250}$$
 = 72 mm,  $\delta_{\rm live} \le \frac{L}{300}$  = 60 mm.

Hence the interior beam satisfies the SLS deflection criteria. Detailed calculations are given in Appendix G.

### Floor layout 2

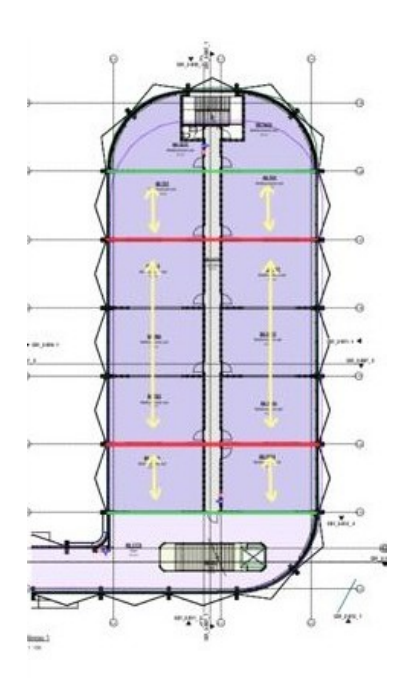


Figure 6.9: Floor plan 2

For calculating the ultimate design line load,

Interior spacing 
$$s = 6.40 \,\text{m}$$
, Edge half-spacing  $\frac{s}{2} = 3.20 \,\text{m}$ 

Ultimate design line-load

Support line	$1.35G_k b \; (kN/m)$	$1.50  Q_k b   (kN/m)$	$w_{\rm Ed}$ (kN/m)
Beam L (edge)	25.4	24.0	49.4
Truss 1	101.4	96.0	197.4
Truss 2	101.4	96.0	197.4
Beam R (edge)	25.4	24.0	49.4

*Table 6.12: Design line loads* 

Along with the line loads, the point load from Ferris wheel will be acting on the truss with values as shown in table 6.4 and table 6.5. In this option, the hollow core spans 19.2 m. Using the VBI tool, it was understood that producing such a slab is not possible. Hence, this option is disregarded.

### **6.3.2** Truss to Floor connection

Figure 6.10 shows a how the steel truss is placed in the floor system. This is similar for the top and bottom of the truss.

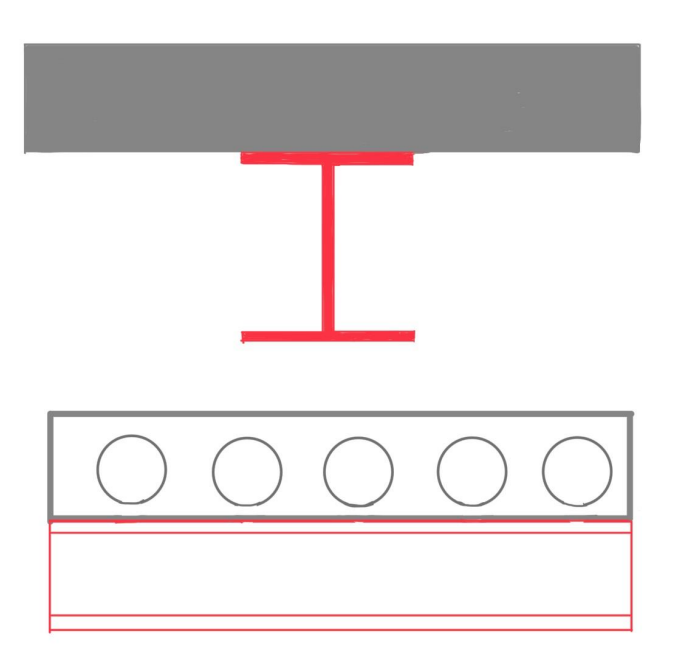


Figure 6.10: Truss to floor connection

## **6.4** Truss topology alternatives

In this section, four truss topologies were developed considering both structural and architectural constraints. These designs were modelled using Grasshopper and Karamba3D to optimise the cross-sections and minimise the overall weight.

## 6.4.1 Truss topology 1

Truss Topology 1 adopts a Pratt truss configuration, split into two separate trusses by a 3.4 m corridor that bisects the floor plan. This configuration was chosen to respect architectural requirements, while

structurally aiming to keep the diagonals in tension and verticals in compression. The upper chord is designed to resist compression, while the bottom chord resists tension forces under applied loads.

Figure 6.11 illustrates the basic Pratt truss geometry.

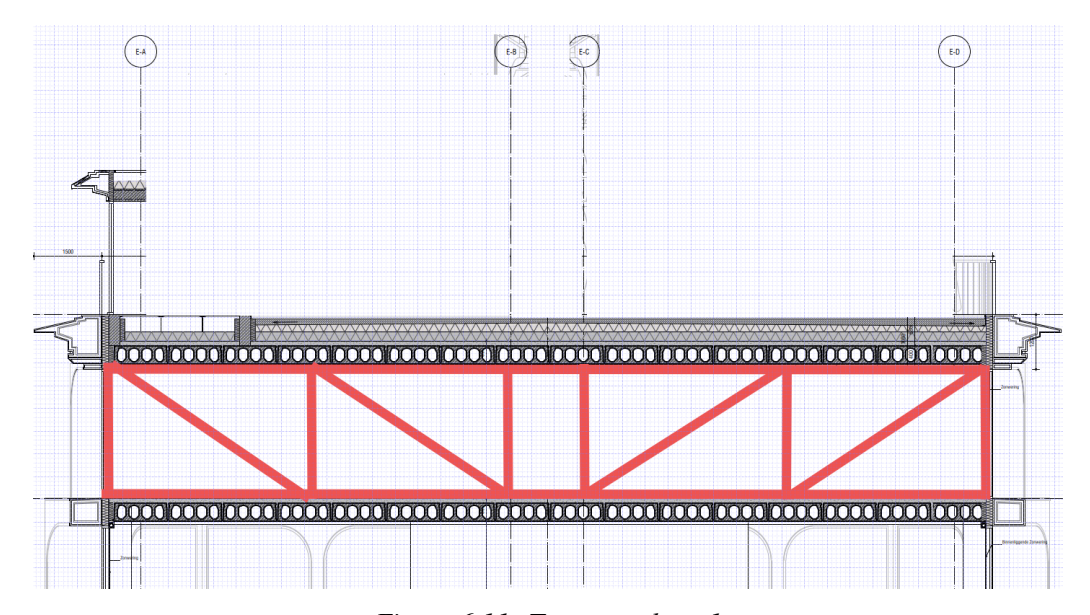


Figure 6.11: Truss topology 1

Figure 6.12 shows the parametric model in Grasshopper, indicating how the truss adapts to the pier's constraints. This simply supported truss has 40 members of steel S355.

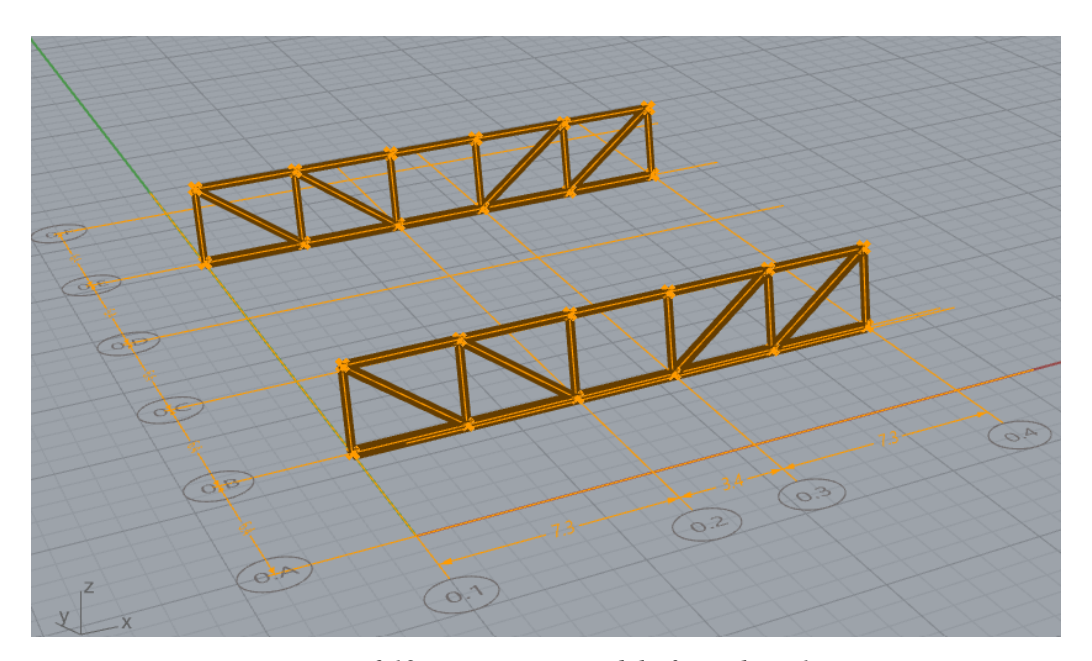


Figure 6.12: Parametric model of Topology 1

All the loads are defined in one load combination, LCO, in Grasshopper as per section 6.2.

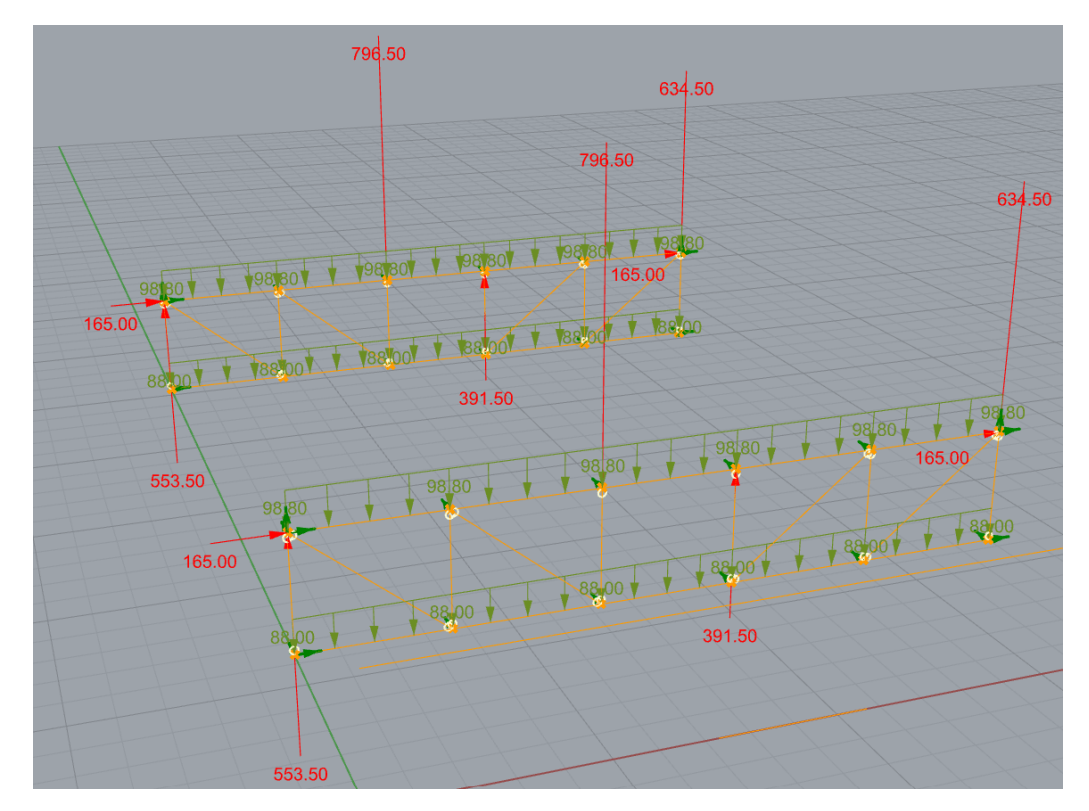


Figure 6.13: Loads- Model 1

For constructability, standardisation of components is important. To reduce high variety of profiles, a grouping strategy is used here. Grouping is based on expected similar stress levels. Upperchords, bottomchord, verticals and diagonals are the 4 different groups and are given member ID's as shown in figure 6.14. So in total, the truss will always have a maximum of 4 different profiles. The downside of this is that, because the load is not always uniform as in this case, due to points loads at different nodes, some members will be under-utilised. Overall this scenario is better than having too many varieties of profiles in the truss. The same grouping strategy is used in all models as shown in figure 6.14.

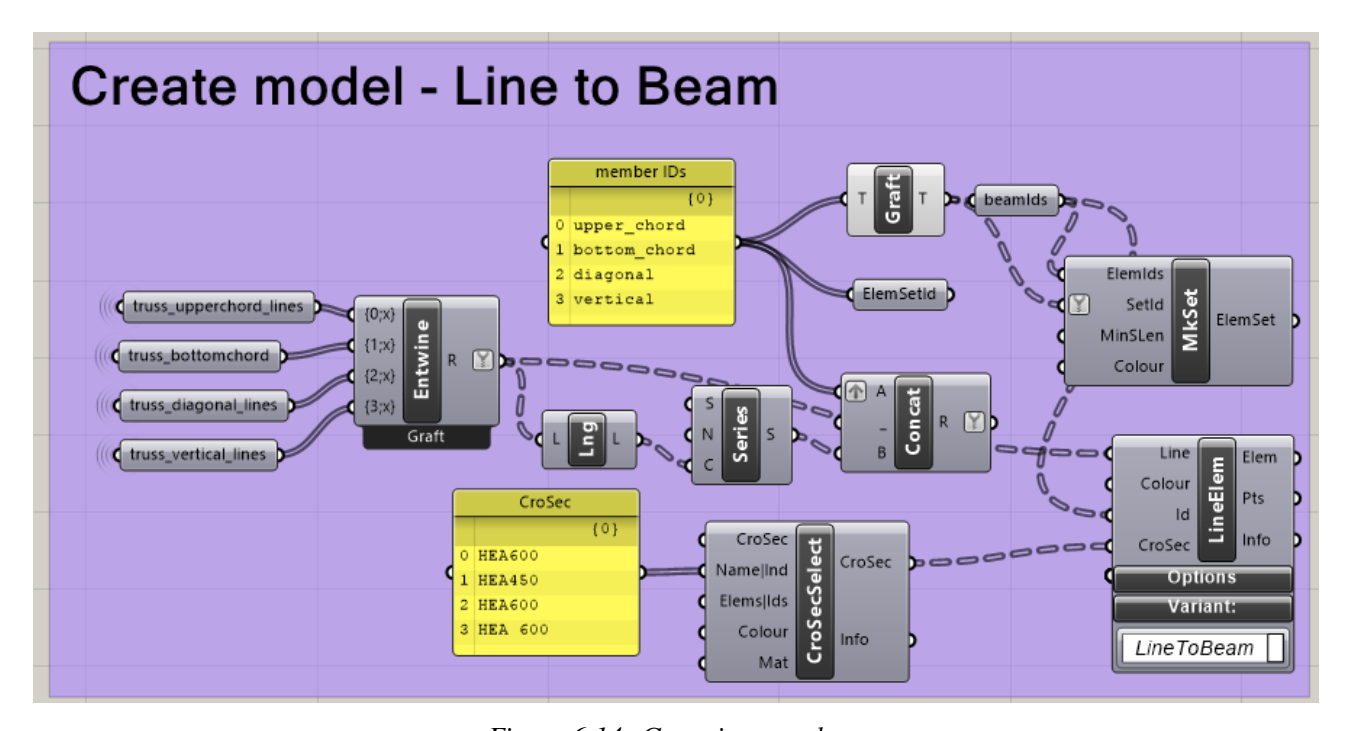


Figure 6.14: Grouping members

### 6.4.2 Results

In Grasshopper, using componets called ModelView, BeamView, Deformation energy, Utilisation, ElemQuery results from the analysis can be visualised. The resulting geometry is shown in figure 8.1. There are only 4 distinct profiles as a result of the grouping of members.

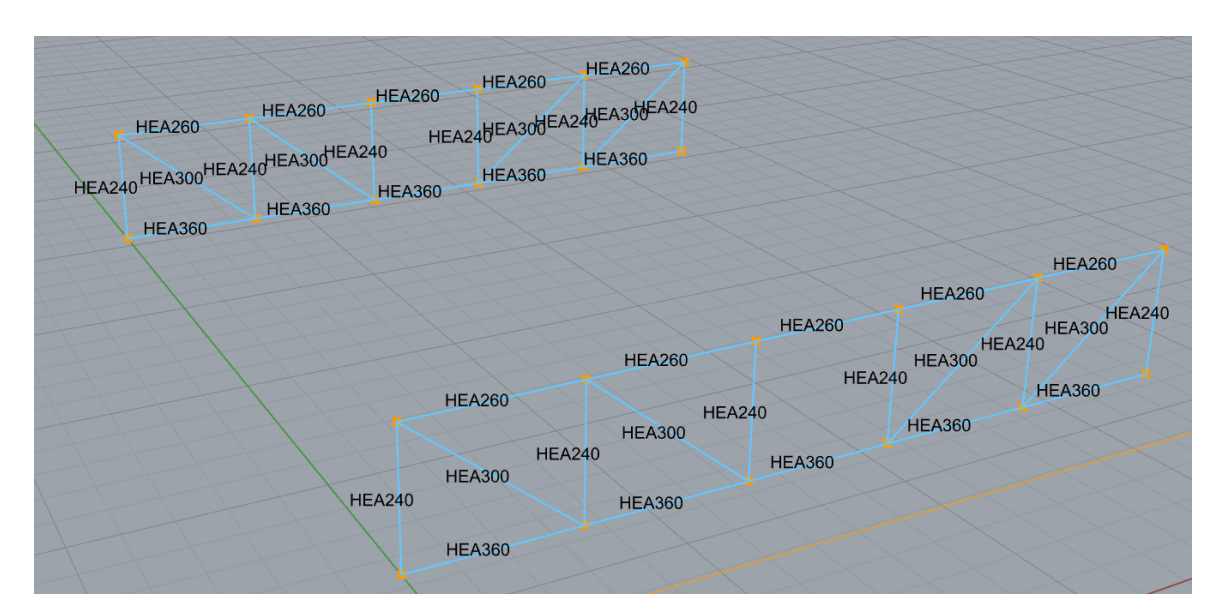


Figure 6.15: Cross section- Model 1

Name	▼ Material	<b>▼</b> Shape	🕶 A [m2] 💌	Wply [m3]	Wplz [m3]
HEA240	S355	I rolled	0,008	0,001	0,000
HEA260	S355	I rolled	0,009	0,001	0,000
HEA300	S355	I rolled	0,011	0,001	0,001
HEA360	S355	I rolled	0,014	0,002	0,001

Figure 6.16: Cross section- Model 1

The figures 6.17 and 6.18 show the shear force diagram and bending moment diagram respectively. The presence of significant shear force and bending moment in the bottom chord is due to the uniformly distributed load applied along the bottom chord members.

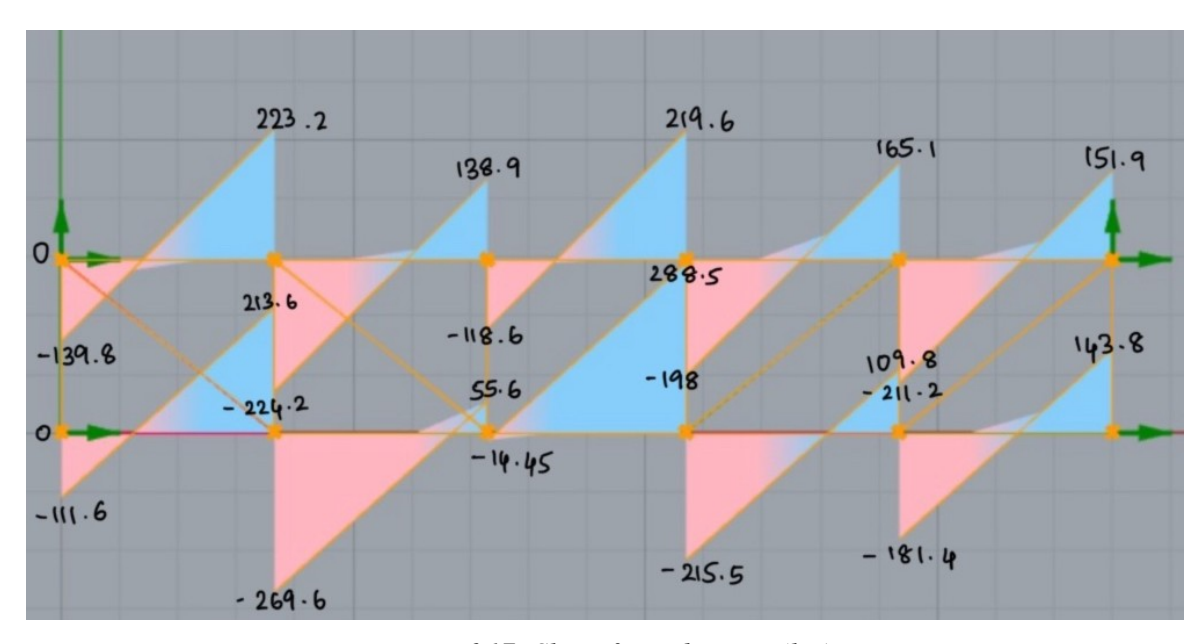


Figure 6.17: Shear force diagram (kN)

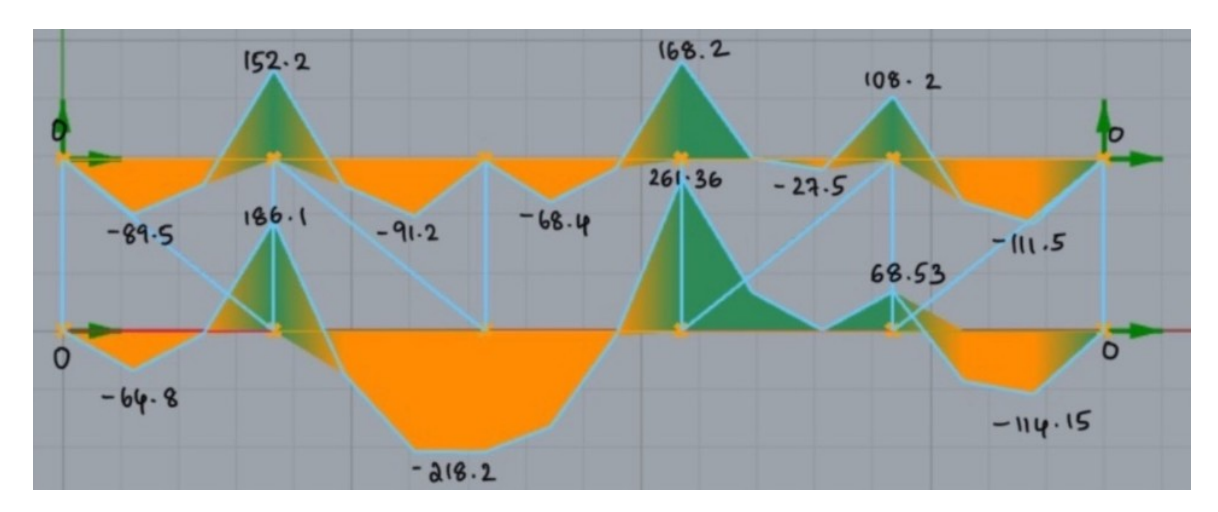


Figure 6.18: Moment diagram (kNm)

The maximum bending moments occur at the midspan of the bottom chord, which is typical for members subjected to UDL. Overall, the SFD and BMD validate the structural model and loading configuration, with all members responding as anticipated under the given loading scenario.

Figure 6.19 visualises the deformation of the truss under applied load. This matches the expectations based on the previously observed bending moment and shear force diagrams.

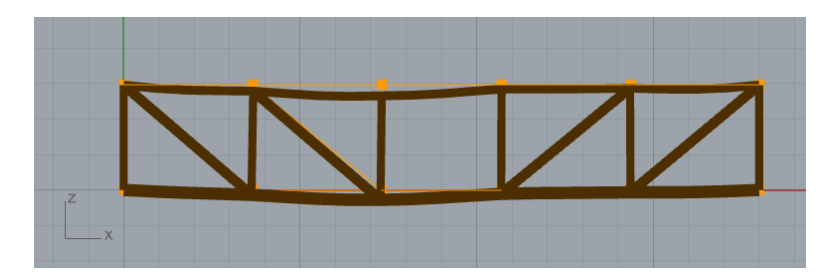


Figure 6.19: Deformation

Table 6.13 shows the maximum displacement of 2.96 cm, which is within acceptable serviceability limits for a span of 18 meters, confirming the adequacy of the structural design under the applied loads.

Result	Value
Mass of truss (kg)	11 951.4
Mass of beam (kg)	33444
Total weight of structural steel (kg)	45395.4
Maximum displacement (cm)	2.96
Maximum utilization	0.9

Table 6.13: Results 1

## 6.4.3 Truss topology 2

Truss topology 2 adopts a similar Pratt truss configuration with a higher number of panels. This was done to see the difference when the number of panels increases within a certain topology. The truss is split into two parts by a 3.4 m corridor. Under applied load, the diagonals are designed to be in tension and the verticals in compression.

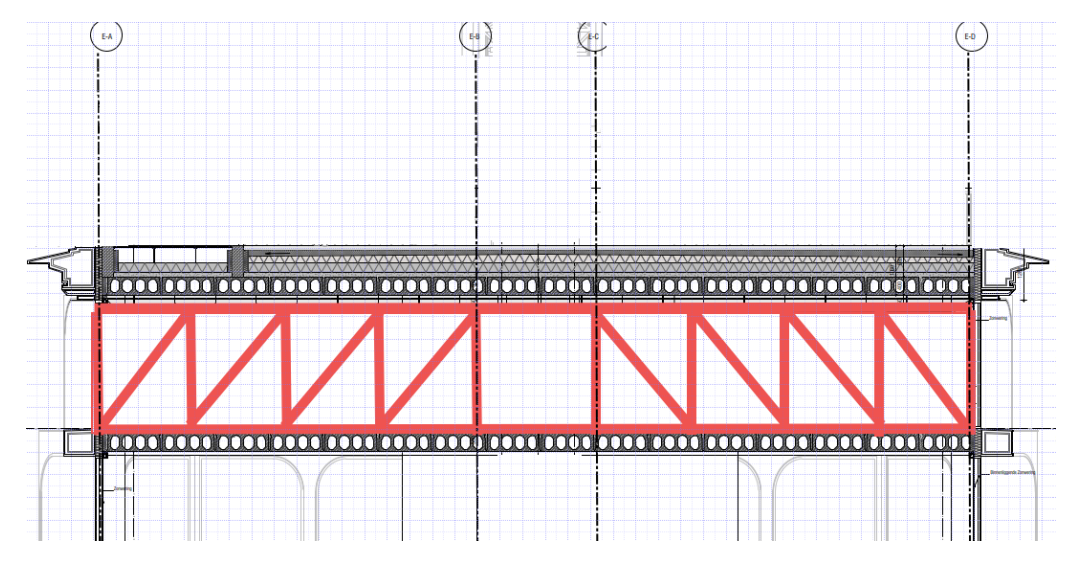


Figure 6.20: Truss topology 2

Figure 6.21 shows the parametric model in Grasshopper. This is a simply supported truss with 72 members of S355.

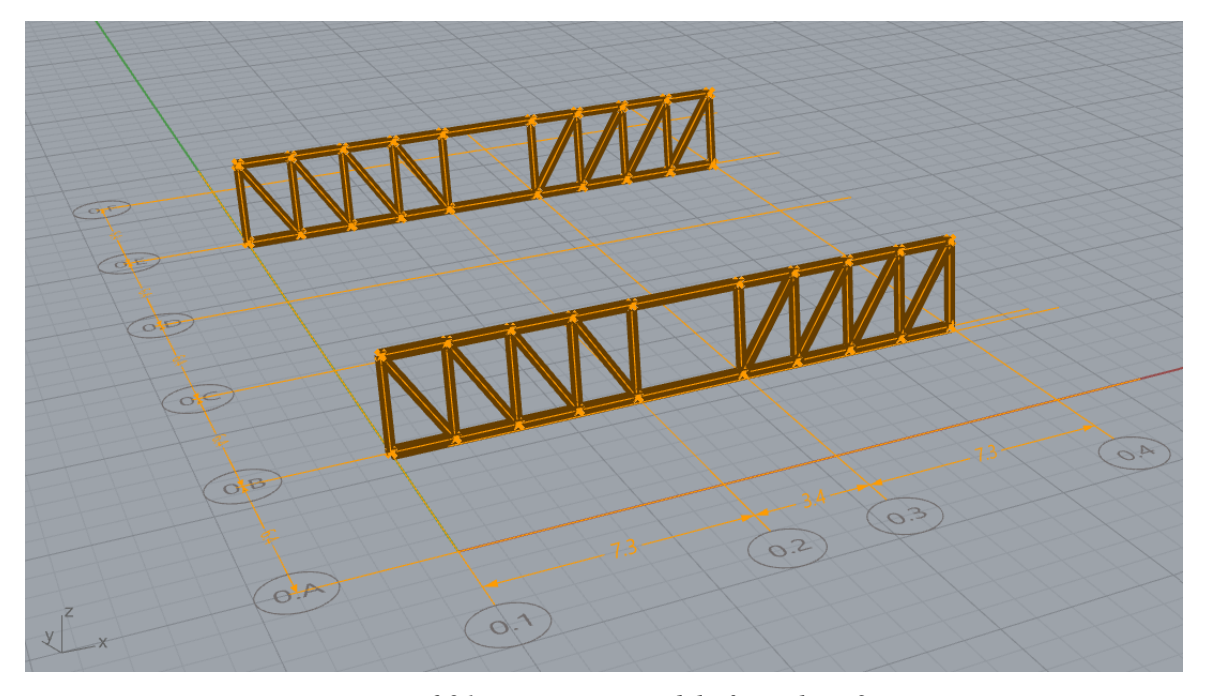


Figure 6.21: Parametric model of Topology 2

Loads are defined as per section 6.2 and it is the same as topology 1.

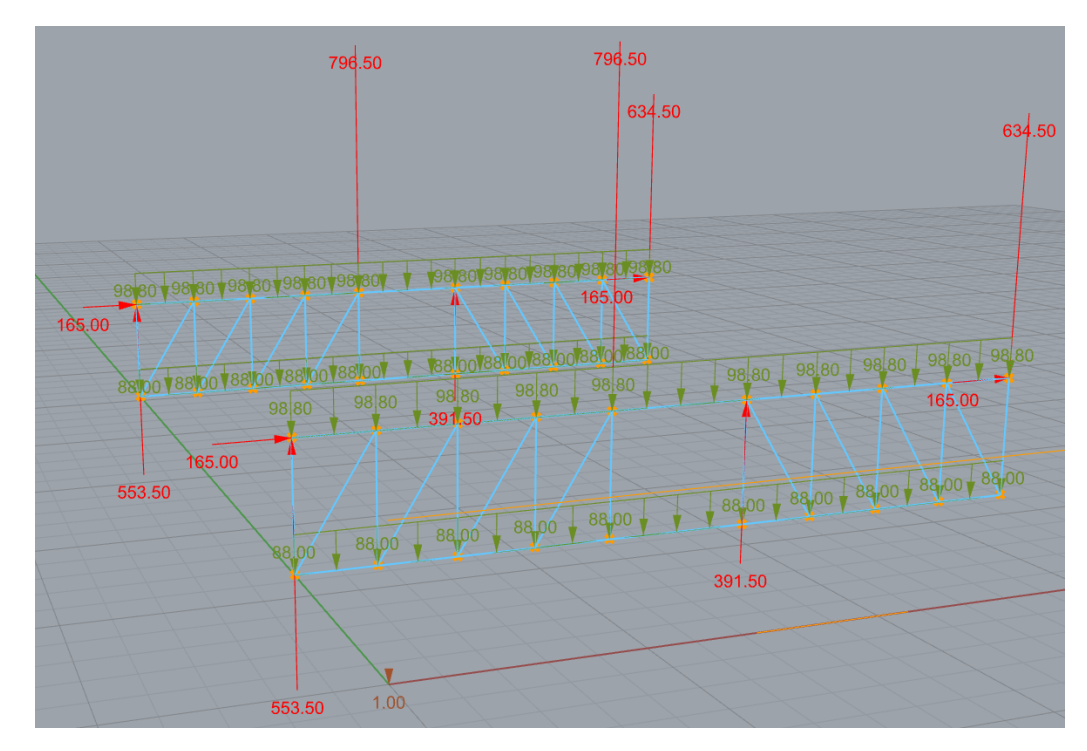


Figure 6.22: Loads- Model 2

### 6.4.4 Results

The resulting geometry and cross-section from Grasshopper is given in figure 6.23. There are only 4 distinct profiles as a result of the grouping of members.

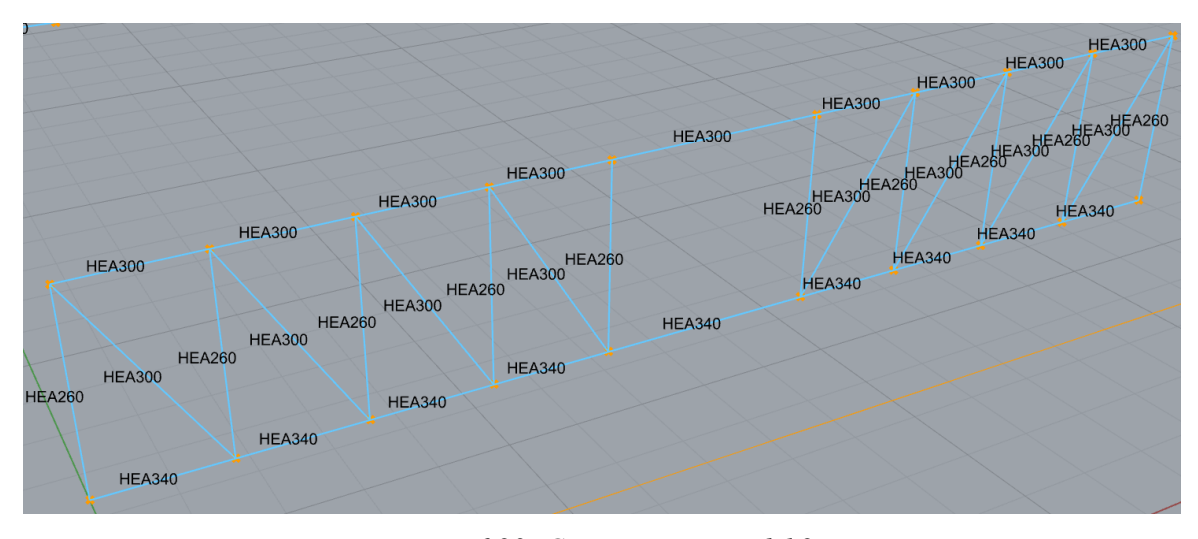


Figure 6.23: Cross section- Model 2

Name	¥	Material	¥	Shape	¥	A [m2]	¥	Wply [m3]	¥	Wplz [m3]	~
HEA240		S355		I rolled		0,0	08	0,0	01	0,0	000
HEA260		S355		I rolled		0,0	09	0,0	01	0,0	000
HEA300		S355		I rolled		0,0	11	0,0	01	0,0	001
HEA360		S355		I rolled		0,0	14	0,0	02	0,0	01,

Figure 6.24: Cross section- Model 2

Figure 6.25 and 6.26 show the shear force diagram and bending moment diagram respectively. The internal forces, moments and shear force values of each member are shown in Appendix G.

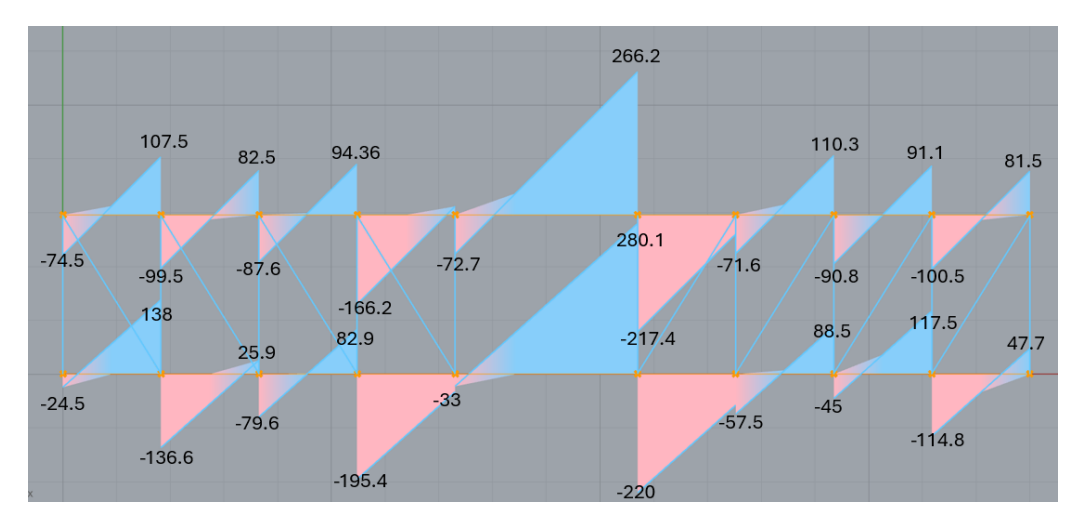


Figure 6.25: Shear force diagram (kN)

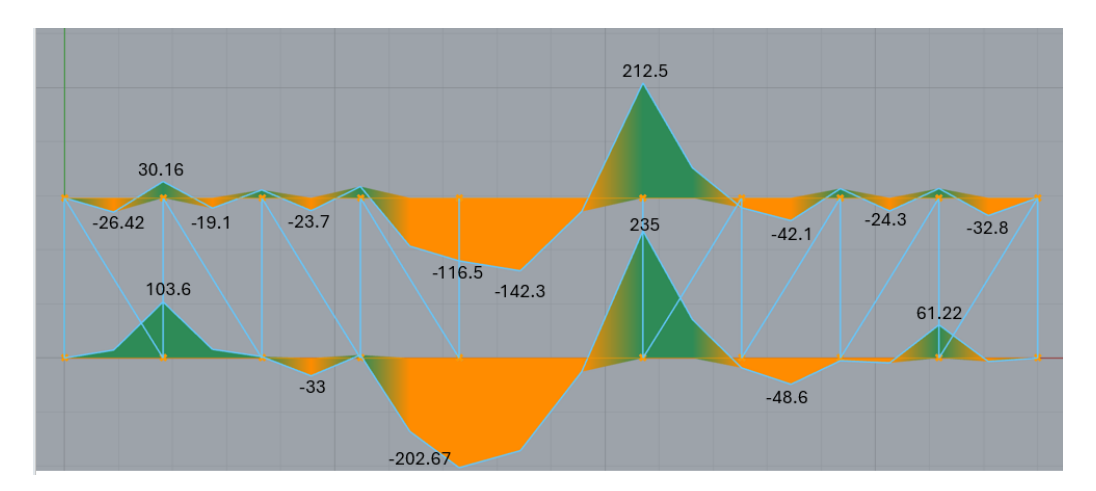


Figure 6.26: Moment diagram (kNm)

The maximum bending moments occur at the midspan of the bottom chord, which is typical for members subjected to UDL. Abrupt changes in the shear force diagram correspond to concentrated loads in the nodes in the middle, confirming the proper transfer of loads through the structure. Overall, the SFD and BMD validate the structural model and loading configuration, with all members responding as anticipated under the given loading scenario.

Figure 6.27 visualises the deformation of the truss under applied load. This matches the expectations based on the previously observed bending moment and shear force diagrams.

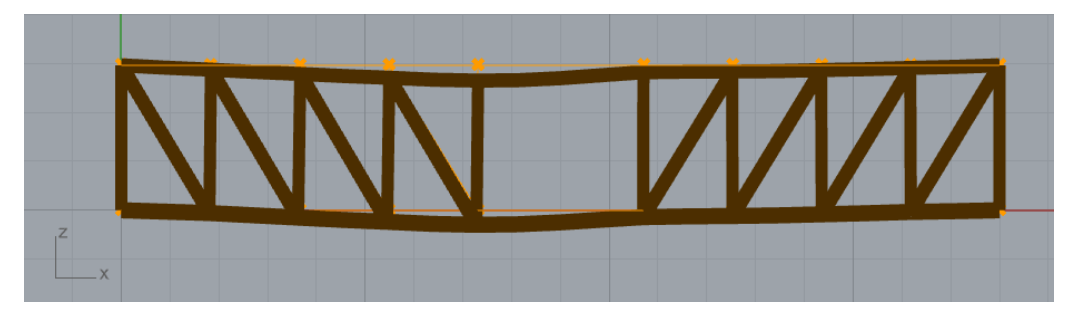


Figure 6.27: Deformation

Table 6.14 shows the maximum displacement of 2.98 cm, which is within acceptable serviceability limits for a span of 18 meters, confirming the adequacy of the structural design under the applied loads.

Result	Value
Mass of truss (kg)	15 900.8
Mass of beam (kg)	33444
Total weight of structural steel (kg)	49344.8
Maximum displacement (cm)	2.98
Maximum utilization	0.9

Table 6.14: Results 2

### 6.4.5 Truss topology 3

Truss topology 3 adopts a Warren truss configuration without verticals. This topology uses the minimum number of members. Under the applied load the topchord is in compression and bottom chord is in tension. Figure 6.28 illustrates the geometry of the warren truss with a 3.4 meter corridor in the middle.

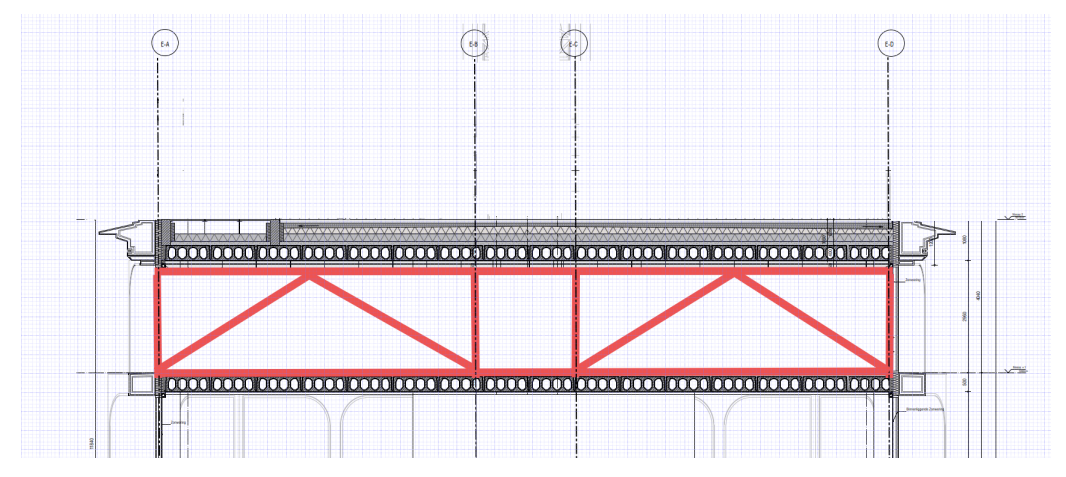


Figure 6.28: Truss topology 3

Figure 6.29 shows the parametric model of the simply supported truss in Grasshopper.

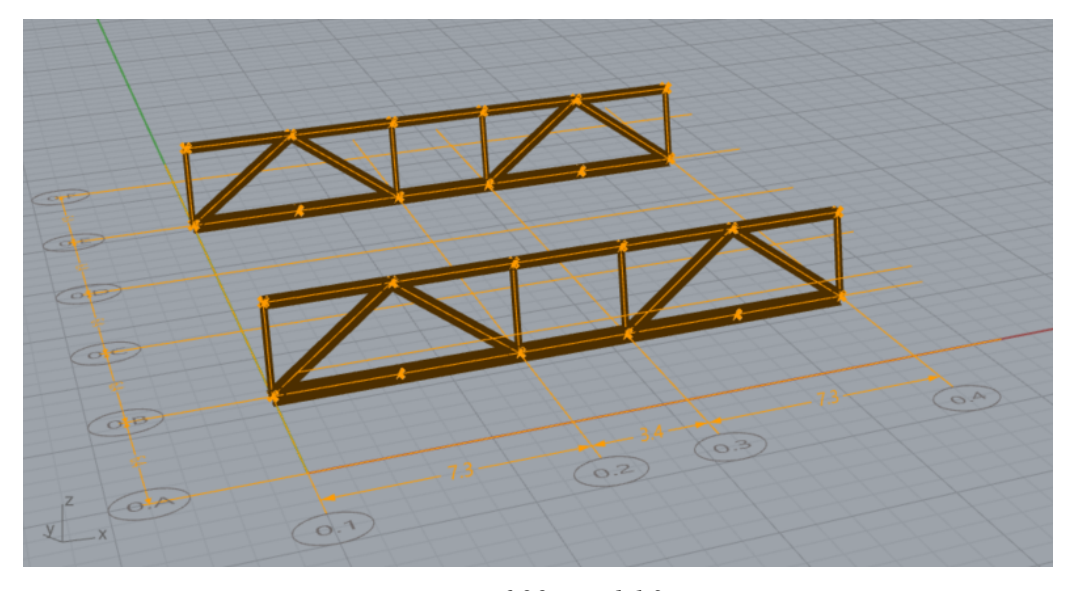


Figure 6.29: Model 3

Loads are defined as per section 6.2.

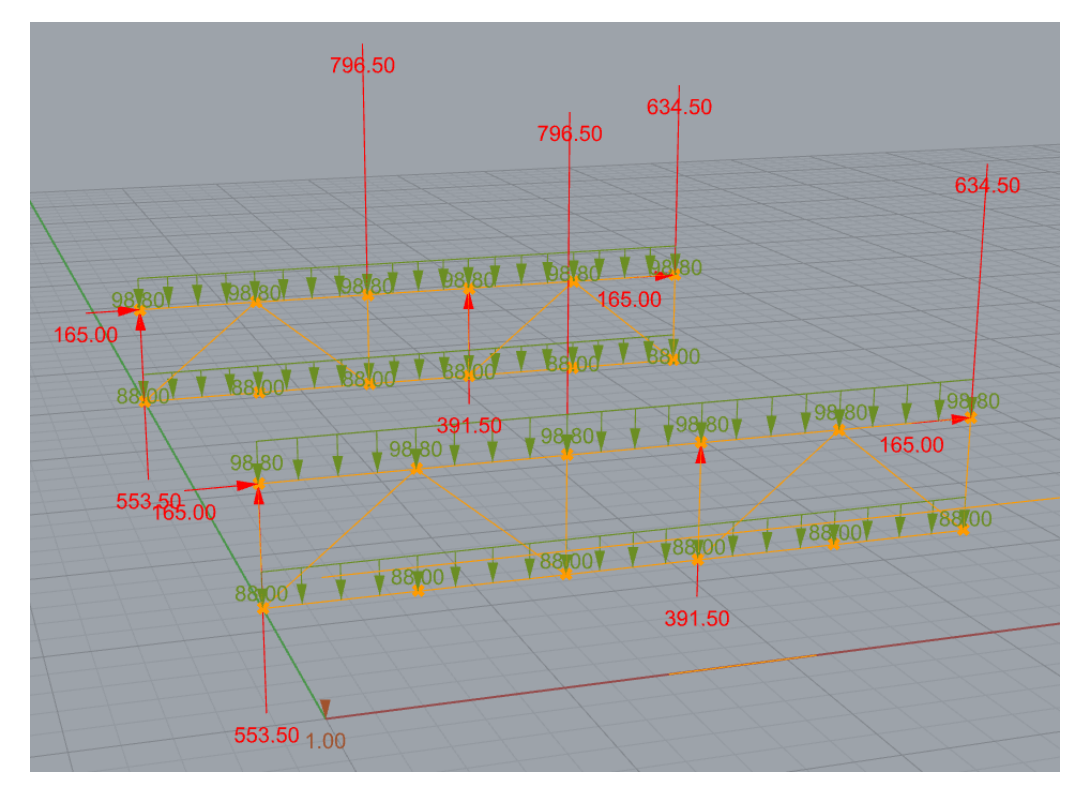


Figure 6.30: Loads- Model 3

### 6.4.6 Results

Members are grouped into 4 groups as mentioned earlier to limit number of different profiles. The profiles for each member obtained after cross-section optimisation is shown in figure 6.31

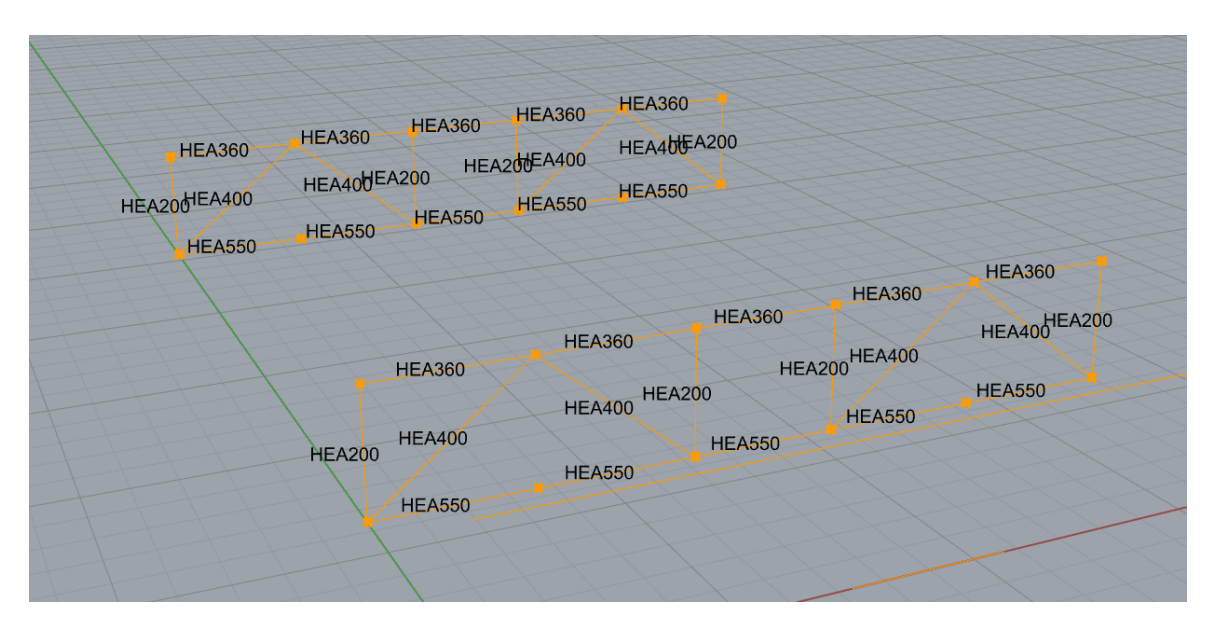


Figure 6.31: Cross section- Model 3

Name	<b>▼</b> Material	<b>▼</b> Shape	▼ A [m2] ▼	Wply [m3]	Wplz [m3]
HEA550	S355	I rolled	0,021	0,005	0,001
HEA400	S355	I rolled	0,016	0,003	0,001
HEA360	S355	I rolled	0,014	0,002	0,001
HEA200	S355	I rolled	0,005	0,000	0,000

Figure 6.32: Cross section- Model 3

Figure 6.33 and 6.34 shows the shear force diagram and bending moment diagram respectively. The internal forces, moments and shear force values of each member are shown in Appendix G.

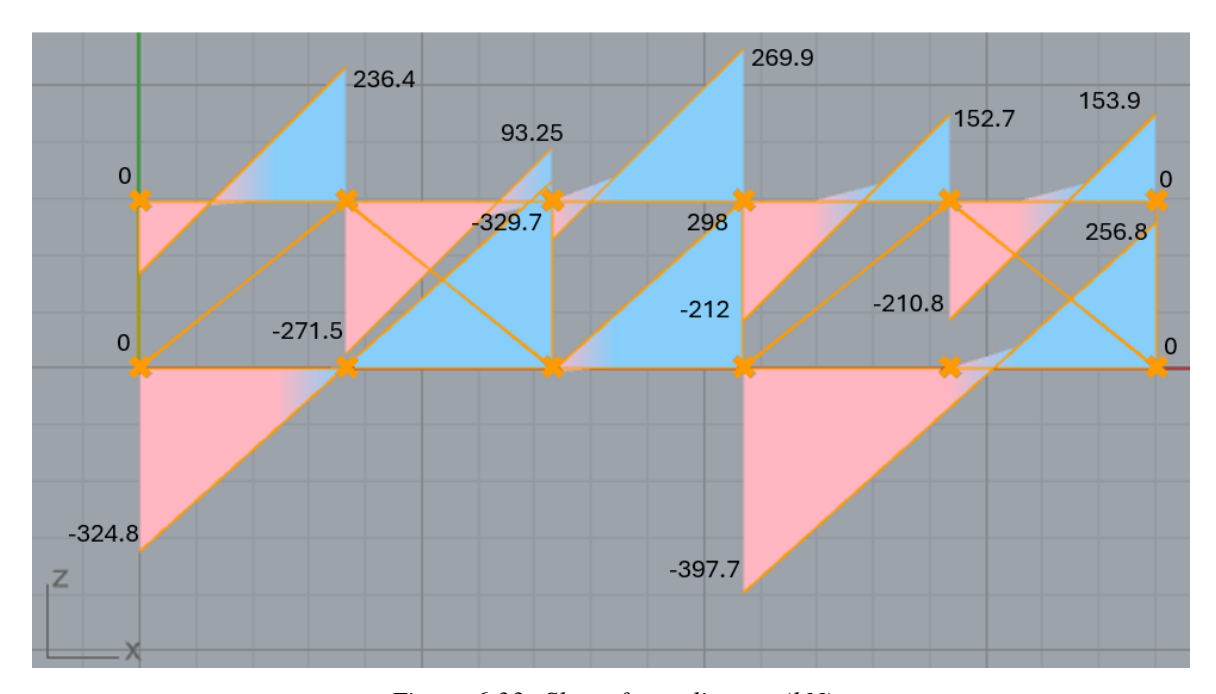


Figure 6.33: Shear force diagram(kN)

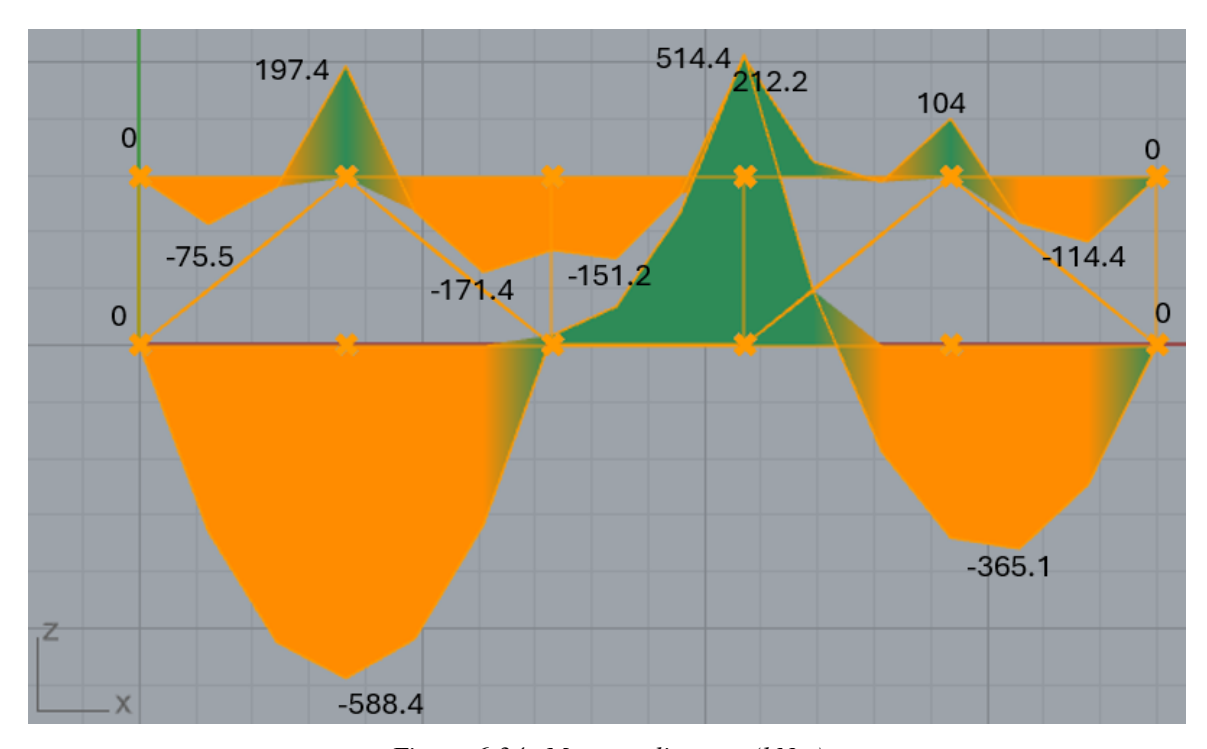


Figure 6.34: Moment diagram (kNm)

Figure 6.35 visualises the deformation of the truss under applied load. Maximum displacement is 2,5 cm and is within acceptable serviceability limits for a span of 18 meters, confirming the adequacy of the structural design under the applied loads.

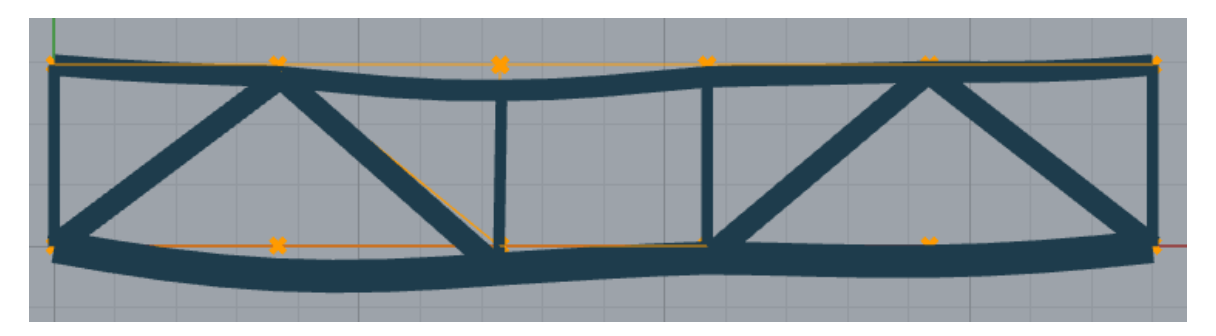


Figure 6.35: Deformation

Result	Value
Mass of truss (kg)	15714
Mass of beam(kg)	33444
Total weight of structural steel(kg)	49158
Maximum displacement (cm)	2.5
Maximum utilization	0.9

### 6.4.7 Truss topology 4

Topology 4 spans the longer building direction, reducing the number of required trusses but increasing individual span lengths. Figure 6.36 illustrates a typical Pratt truss topology. The truss is spanning 25.6 meters.

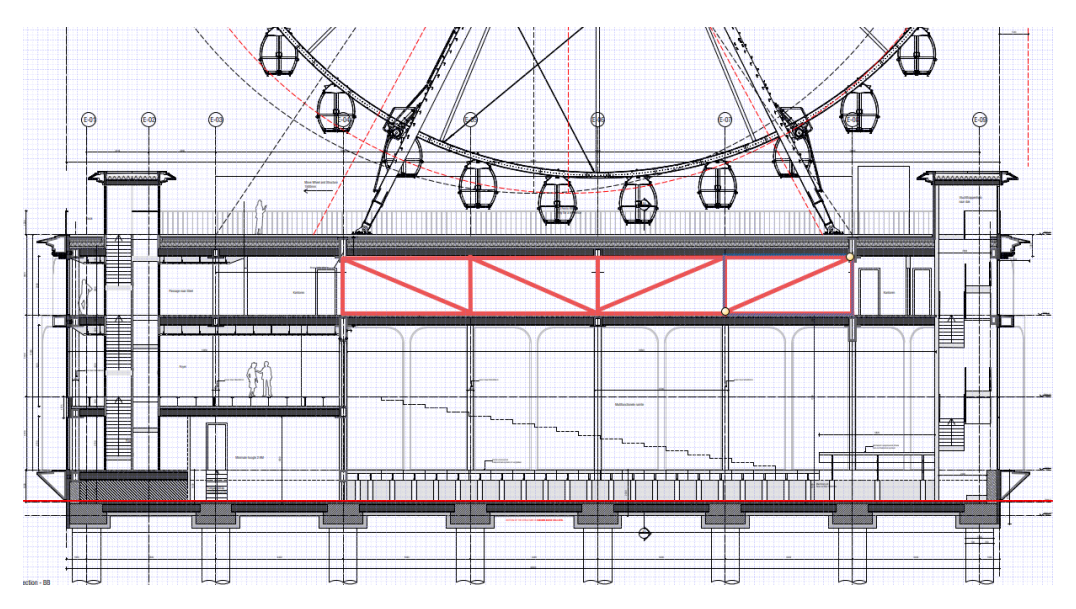


Figure 6.36: Truss Topology 4

Figure 6.37 shows the floor span of this option. The red line represent the truss and beams are represented in green lines. There is only 2 truss on either side of the corridor as the facade has beams and columns to take up the load. Having a truss in the facade obstructs view hence not preferred in this design. The direction of the hollowcore slabs are shown with the yellow arrow. Prefabricated HC slab for a span of 7.3 meter is available according to calculations using VBI tool. Design checks for the hollow core slab is given in the Appendix D.

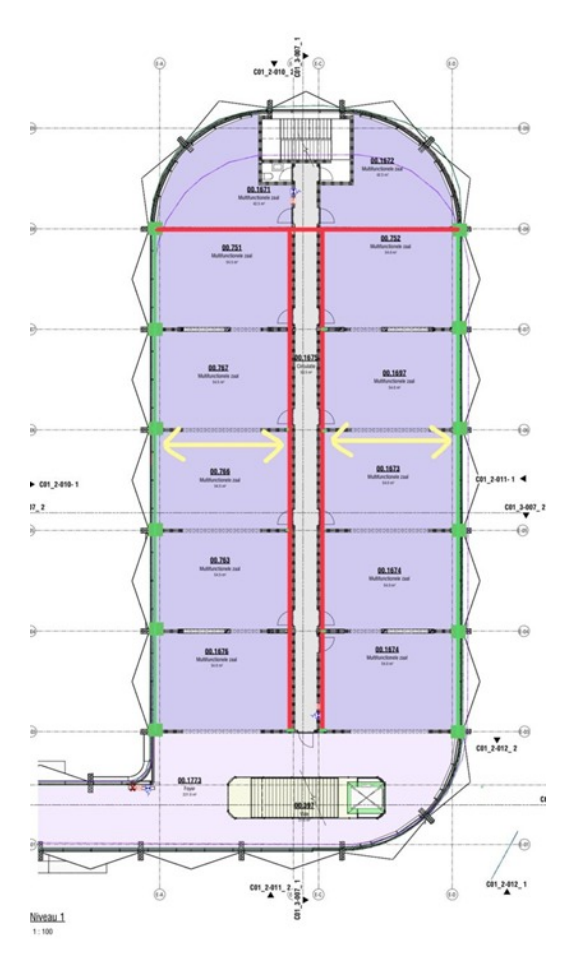


Figure 6.37: Topology 4

According to figure 6.37 a truss in lateral direction is also designed in Grasshopper and the self is added with the other trusses. Thus the truss layout is shown in figure 6.38.

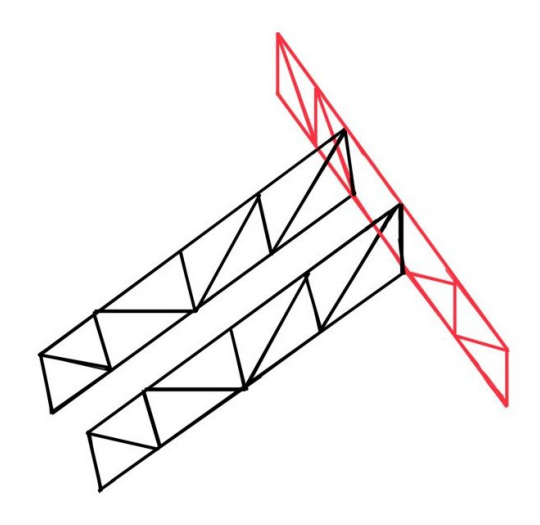


Figure 6.38: Option D

### 6.4.7.1 Beam design

Beams (Span = 6.40 m) were sized using of cross–section-optimisation study carried out in Grasshopper using the Karamba3D. The design input was a uniformly distributed load of  $q = 56.7 \text{ kN m}^{-1}$  (see Table 6.15).

<b>Support line</b>	<i>b</i> (m)	$1.35 G_k b \ (kN/m)$	$1.50 Q_k b \ (kN/m)$	$\mathbf{w}_{\mathrm{Ed}}$ (kN/m)
Beam	3.65	29.4	27.3	56.7

Table 6.15: Design line loads for beam

Karamba iteratively assessed the cross-section catalogue and identified IPE 330 (S355) as the lightest section that satisfies Eurocode requirements in bending, shear and deflection.

• Maximum bending moment (at mid-span):  $M_{\text{max}} = 284.3 \text{ kN m}$ 

• Maximum shear force (at supports):  $V_{\text{max}} = 181.5 \text{ kN}$ 

• Maximum deflection:  $\delta_{\text{max}} = 14.7 \text{ mm}$ 

• Self-weight per beam: m = 179 kg

All utilisation ratios returned by the Karamba cross-section optimisation component are below unity, confirming that the IPE 330 section meets the ultimate and serviceability limit-state criteria without further modification.

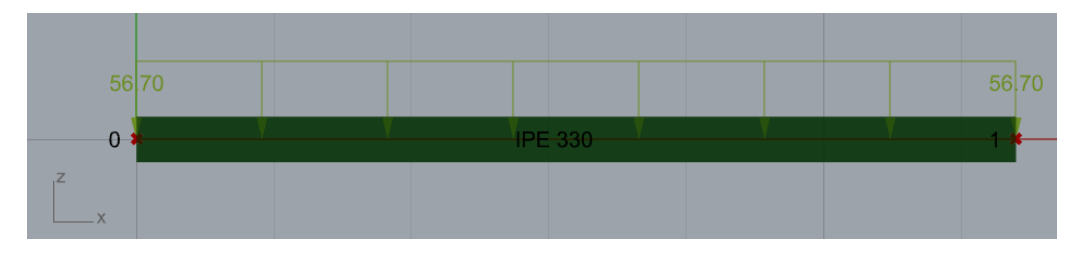


Figure 6.39: Grasshopper model of beam

#### **6.4.7.2** Loads on truss

The loads acting on the trusses are given in table below. For ULS, the governing load combination is determined by the following formula;

$$w_{Ed} = 1.35 G_k b + 1.50 Q_k b$$

<b>Support line</b>	<i>b</i> ( <b>m</b> )	$1.35G_k b \; (kN/m)$	$1.50  Q_k b   (kN/m)$	$w_{Ed}$ (kN/m)
Truss 1	5.35	43.1	40.13	83.3
Truss 2	5.35	43.1	40.13	83.3

*Table 6.16: Design line loads for top chord* 

Support line	b ( <b>m</b> )	$1.35G_k b \; (kN/m)$	$1.50  Q_k b   (kN/m)$	$w_{Ed}$ (kN/m)
Truss 1	5.35	33.45	40.13	73.5
Truss 2	5.35	33.45	40.13	73.5

Table 6.17: Design line loads for bottom chord

Along with the line loads, point loads from Ferris wheel is applied according to the table 6.4 and 6.5.

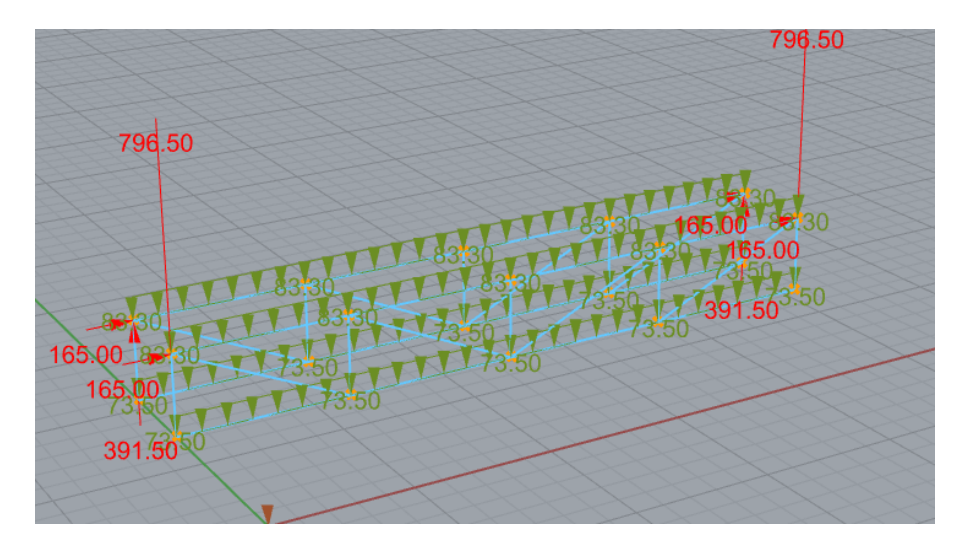


Figure 6.40: Loads- Model 4

Figure 6.41 shows the parametric model of the longer truss in Grasshopper and figure 6.42 shows the typical welded connection for this truss.

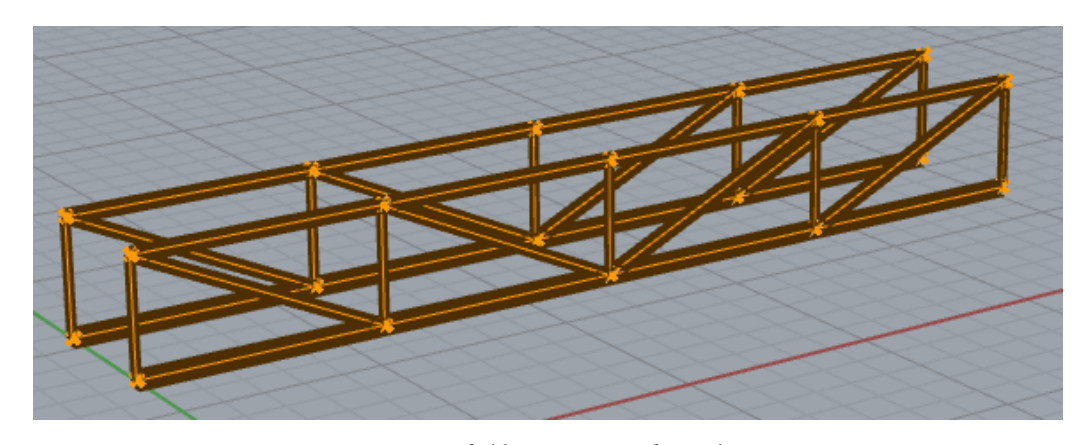


Figure 6.41: Truss topology 4

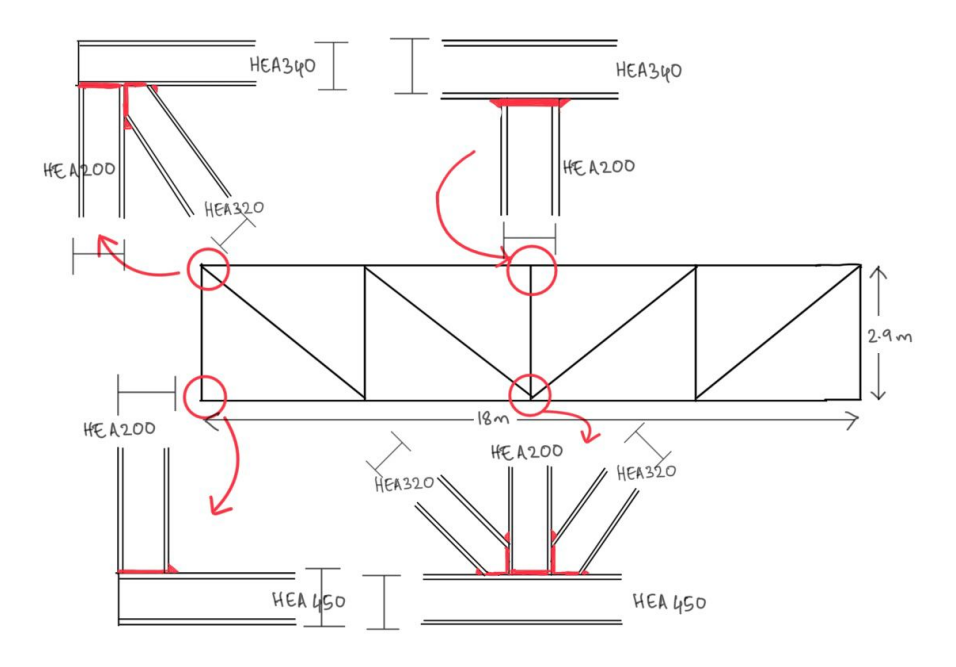


Figure 6.42: Typical welded connection

### 6.4.8 Results

The profiles for topchord, bottom chord, diagonals and verticals are given in table 6.44

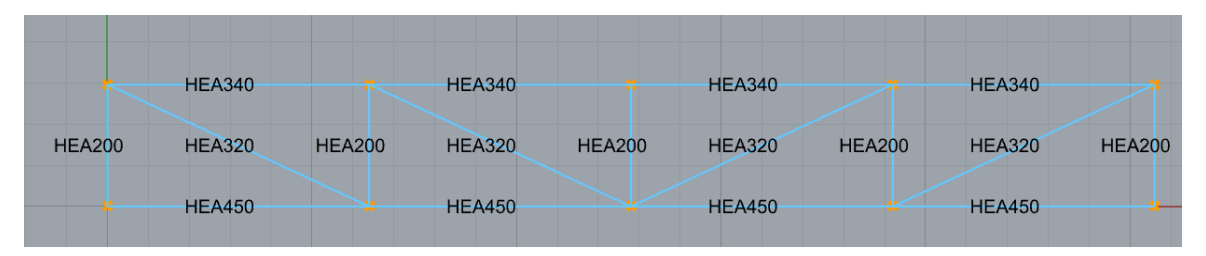


Figure 6.43: Cross section- Model 4

Name	▼ Material	<b>▼</b> Shape	🕶 A [m2] 💌	Wply [m3]	Wplz [m3]
HEA450	S355	I rolled	0,018	0,003	0,001
HEA200	S355	I rolled	0,005	0,000	0,000
HEA340	S355	I rolled	0,013	0,002	0,001
HEA320	S355	I rolled	0,012	0,002	0,001

Figure 6.44: Cross section- Model 4

Figure 6.45 and 6.46 show the shear force diagram and bending moment diagram, respectively.

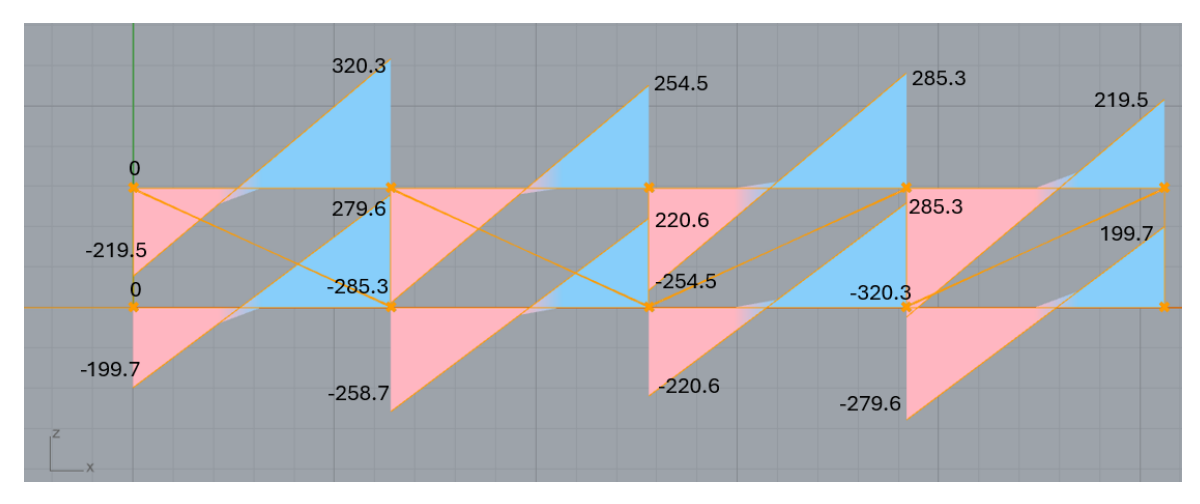


Figure 6.45: Shear force diagram (kN)

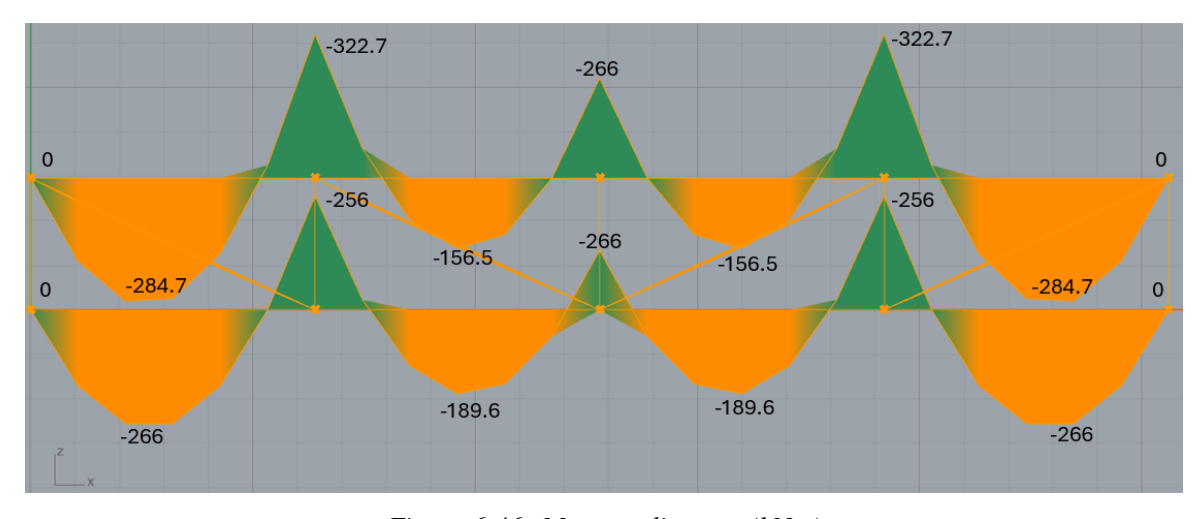


Figure 6.46: Moment diagram (kNm)

Figure 6.47 visualizes the deformation of the truss under load. Maximum displacement is 4.93 cm which is within acceptable serviceability limits for a span of 25.6 meters.

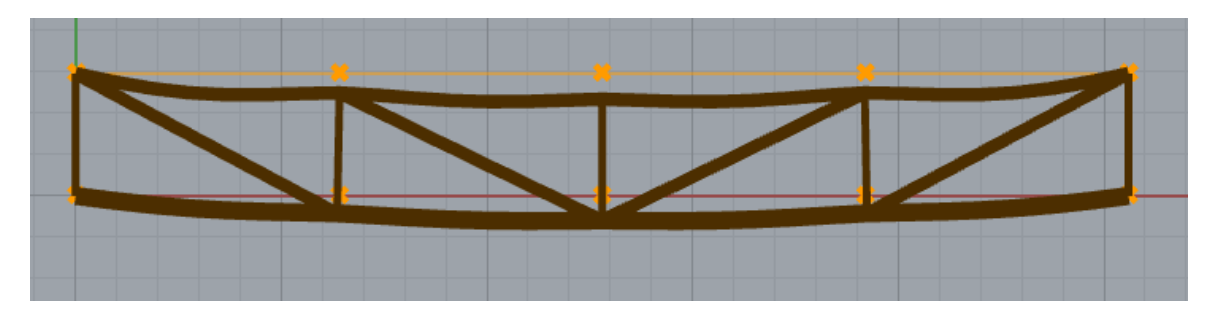


Figure 6.47: Deformation

Result	Value
Mass of trusses (kg)	30100.5
Total mass of beams (kg)	1790
Total weight of structural steel(kg)	31890.5
Maximum displacement (cm)	4.93
Maximum utilization	0.9

Using the same truss layout and topology, the members were redesigned with square hollow sections to compare self-weight. The results are summarized in Table 6.18.

Result	Value
Truss members (hollow sections)	32,455.25 kg
Beam IPE 330	1,790 kg
Total steel weight	34,245.25 kg

Table 6.18: Self-weight for hollow-section redesign

The total steel weight for the hollow-section option is higher than for the open-section scheme and the cost for hollow steel sections in euro/kg is almost twice as compared to open sections. Higher cost for hollow sections is due to extra processing steps, tighter tolerance and higher demand due to application not just in civil construction. Hence the open-section design is preferable for this layout.

### **6.5** Segmentation and Connection

In this section, the segmentation strategies discussed in chapter 4 is applied to The Pier. The truss for the Pier was designed to be divided into modular segments to facilitate transport and erection. At each segment interface, a bolted splice connection is introduced.

Model 1 is used as an example to discuss the segmentation plan and design the connections. Figure H.1 shows the numbers given to the members of model 1 in Grasshopper. Members 4, 5, 14 and 15 encloses the corridor and no diagonals are present in the corridor making it the ideal location to segment the truss. In this location, only two members needs to be spliced for each truss and internal forces are relatively low.

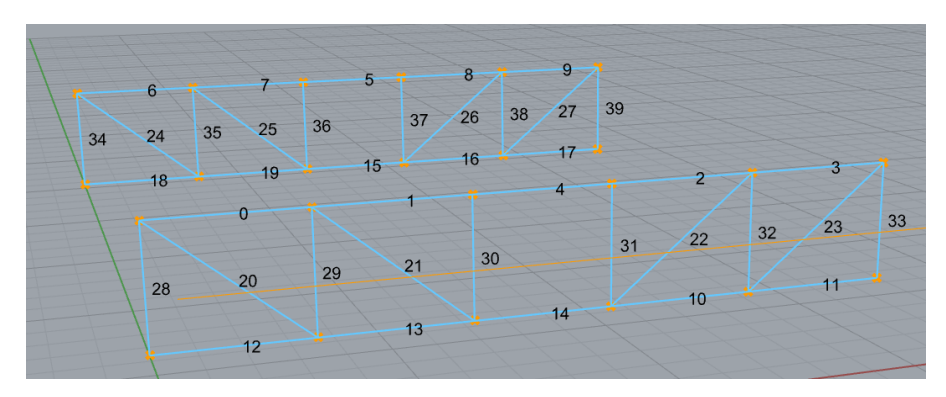


Figure 6.48: Member Numbers

Connections are modelled using the software IDEA StatiCa, which employs the Component-Based Finite Element Method (CBFEM) for the design of steel connections [40]. CBFEM builds on the component method outlined in Eurocode 3 for joint design, combining it with finite element analysis. In the component method, each part of the connection is modelled as a spring, and various design formulas are used to determine their individual stiffness. These stiffness values are then combined to calculate the overall stiffness of the joint [38]. CBFEM uses this approach to analyze the stress distribution in individual components, such as bolts and plates [40].

In this section, stiffness analysis is not done as the truss is assumed to be entirely pinned and the connection is designed for zero moment. Therefore component based design is not done; checks are done for strength only.

Table 6.19 shows the axial forces in members extracted from structural analysis using Karamba3D. The top chord is in compression and bottom chord in tension according to the table 6.19.

Members	N [kN]
Beam4	-415.1
Beam5	-415.2
Beam15	1648.5
Beam14	1648.6

Table 6.19: Axial forces in selected members

#### Connection for the top chord

The topchord in the corridor is in axial compression and to simplify the connection, the truss is segmented at the point of zero moment as shown in figure 6.49. Total length of the members 4 and 5 is 3.4 m. Point of zero moment is obtained at 2.4 from the left. Shear force and axial force at the point is used to design the connection. The cross section is HEA260 and material S355 is used.

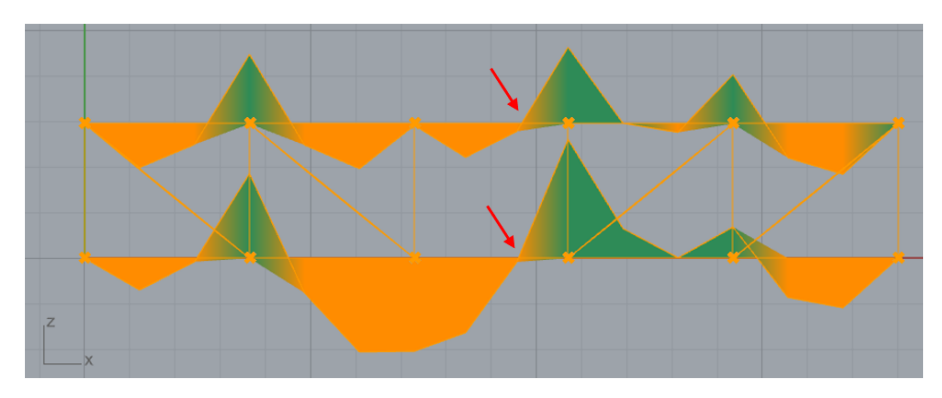


Figure 6.49: Segmentation point

Figure 6.50 shows for topchord 4 and 5 at the splice, a bolted flange plate connection is employed.

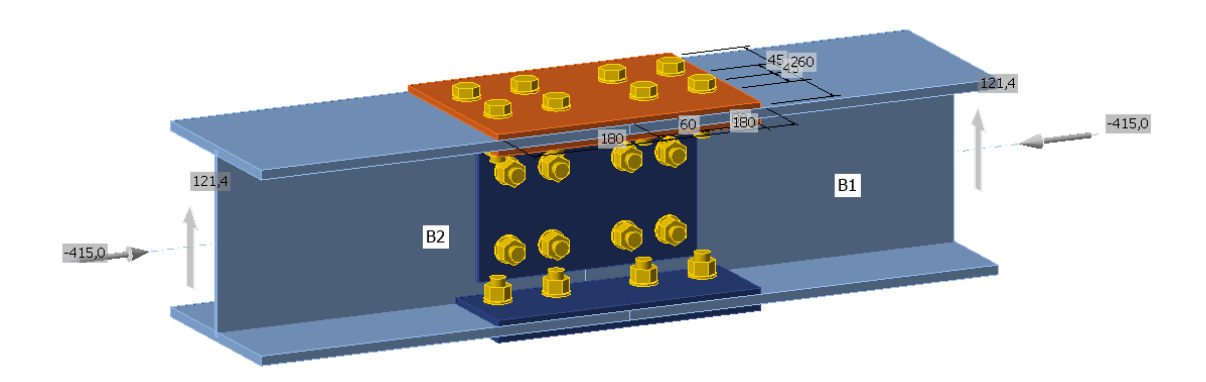


Figure 6.50: Splice connection for compression member

#### **Structrual Configuration**

- 8 x M20 8.8 bolts are used in the flanges and flange plates are 8 mm thick on top and bottom flange.
- Web plate is 6 mm think and 8 x M20 8.8 bolts are used in web.
- Bolt assembly consists of bolt, washer, and nut and is simulated by a nonlinear spring based on CBFEM method in IDEA StatiCa[40].

The section which is considered is for pure shear, and no bending moment. Theoretically, there is no need for flange plates, only web is sufficient for the most optimum connection. But in a real life case, there is chance that there could be a moment at this section, due to lateral load, accidental loads, etc. therefore, flange plates are given so that they takes moment also.

#### Result

Strength analysis, strain checks of plates, together with code checks of components are performed by elastic-plastic analysis. In this design the response of the joint to overall load is calculated. Design checks based on EN1993-1.8 for bolts such as bearing resistance check, utilisation in tension, utilisation in shear, tension resistance check, punching resistance check, shear resistance check were done by IDEA StatiCa and results and calculation is given in the appendix along with bearing and net section check for the plates.

#### Connection for the bottom chord

The bottom chord in the corridor is in axial tension and to simplify the connection, the truss is segmented at the point of zero moment as shown in figure 6.49 similar to top chord. The cross section is HEA360 and material S355 is used.

Figure 6.51 shows the connection designed for the bottomchord member 14 and 15.

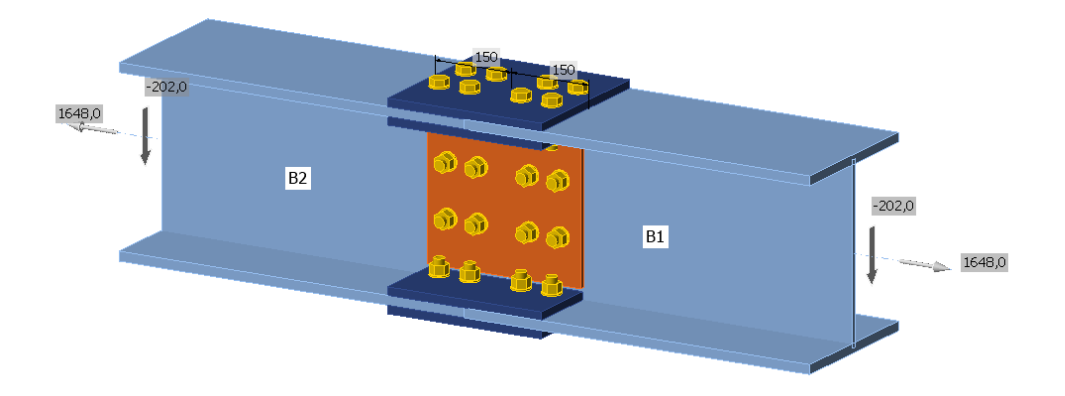


Figure 6.51: Splice connection for tension member

### **Structrual Configuration**

- 8 x M20 8.8 bolts are used in the flanges and flange plates are 15 mm thick on top and bottom flange.
- Web plate is 10 mm think and 6 x M20 8.8 bolts are used in web.
- Bolt assembly consists of bolt, washer, and nut and is simulated by a nonlinear spring based on CBFEM method in IDEA StatiCa[40].

#### Result

In this design, the response of the joint to overall load is calculated. Design checks based on EN1993-1.8 for bolts such as bearing resistance check, utilisation in tension, utilisation in shear, tension resistance check, punching resistance check, shear resistance check are done by given in the appendix along with bearing and net section check for the plates.

## Chapter 7

## **Findings**

## 7.1 Optimisation workflow

The optimisation workflow was first tested on two problems: a 5 m simply-supported beam and a 50 meter Warren truss by running each model in Karamba3D, RFEM and manual Eurocode checks. In both cases, the key response metrics (mass, stresses, deflection) differed by less than 1% and, for the truss, the difference in mass was only 0.3% while maximal deflection differed by 0.02 cm, which is inside allowable tolerances. The same Warren truss was then subjected to optimisaiton based on genetic algorithm in Galapagos in which the height and width ratios acted as genomes to minimise the weight of the truss. In addition to that, OptiCroSec (OCS) re-sized members in every fitness evaluation; the algorithm converged to a minimum weight of 16842.7 kg, confirming that the nested GA + OCS loop works.

For the Pier case study that follows, the geometric ratios are fixed by architectural constraints as established in Chapter 6, so only the OCS optimiser is required. The earlier GA exercise therefore, serves a different purpose: it identified that height and panel count changes influence the performance and weight of the truss.

These validation exercises done in chapter 3 demonstrate that the Grasshopper  $\rightarrow$  Karamba3D  $\rightarrow$  OCS chain produces results that are code compliant, giving confidence in all subsequent analyses for the Pier redevelopment.

### 7.2 Pier truss design

By applying the methodology mentioned in chapter 3 with the height and width ratio fixed for The Pier, weight of steel trusses were produced. Along with this beams were designed for each out option so that the total structural steel weight can be calculated as shwon in the table 7.1.

Option	Mass [kg]
A	45395.4
В	49344.8
С	49158
D	31890.5

Table 7.1: Weight comparison

Option D, is the lightest truss according to the results from Grasshopper (Karamba3D).

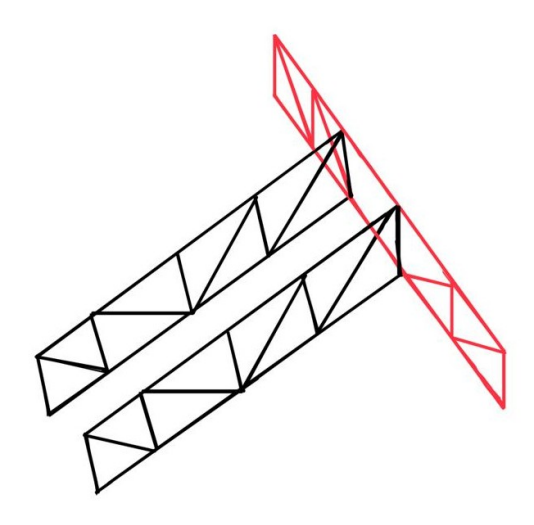


Figure 7.1: Option D -lightest design

#### **Embodied carbon calculation**

Embodied carbon refers to the total greenhouse gas emissions (expressed in CO<sub>2</sub>-equivalents) associated with the production, processing, transport, and assembly of construction materials before the building or infrastructure is in use. In this study, the embodied carbon of steel truss options is assessed by calculating the Global Warming Potential (GWP) from cradle-to-gate, i.e., covering production stages A1-A3 as defined by EN 15804.

The calculation uses emission factors from the Dutch National Environmental Database (NMD), specifically for hot-rolled structural steel profiles (e.g., HEA sections in S355 grade). For each truss option, the total mass of steel is determined using parametric modeling in Grasshopper. The embodied carbon (GWP) is then calculated by multiplying the total steel mass by the emission factor:

GWP = Mass of steel [kg] × Emission factor [kg 
$$CO_2$$
-eq/kg]

The table 7.2 allow a direct comparison between different design alternatives based on their environmental impact.

$$M_{\text{steel}} = 25\,106.5\,\text{kg}$$
 (7.1)

$$EF_{\text{NMD}} = 1.51 \,\text{kg CO}_2 - \text{eq/kg} \tag{7.2}$$

$$GWP = M_{\text{steel}} \times EF_{\text{NMD}} \tag{7.3}$$

= 
$$25\,106.5\,\mathrm{kg} \times 1.51\,\mathrm{kg}\,\mathrm{CO}_2$$
-eq/kg (7.4)

$$= 37911 \,\mathrm{kg} \,\mathrm{CO}_2 - \mathrm{eq}$$
 (7.5)

Option	Mass [kg]	EF [kg CO <sub>2</sub> -eq/kg]	GWP [kg $CO_2$ -eq]
A	45395.4	1.51	68546.5
В	49344.8	1.51	74510.6
С	49158	1.51	74228.5
D	31890.5	1.51	48154.6

Table 7.2: Embodied carbon results per design option (Dutch NMD factors).

Because a single cradle-to-gate factor was applied to all sections, any kilogram saved translates dir-

ectly into 1.5 kg CO-eq. Weight optimisation is therefore an effective proxy for carbon reduction in this study. Comparing the two extreme options, Option D and Option B, the former is not only the lightest but also the lowest-carbon alternative. Choosing Option B would be almost double the amount of steel and CO-eq with no compensating functional benefit; the excess stems mainly from the box beams that were needed to control deflection on the 18 meter span.

### 7.3 Segmentation strategies for large span

The findings from chapter 4 are used to segment the truss in the pier and design an example connection. Steel trusses often exceed standard transport dimensions and crane capacities. In the Netherlands, road transport generally permits a maximum of , 23 m in length, 2 m in width and 3.5 m in height under standard permit conditions. Site cranes typically have a 25-ton lifting limit. These constraints are the number, size, and location of truss segments. The ambition to make steel structures reusable adds another layer of importance to segmentation. Splices must be demountable and be reversible, favouring bolted rather than welded joints. So segmentation must be considered early in the design process, and not as an afterthought.

Two primary segmentation approaches are discussed: Member-Level Segmentation and Node-Level Segmentation. Member-level segmentation is only viable when cuts avoid peak force zones. For nodal level segmentation, all members remain intact from node to node with their full section capacity, but it concentrates multiple member forces into one joint region, which must be designed to transfer all those forces between modules. This could result in a more complex or expensive connection. These two options are used in different project based on the engineer's and contractor's discretion and there is no definite right or wrong way. In the four case studies discussed in chapter 4, different approaches are used. In Omnisport Apeldoorn, segmentation was required to meet truck length and height limits. The solution was to segment near nodes, not mid-member, to limit cantilever deflection and simplify transport. For Adam Tower Crown, the assembly of the segments on the site at 74 m height was the difficult part. Splices were positioned where chord forces were lowest to simplify the assembly. The 29 m Viereendel truss on two sides were built as continuous modules and two sides were segmented into smaller bolted units. Here, logistics at height dictated segment size. In the case study X, the length and width of the truss made it difficult to transport it on road and hence cutting the truss vertically and horizontally was discussed. Case study Y involved a hot dipped galvanised truss and the size of the galvanising tub and truck dimensions were the major concerns in this case. Special member level segmentation with double columns was discussed to be implemented by taking the temperature effects in galvanised truss into consideration.

In Section 6.5, segmentation was applied to an 18 m truss design for Island 3 of The Pier. The truss was split in the corridor zone, where only two chords needed to be cut both at points of zero moment, which reduces joint complexity.

Optimal segmentation balances internal force flow, transportation logistics, fabrication method, site assembly, client demands and disassembly goals and is most often than not tailored to specific project demands.

### 7.4 Cost optimisation

Cost optimisation was included in the methodology to see the tradeoff cost of material and connection and fabrication has with weight of the structure. Through expert interviews, it could be found out that the weight of the profiles is the main cost driver and practically a fraction of that cost is calculated as cost of connection and fabrication. The detail calculation about the cost of connection and fabrication

was not obtained during study.

### 7.5 Limitations

- 1. The "OptiCrosec" component in Karamba3D can only select from the discrete list of commercially available profiles provided by the user. As a consequence, any cross-section outside that catalogue remains unexplored.
- 2. At each iteration every member is resized independently to the first section in its family that satisfies the target utilisation. Although this heuristic converges rapidly, it favours local rather than global improvements and may overlook lighter configurations that require a temporary increase in utilisation elsewhere. That means the routine halts once two consecutive analyses return identical sections. It never revisits earlier decisions or explores alternative sizing paths, so the final solution is near-optimal but not provably the minimum-mass arrangement.
- 3. OptiCroSec minimises weight subject to strength constraints only. Other pertinent objectives like cost, embodied carbon, and fabrication complexity are excluded and may yield different "best" solutions.
- 4. Limited data obtained on cost estimates of different type of connections, fabrication process and handling, forced to conclude the result based on the weight of the structure only. A detailed study might result in a different solution.

## **Chapter 8**

## **Conclusion and Recommendations**

### 8.1 Conclusion

This thesis developed and validated a parametric workflow to optimise truss for The Pier Redevelopment in Scheveningen and was structured around three main objectives, each addressed through a combination of parametric modeling, case study analysis, and expert interviews. The first objective:

# Determine a material-efficient design for a large-span steel truss for The Pier Redevelopment project.

This question is answered by generating a parametric model in Grasshopper (Karamba3D) and optimising cross-section to get a lightweight design. Among the four architecturally feasible layouts studied, Option D: trusses spanning the long direction with short 6.4 m secondary beams, proved the most efficient. The final design requires 31 t of structural steel and 48 t CO2-eq cradle-to-gate (A1–A3). Compared to the heaviest alternative, Option B at 49.34 t, this represents a material saving of 18.35 t (37 %) and a GWP reduction of 26.5 t CO2-eq (36 %). Even relative to the next lightest alternative, Option A at 45.40 t, the saving is 14.4 t steel (32%). These results confirm that rethinking the truss span direction and beam arrangement at the concept stage can deliver substantial, measurable reductions in both material use and embodied carbon.

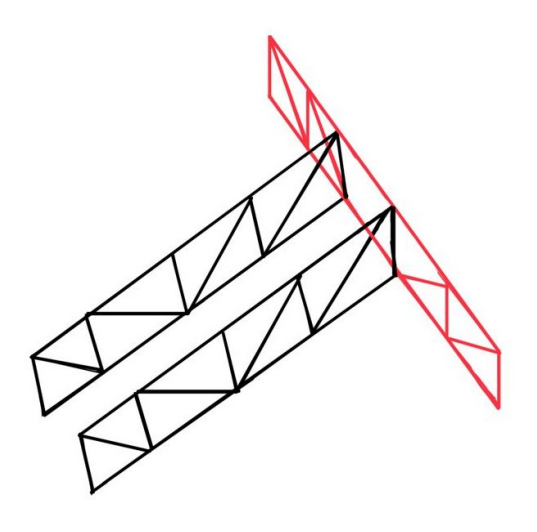


Figure 8.1: Final Truss Design

The primary reason for Option D's advantage is the efficiency of its beam system. Short 6.4 m interior beams can be sized to IPE 330 sections with a self-weight of 179 kg each, giving only 1.79 t total beam mass. In contrast, Options A–C use 18 m interior beams that require heavy box sections

to satisfy serviceability limits, pushing beam mass to 33.44 t. Although the long-span trusses in Option D are heavier (30.10 t) than those in short-span layouts, the 31.6 t reduction in beam mass more than compensates, resulting in the lowest overall weight. The validation of the Grasshopper  $\rightarrow$  Karamba3D  $\rightarrow$  OptiCroSec workflow helped ensure that the weight and GWP differences reported here result from actual design changes rather than inaccuracies in the analysis, as it showed less than 1 % difference from RFEM and hand calculations.

To apply the knowledge gained from the segmentation study conducted using four different case studies, truss option A was selected. Segmenting the truss into two pieces was the best strategy identified for option A and therefore, segmentation was applied in the corridor span, where two splices were placed in shear-dominant, zero-moment zones because force aligned segmentation improves constructability and reduces joint complexity, with minimal excess material. Connection design and verification for this were done using IDEA StatiCa.

The second objective:

# How can segmentation strategies and connection methods for steel trusses balance constructability, transportation, and sustainability requirements?

This was answered through detailed case studies of projects done by Haskoning and interviews with their structural engineers involved in these projects. The case studies demonstrated that segmentation is most effective when treated as an integral part of the design process rather than an afterthought. Two main strategies emerged, each suited to different constraints: member-level splices placed in low-force or zero-moment regions, which simplify detailing and support disassembly, and node-level segmentation, which avoids cutting members but concentrates forces into larger joints and is useful when transport size or lifting capacity is the dominant limit. Across projects at Haskoning, designs placed splices in shear-dominant, low-moment zones away from peak axial forces, kept the number of field joints to a minimum, and located them where access for assembly is good.

Practical constraints such as the Dutch transport limit of approximately  $23 \text{ m} \times 2 \text{ m} \times 3.5 \text{ m}$ , typical crane capacities of 25 t, and galvanizing bath limits were shown to directly influence segment size and splice placement. The case studies also reinforced the benefits of standardising plate thicknesses and bolt sizes to simplify procurement, assembly, and potential future disassembly. Minimising joint numbers was consistently associated with lower risk, faster erection, and fewer tolerance issues, while still meeting logistical and safety requirements.

The third objective:

# To integrate direct cost modelling into parametric truss design for improved decision-making on trade-offs between weight and total cost.

Expert interviews confirmed that material weight is the dominant driver of total cost for steel trusses at concept stage, meaning that changes in weight can be used as a good early indicator of cost changes. Industry data indicates that fabrication and connections typically add only a small percentage to material cost, while material grade and profile choices can cause differences in unit prices. While reducing weight usually lowers total cost, this is not always the case. If the lighter design requires many more joints or involves complex fabrication, the extra labour and materials for connections can offset the savings, making it important to track joint numbers and detailing as well as weight. This study focused on direct costs and excluded indirect costs, which are relatively insensitive to geometry at this stage. Due to limited detailed data on fabrication and joint costs, conclusions were primarily weight-based, and future work should quantify process-level costs and enable multi-objective optimisation for weight and cost.

### 8.2 Recommendations

#### **Recommendations for further research:**

- 1. In cost optimisation of a structure, quantify costs for fabrication steps (sawing, drilling, welding, blasting, coating etc) to provide a more accurate total cost estimation beyond weight based estimates.
- 2. Automate joint checks with the Rhino/Grasshopper plug-in for IDEA StatiCa so that GH script can also generate connection geometry, run bulk calculations and pull stiffness or utilisation results back into the optimisation loop without manual export-import cycles. The plug-in is still a preview tool and IDEA warns that version-to-version compatibility is not guaranteed [41].
- 3. Adopt multi-objective optimisation that evaluates weight and cost and produce a Pareto front to evaluate the tradeoffs.

### Recommendations for case study: The Pier

- 1. Extend optimisation loop to more load cases from Eurocode, such as wind actions, accidental actions, and dynamic service loads. Verify governing combinations using EN 1990 Annex A1 [39].
- 2. Integrate durability, corrosion, ease of disassembly, component re-use and recyclability in the design. Designing for a second life rather than end-of-life recycling will align the truss with circular-economy standards.
- 3. Evaluate erection strategy such as lifting sequence, crane selection, temporary works and on-site cycle time as these logistics factors will reveal module sizes and splice locations that minimise construction risk, programme duration and embodied carbon from site activities.
- 4. Model hot-finished CHS, SHS and RHS hollow structural sections, applying EN 1993-1-1 section-class checks and ISO 14346 fatigue limits while verifying joints in IDEA StatiCa so weld-access solutions are tested, thereby demonstrating whether hollow sections deliver their torsional and buckling advantages without compromising constructability.

## **Bibliography**

- [1] Designing Buildings Wiki. *Parametricism*. 2021. URL: www.designingbuildings.co. uk.
- [2] Grasshopper3D Community-Scott Davidson. *Grasshopper, Algorthmic modelling for Rhino*. 2025. URL: www.grasshopper3d.com.
- [3] RE:BORN Real Estate. *The Pier.* 2024. URL: https://re-born.com/en/projecten/the-pier/(visited on 26/05/2025).
- [4] Wikipedia contributors. *Scheveningse pier*. Dutch Wikipedia. 2025. URL: https://nl.wikipedia.org/wiki/Scheveningse\_pier (visited on 26/05/2025).
- [5] European Committee for Standardization (CEN). EN 15804:2012+A2:2019 Sustainability of construction works Environmental product declarations Core rules for the product category of construction products. European Standard. Brussels, Belgium: European Committee for Standardization, 2019.
- [6] Weiwei Lin and Teruhiko Yoda. 'Truss Bridges'. In: *Bridge Engineering*. Elsevier, 2017, pp. 137–153. DOI: 10.1016/b978-0-12-804432-2.00008-6.
- [7] Post Graduate Student and S. G. Balekundri Institute Of Technology Associate Professors. 'Geometry shape and section optimization of steel trusses'. In: *International Research Journal of Modernization in Engineering Technology and Science (IRJMETS)* 04.08 (2022), pp. 903–908. DOI: e-ISSN:2582-5208.
- [8] Laurin ernst. 11 Type of Trusses. Nov. 2023. URL: www.structuralbasics.com.
- [9] Raffaele Cucuzza. 'Constructability-based design approach for steel structures: From truss beams to real-world inspired industrial buildings'. In: *Automation in Construction* 166 (2024), p. 105630. ISSN: 0926-5805. DOI: https://doi.org/10.1016/j.autcon.2024. 105630. URL: https://www.sciencedirect.com/science/article/pii/S0926580524003662.
- [10] C. Pasquire and A. Gibb. 'Considerations for Assessing the Benefits of Standardisation and Pre-Assembly in Construction (The Findings of a Pilot Study)'. In: CIBSE Seminar on Standardisation in the Design and Construction of Building Services Installations. Vol. 26. Report presentation. Chartered Institution of Building Services Engineers (CIBSE). 1999.
- [11] F. W. Wong et al. 'A Study of Measures to Improve Constructability'. In: *International Journal of Quality & Reliability Management* 24.6 (2007), pp. 586–601. DOI: 10.1108/02656710710757781
- [12] F. W. Wong et al. 'Factors Affecting Buildability of Building Designs'. In: *Canadian Journal of Civil Engineering* 33.7 (2006), pp. 795–806. DOI: 10.1139/L06-022. URL: https://doi.org/10.1139/L06-022.
- [13] J. P. G. Carvalho et al. 'Multi-objective Structural Optimization for the Automatic Member Grouping of Truss Structures Using Evolutionary Algorithms'. In: *Computers & Structures* 292 (2024), p. 107230. DOI: 10.1016/j.compstruc.2023.107230. URL: https://doi.org/10.1016/j.compstruc.2023.107230.

- [14] R. Walls and A. Elvin. 'An Algorithm for Grouping Members in a Structure'. In: *Engineering Structures* 32.6 (2010), pp. 1760–1768. DOI: 10.1016/j.engstruct.2010.02.027. URL: https://doi.org/10.1016/j.engstruct.2010.02.027.
- [15] Tomas R. van Woudenberg and Frans P. van der Meer. 'A grouping method for optimization of steel skeletal structures by applying a combinatorial search algorithm based on a fully stressed design'. In: *Engineering Structures* 249 (2021), p. 113299. ISSN: 0141-0296. DOI: https://doi.org/10.1016/j.engstruct.2021.113299.
- [16] Jamie Yeung et al. 'Understanding the total life cycle cost implications of reusing structural steel'. In: *Environment Systems and Decisions* 37.1 (2016), pp. 1–20. DOI: 10.1007/s10669-016-9621-6.
- [17] Trayana Tankova. Lecture 2.5.3 Design and Analysis of Simple Joints. Online course material. Lecture notes, CIEM5000 Structural Engineering Base Module, TU Delft. 2025. URL: https://brightspace.tudelft.nl (visited on 29/05/2025).
- [18] G. M. Gasii. 'Structural and Design Specifics of Space Grid Systems'. In: *Poltava National Technical Yuri Kondratyuk University* 16.6 (2017), pp. 475–484. DOI: 10.21122/2227-1031-2017-16-6-475-484. URL: https://doi.org/10.21122/2227-1031-2017-16-6-475-484.
- [19] João Marcos P. Vieira et al. 'Many-Objective Truss Structural Optimization Considering Dynamic and Stability Behaviors'. In: *Dynamics* 5.1 (2025), p. 3. DOI: 10.3390/dynamics5010003. URL: https://doi.org/10.3390/dynamics5010003.
- [20] Nor Atiqah Zolpakar et al. 'Application of Multi-objective Genetic Algorithm (MOGA) Optimization in Machining Processes'. In: *Springer Series in Advanced Manufacturing*. Springer Nature, 2020, pp. 185–199. DOI: 10.1007/978-3-030-19638-7\_8.
- [21] P. Cicconi et al. 'A Design Methodology to Support the Optimization of Steel Structures'. In: *Procedia CIRP* 50 (2016), pp. 58–64. DOI: 10.1016/j.procir.2016.05.030. URL: https://doi.org/10.1016/j.procir.2016.05.030.
- [22] Ruben Koopnam. 'Structural design and optimisation of a topologically reconfigurable modular steel space frame system'. Defended October 2024; retrieved from the TU Delft institutional repository. MSc thesis. Delft, The Netherlands: Delft University of Technology, 2024. URL: http://repository.tudelft.nl/.
- [23] Richard Frans and Yoyong Arfiadi. 'Sizing, shape, and topology optimizations of roof trusses using hybrid genetic algorithms'. In: *Procedia Engineering*. Vol. 95. Elsevier Ltd, 2014, pp. 185–195. DOI: 10.1016/j.proeng.2014.12.178.
- [24] Alemseged Gebrehiwot Weldeyesus et al. 'Truss geometry and topology optimization with global stability constraints'. In: *Structural and Multidisciplinary Optimization* 62 (4 Oct. 2020), pp. 1721–1737. ISSN: 16151488. DOI: 10.1007/s00158-020-02634-z.
- [25] William S. Dorn, Ralph E. Gomory and Harvey J. Greenberg. 'Automatic Design of Optimal Structures'. In: *Journal de Mécanique* 3 (1964), pp. 25–52.
- [26] Ali Mortazavi and Vedat Toğan. 'Simultaneous size, shape, and topology optimization of truss structures using integrated particle swarm optimizer'. In: *Structural and Multidisciplinary Optimization* 54 (4 Oct. 2016), pp. 715–736. ISSN: 16151488. DOI: 10.1007/s00158-016-1449-7.
- [27] Razvan Cazacu and Lucian Grama. 'Steel Truss Optimization Using Genetic Algorithms and FEA'. In: *Procedia Technology* 12 (2014), pp. 339–346. ISSN: 22120173. DOI: 10.1016/j.protcy.2013.12.496.

- [28] Clemens Preisinger. 'Linking Structure and Parametric Geometry'. In: *Architectural Design* 83.2 (2013), pp. 110–113. DOI: 10.1002/ad.1564.
- [29] David Rutten. 'Galapagos: On the Logic and Limitations of Generic Solvers'. In: *Architectural Design* 83.2 (Mar. 2013), pp. 132–135. ISSN: 0003-8504. DOI: 10.1002/ad.1568.
- [30] David Rutten. Evolutionary Principles Applied to Problem Solving. Blog post on Grasshopper3D. Sept. 2010. URL: https://www.grasshopper3d.com/profiles/blogs/evolutionary-principles (visited on 29/05/2025).
- [31] Jukka Maenpaa. 'Algorithm-Aided Structural Engineering of Steel-Framed Warehouse'. Master's Thesis. Tampere, Finland: Tampere University of Technology, Feb. 2018. URL: https://trepo.tuni.fi/handle/123456789/25580.
- [32] Dlubal Software. RFEM 6 Online Manual(Static Analysis Settings). 2023. URL: https://www.dlubal.com/en/downloads-and-information/documents/online-manuals/rfem-6/000255.
- [33] Hans Welleman. *Mechanics of Slender Structures: CIEM5000-U2 (Only Statics)*. Lecture notes, Faculty of Civil Engineering Geosciences, MSc track-base course "Base: Structural Engineering". Academic year 2023–2024, accessed on 25 June 2025 via Brightspace. 2023. URL: https://brightspace.tudelft.nl/%E2%80%A6/CIEM5000-U2-2023-24.
- [34] Mahesh Thakare, P. R. Barbude and Ajay Radke. 'Finding Span to Depth Ratio of Double Warren Steel Truss for Least Weight Subjected to Double Track Railway Loading'. In: *International Journal of Engineering Research and Applications* 11.7 (2021), pp. 29–35. DOI: 10. 9790/9622-1107042935. URL: https://www.ijera.com/papers/vol11no7/Ser-4/E1107042935.pdf.
- [35] Teemu Tiainen et al. 'Steel Building Optimization Applying Metamodel Techniques'. In: *Rakenteiden Mekaniikka (Journal of Structural Mechanics)* 45.3 (2012), pp. 152–161. URL: http://rmseura.tkk.fi/rmlehti/2012/nro3/RakMek\_45\_3\_2012\_5.pdf.
- [36] EN 1993-1-1: Eurocode 3: Design of Steel Structures Part 1-1: General Rules and Rules for Buildings. English version, supersedes ENV 1993-1-1:1992. Brussels: European Committee for Standardization (CEN), May 2005.
- [37] Tony T. P. To. 'Structural optimization of modular high-rise buildings'. Retrieved from the TU Delft Institutional Repository. MA thesis. Delft, The Netherlands: Delft University of Technology, Apr. 2020. URL: http://repository.tudelft.nl/.
- [38] EN 1993-1-8: Eurocode 3: Design of Steel Structures Part 1-8: Design of Joints. See Chapter 6 for the component method, §§6.1–6.4. European Committee for Standardization (CEN), May 2005.
- [39] EN 1990: Eurocode Basis of Structural Design Annex A1: Application for Buildings. English version; incorporates Amendment A1:2005 and Corrigendum AC:2010. Brussels: European Committee for Standardization (CEN), Dec. 2005.
- [40] IDEA StatiCa. *Release Notes IDEA StatiCa Steel & Concrete 23.1*. Software Release Notes. IDEA StatiCa, Oct. 2023.
- [41] IDEA StatiCa. *Release notes IDEA StatiCa v25.0*. Highlights the updated Grasshopper plugin. Apr. 2025. URL: https://www.ideastatica.com/support-center/release-notes-idea-statica-25-0.

# **Appendix A**

# **Grasshopper Scripts**

## A.1 Simply supported beam

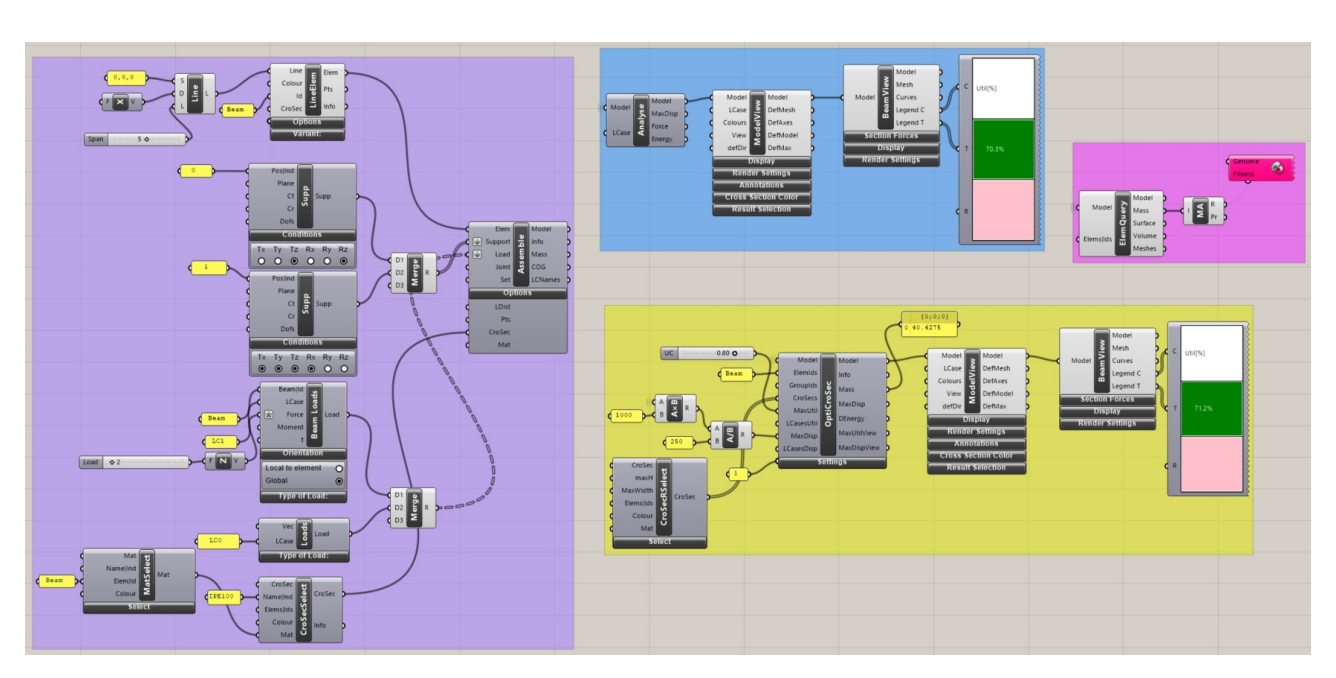


Figure A.1: Grasshopper script for Beam Model

## A.2 Standard truss

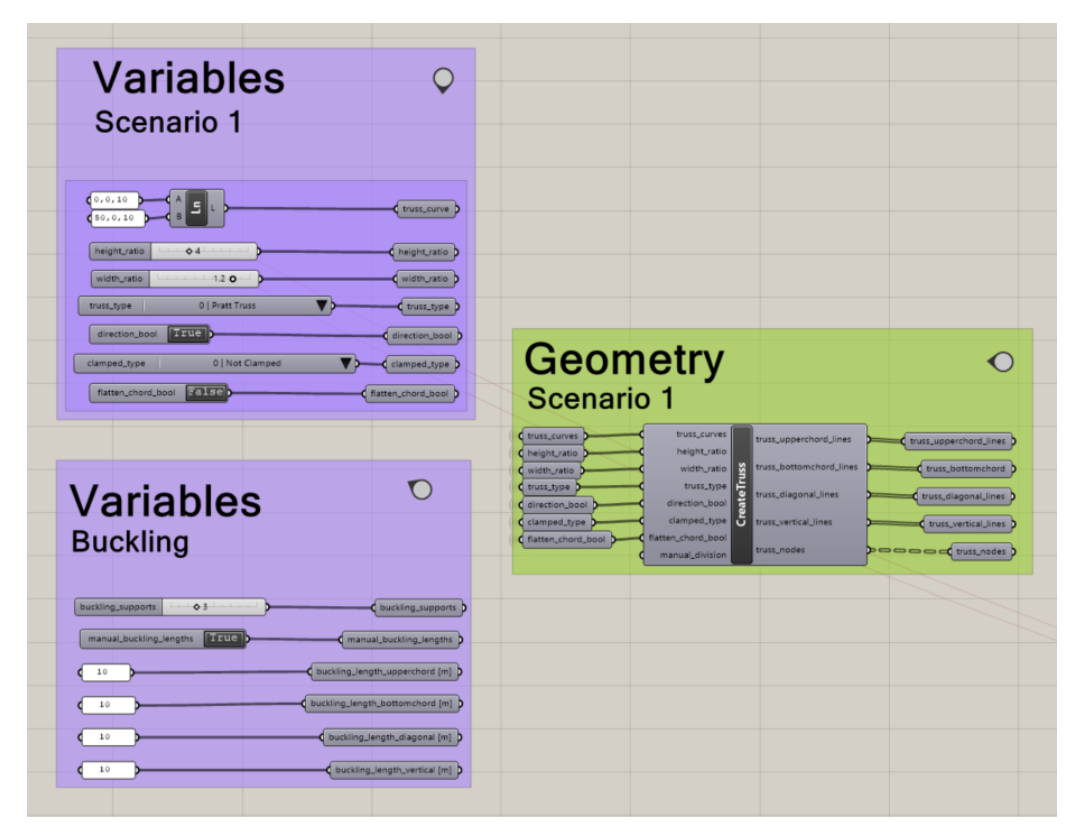


Figure A.2: Grasshopper script for Truss Model-1

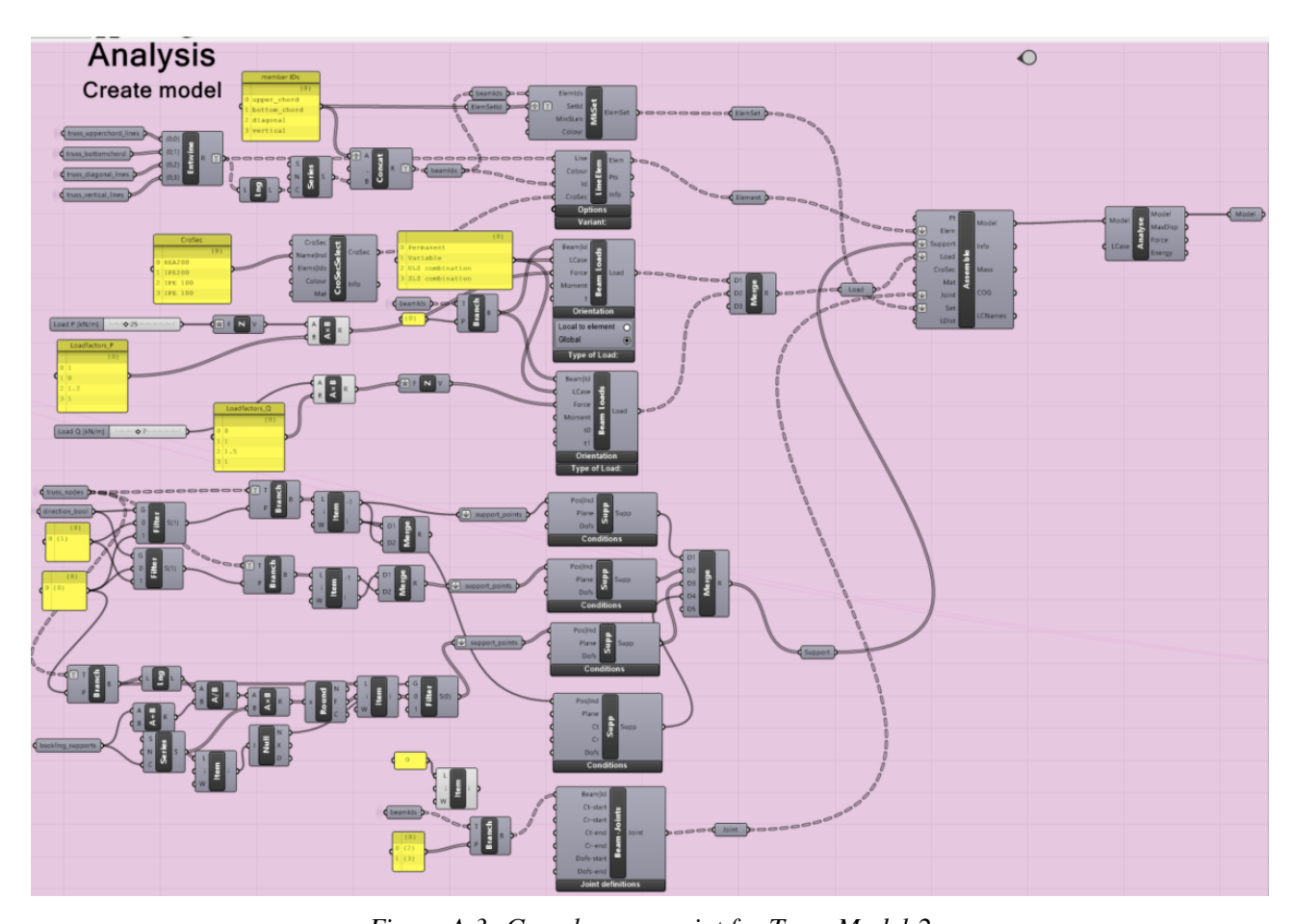


Figure A.3: Grasshopper script for Truss Model-2

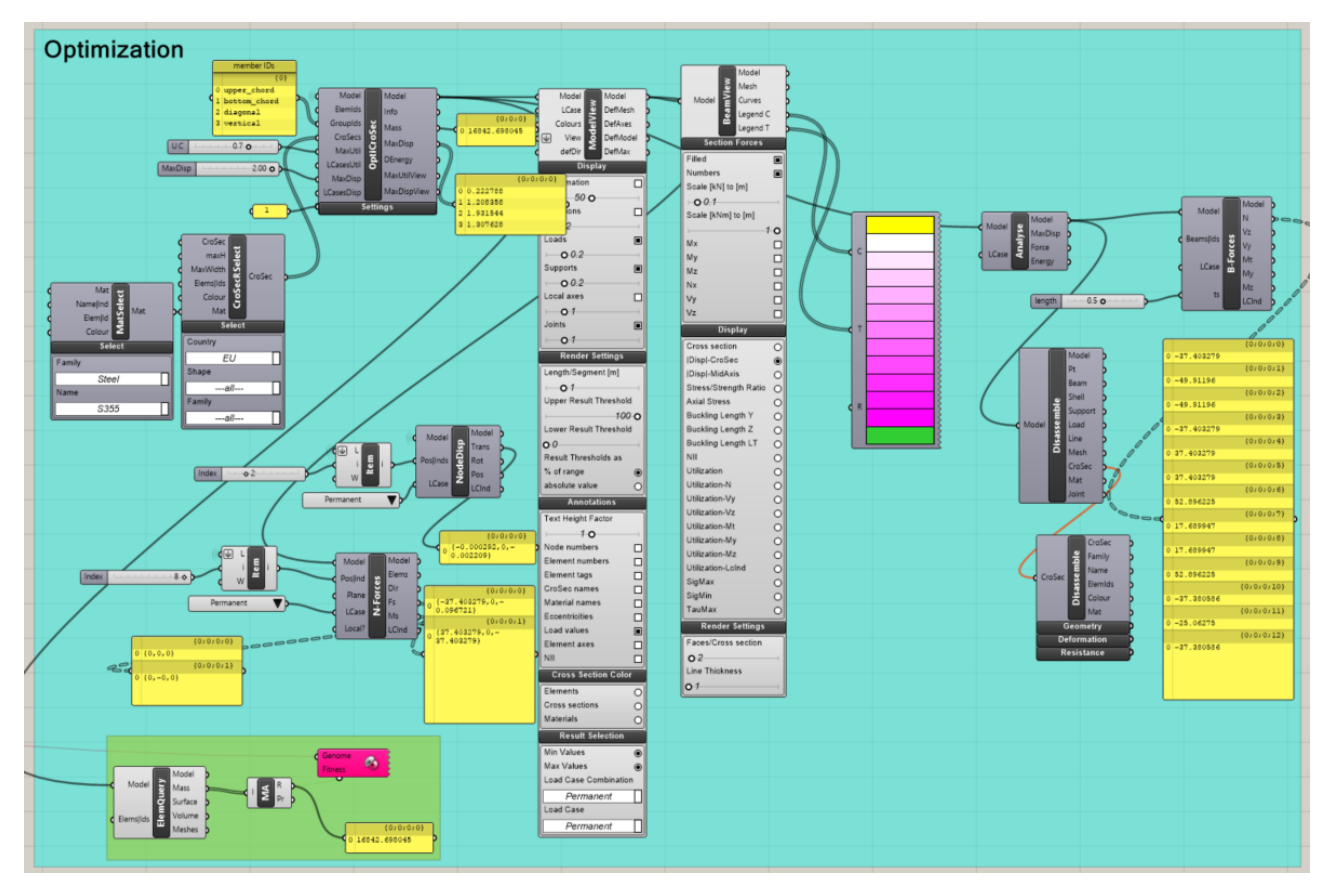


Figure A.4: Grasshopper script for Truss Model-3

## **A.3** Truss for the Pier- Model 1

The grid sizes are based on the design of the Pier from Haskoning. The same grid is used for the first 3 models.

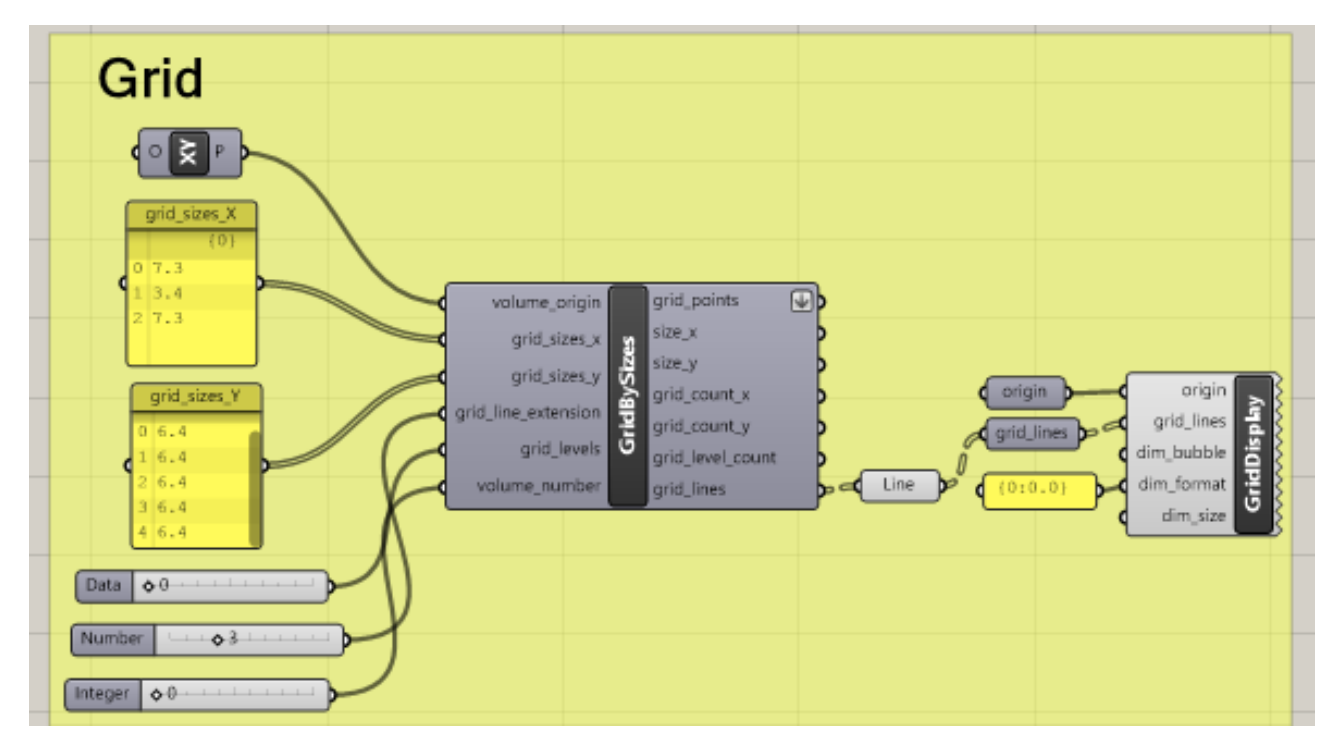


Figure A.5: Grid

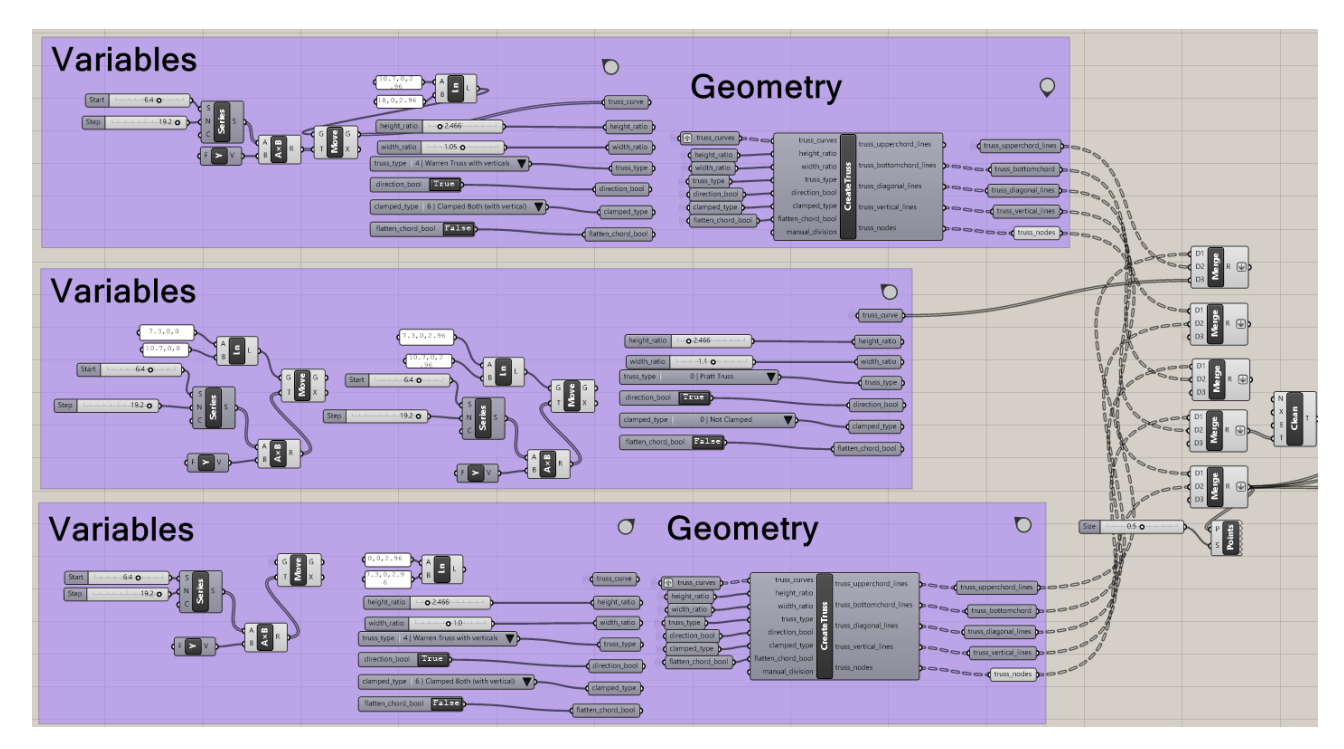


Figure A.6: Variables

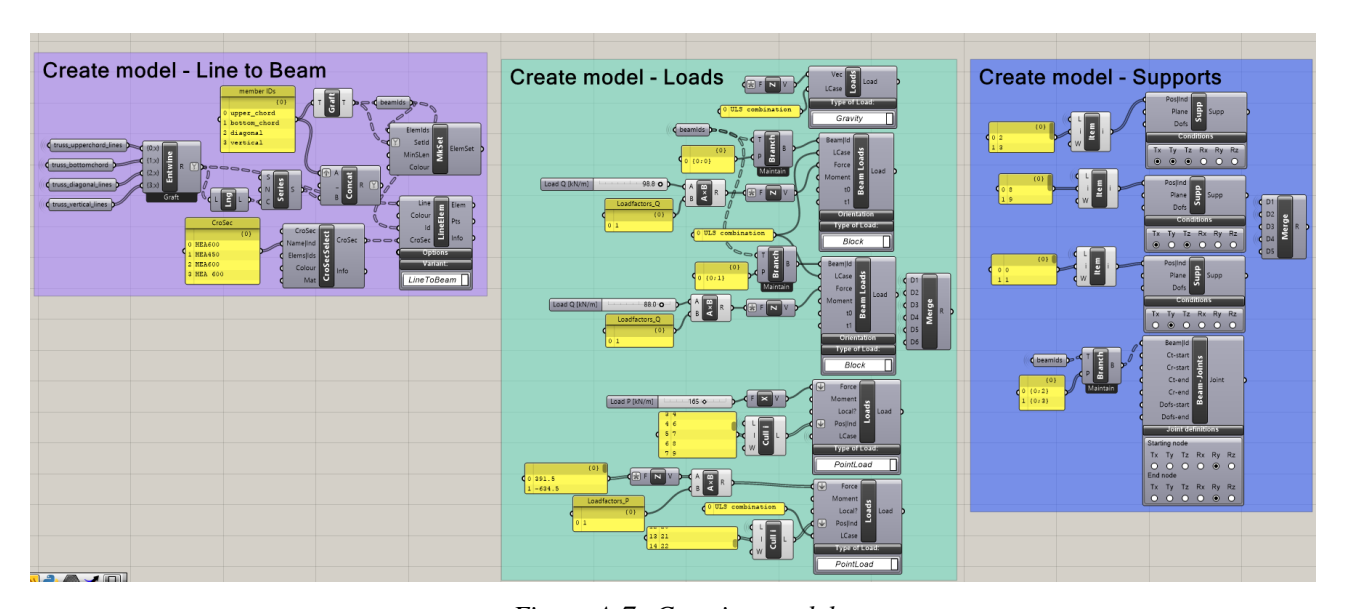


Figure A.7: Creating model

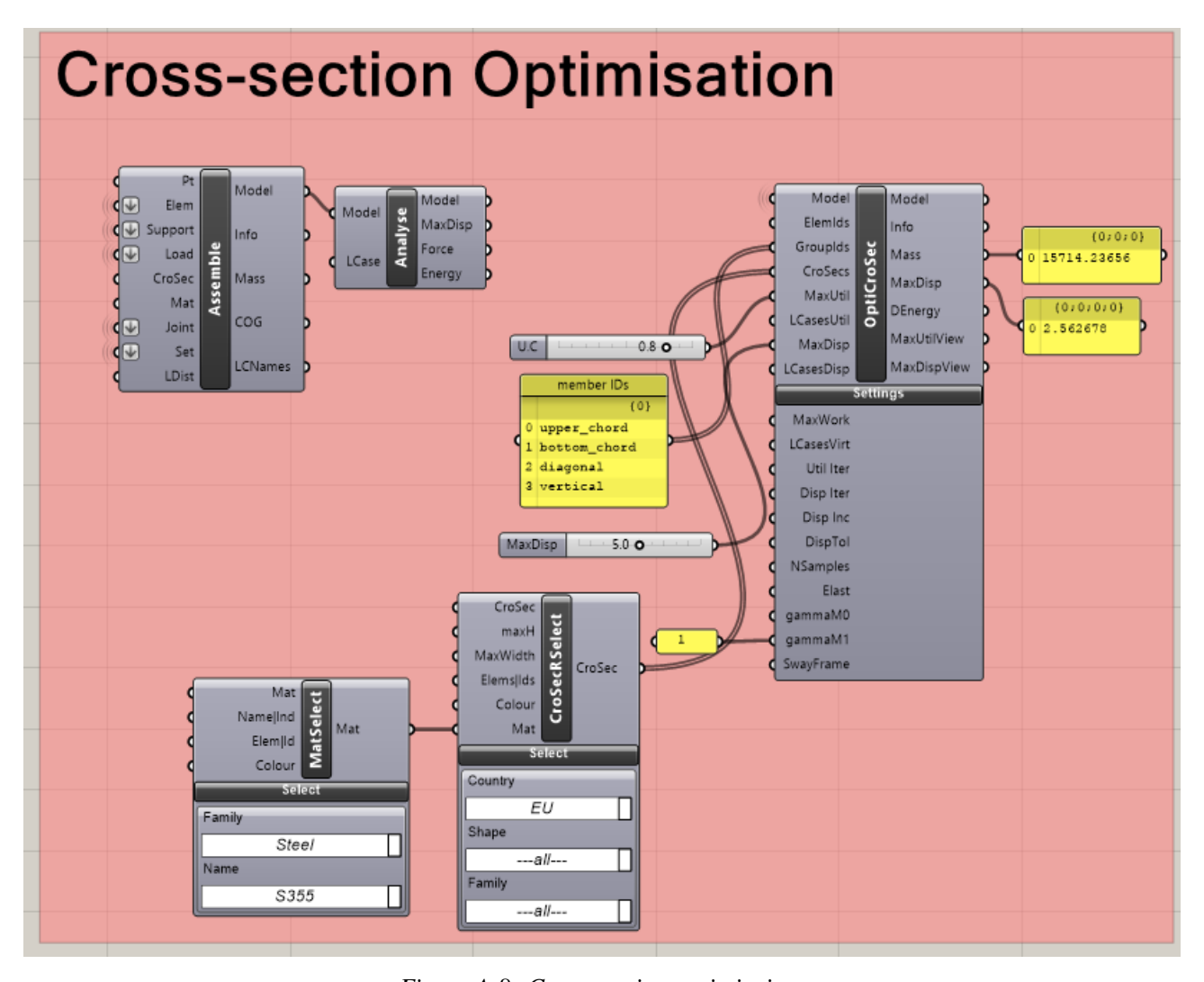


Figure A.8: Cross section optimisaiton

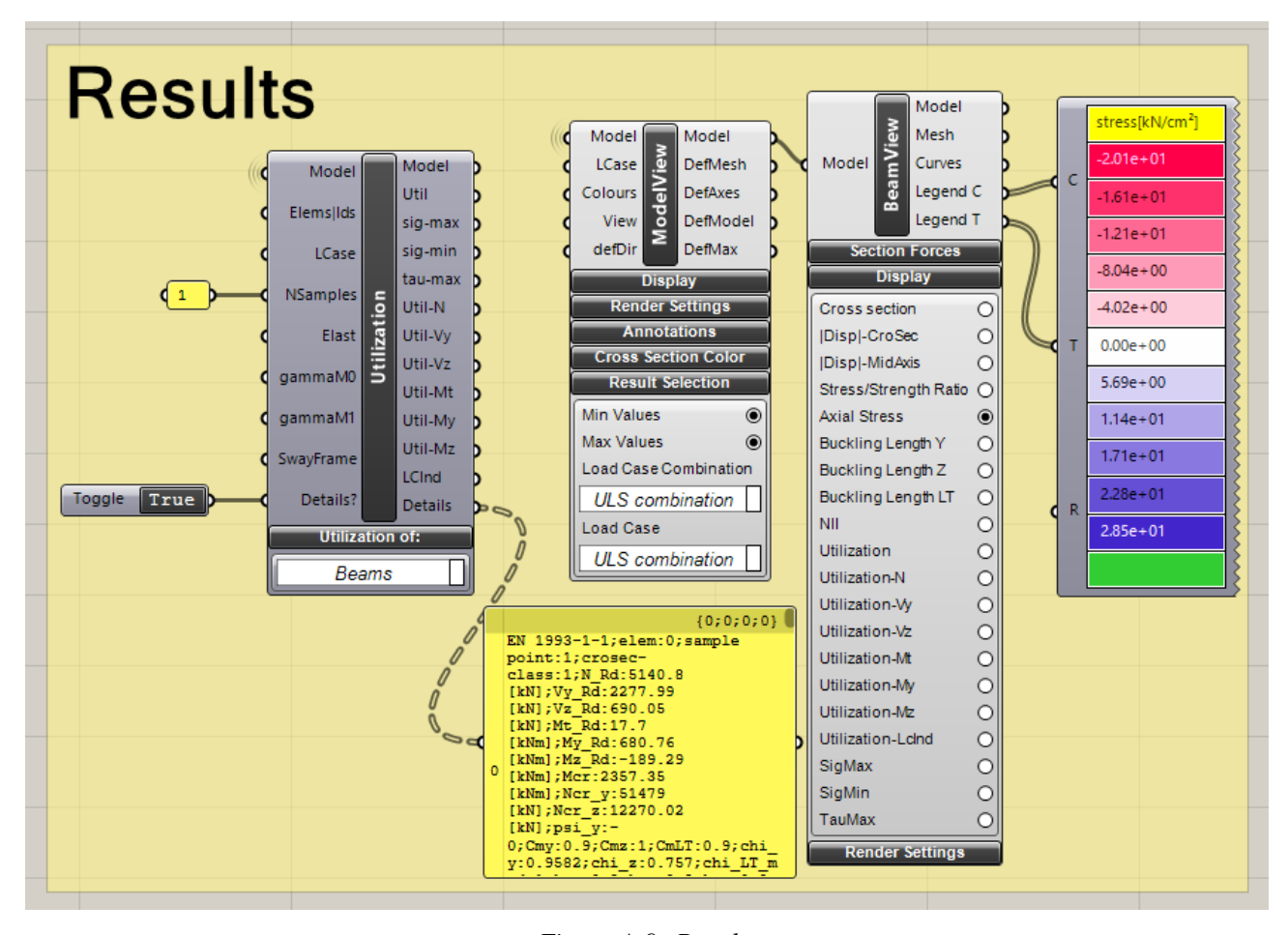


Figure A.9: Results

## A.4 Truss for the Pier- Model 2

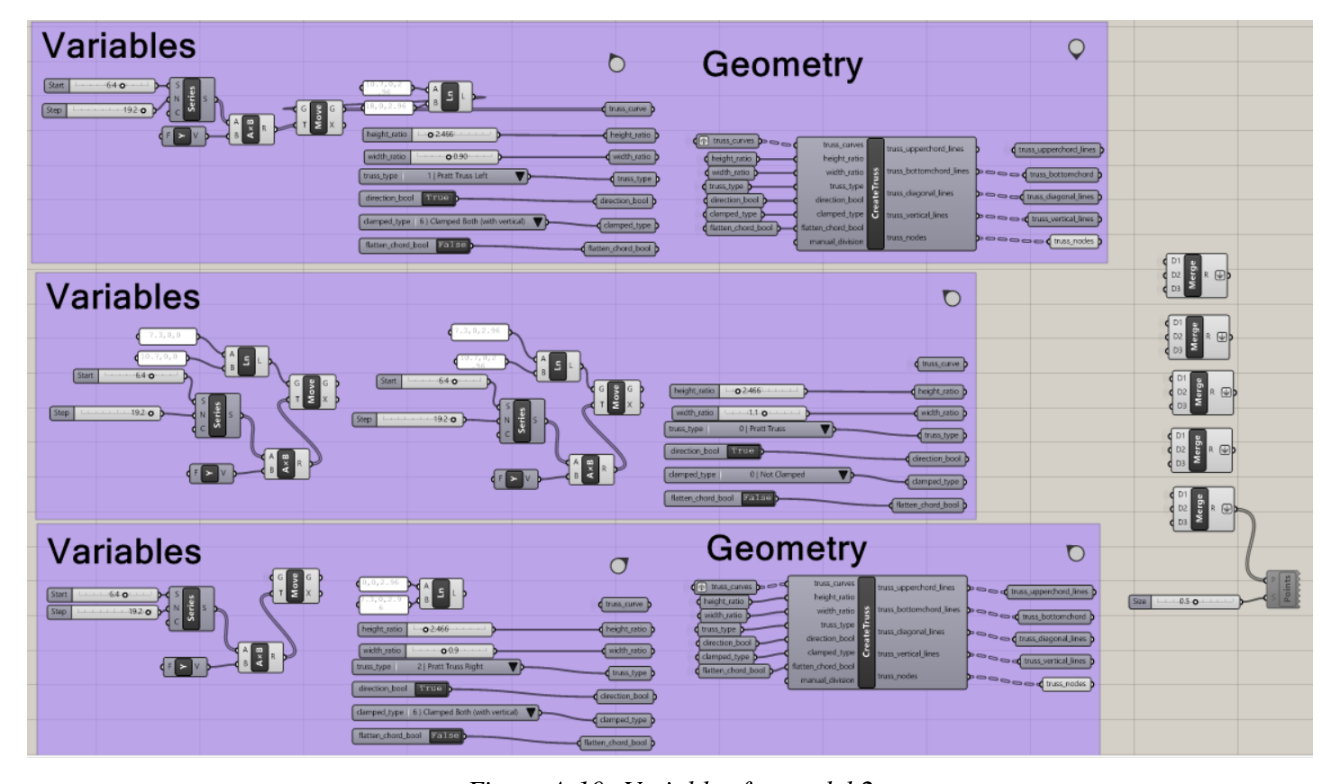


Figure A.10: Variables for model 2

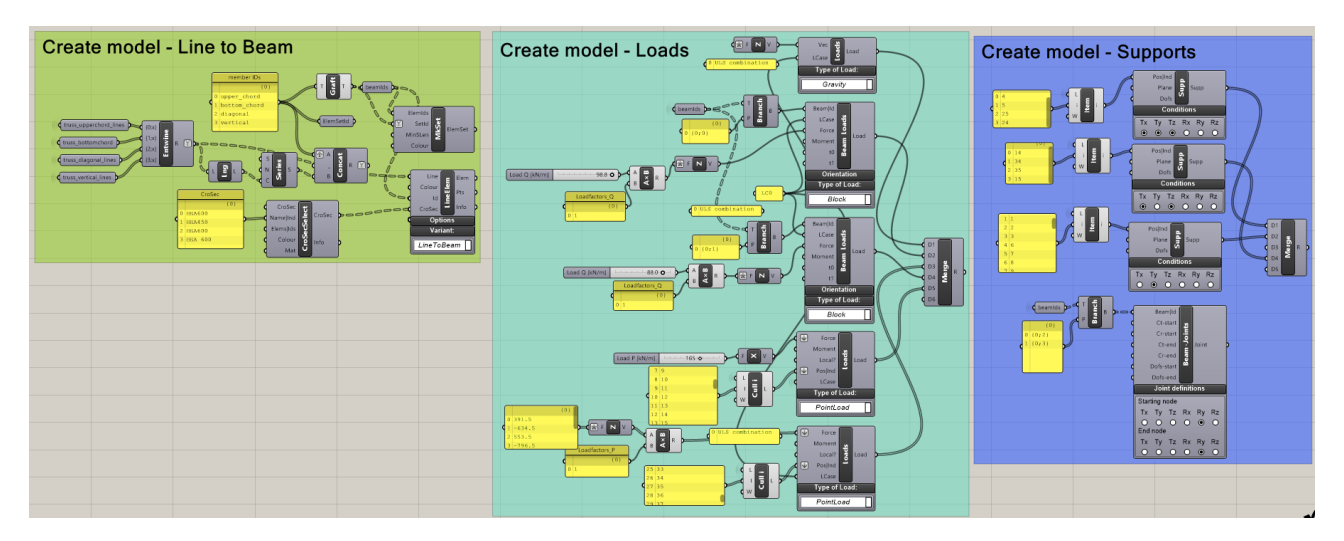


Figure A.11: Creating model 2

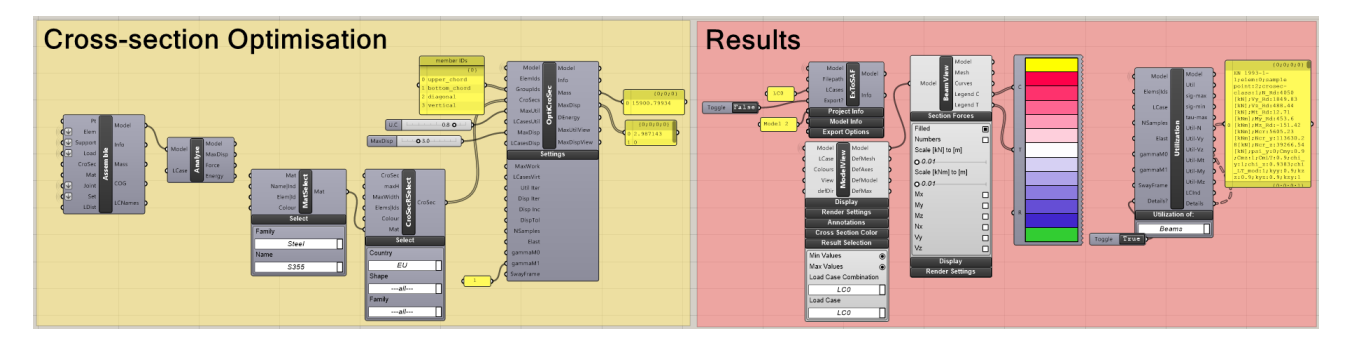


Figure A.12: Cross-section optimisation and results

## A.5 Truss for the Pier- Model 3

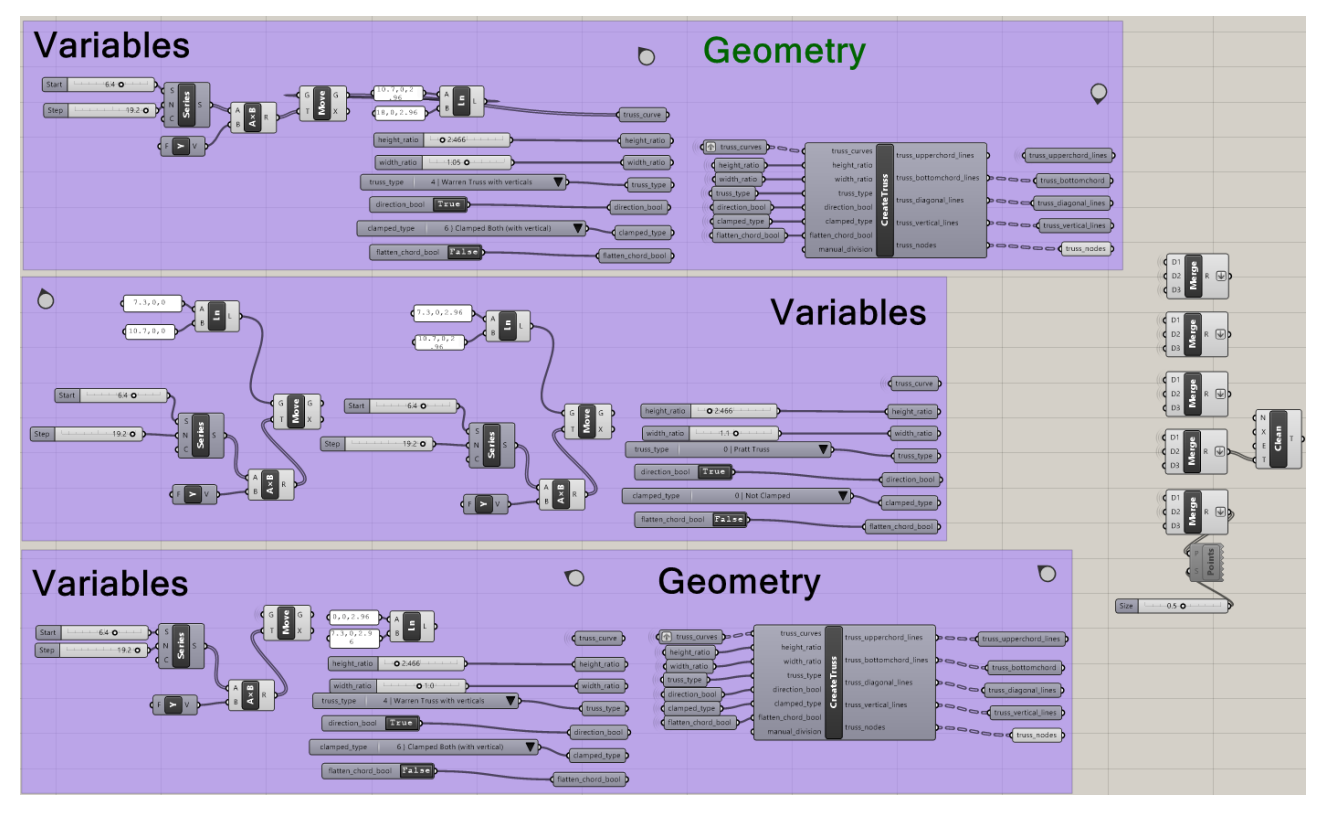


Figure A.13: Variables for model 3

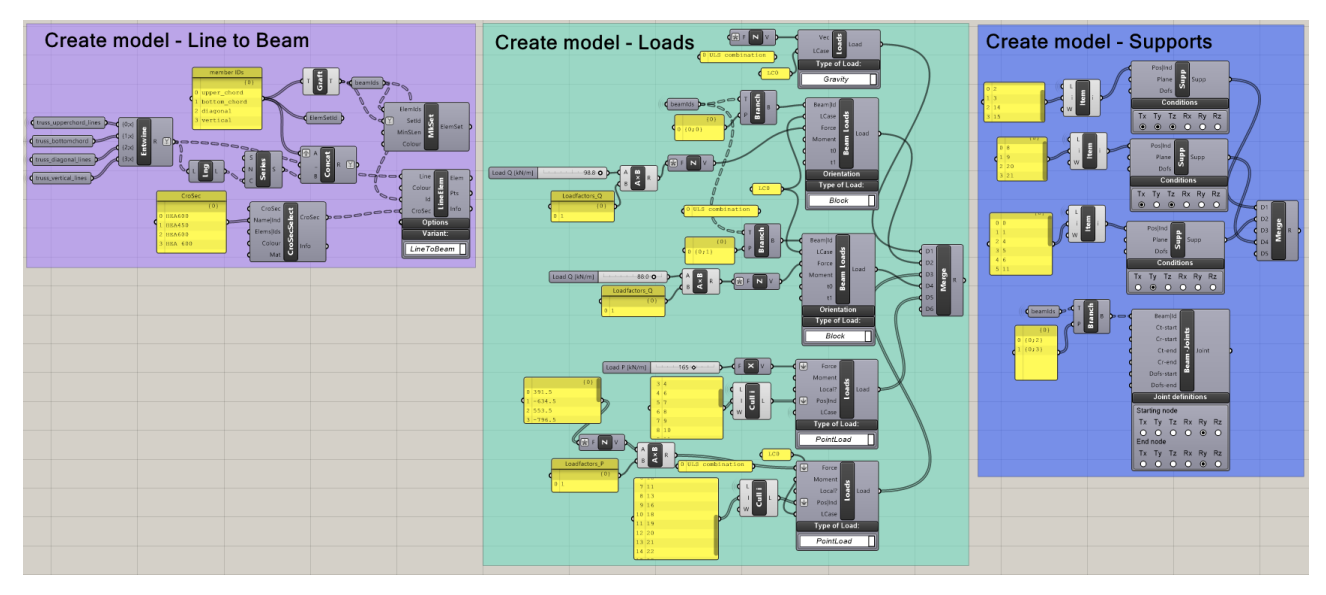


Figure A.14: Creating model 3

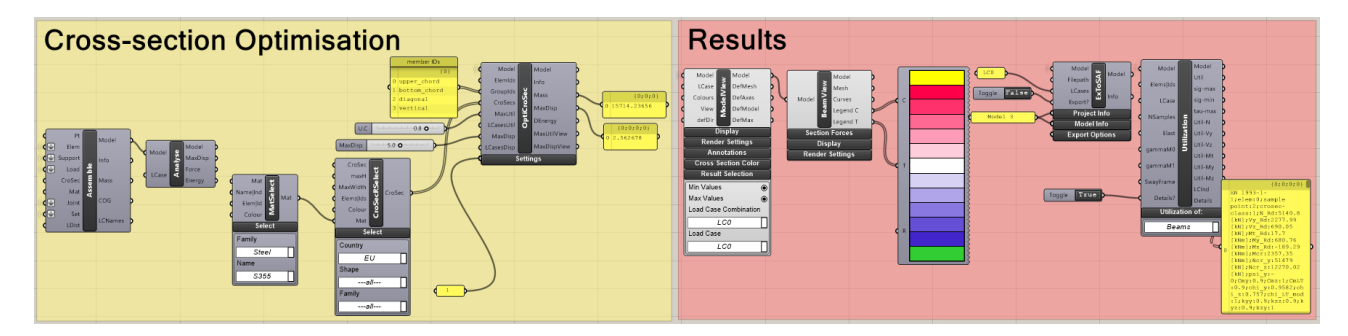


Figure A.15: Cross-section optimisation and results

## A.6 Truss for the Pier- Model 4

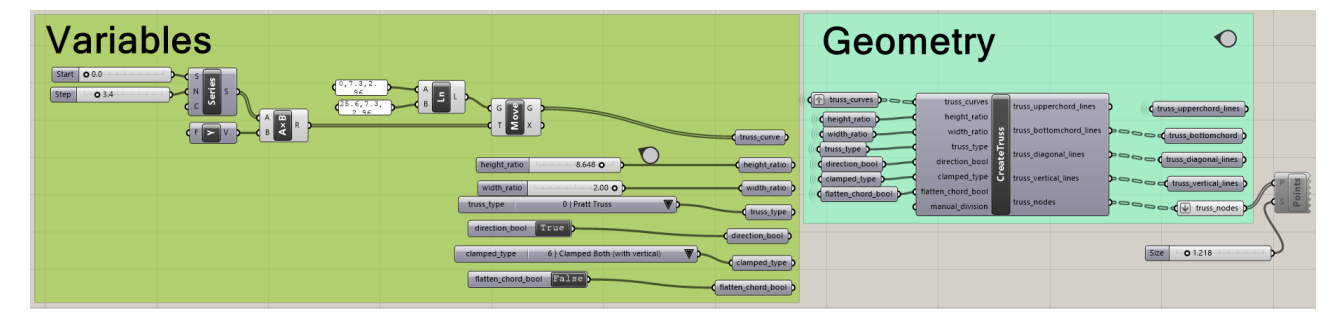


Figure A.16: Variables for model 4

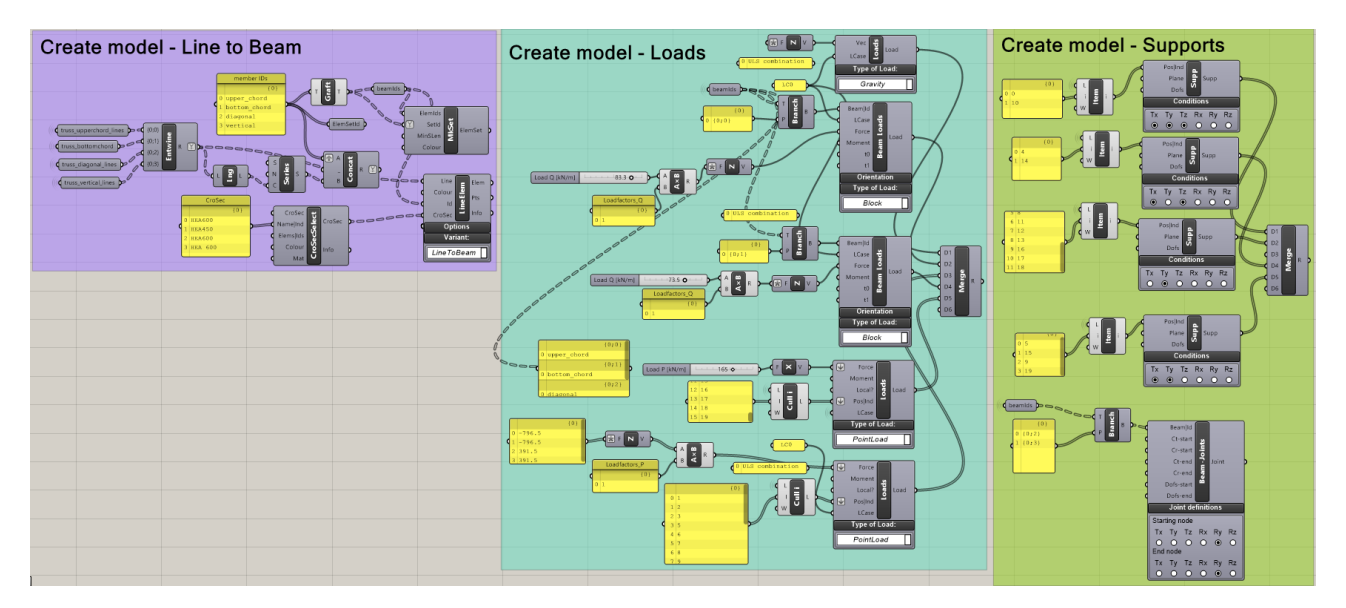


Figure A.17: Creating model 4

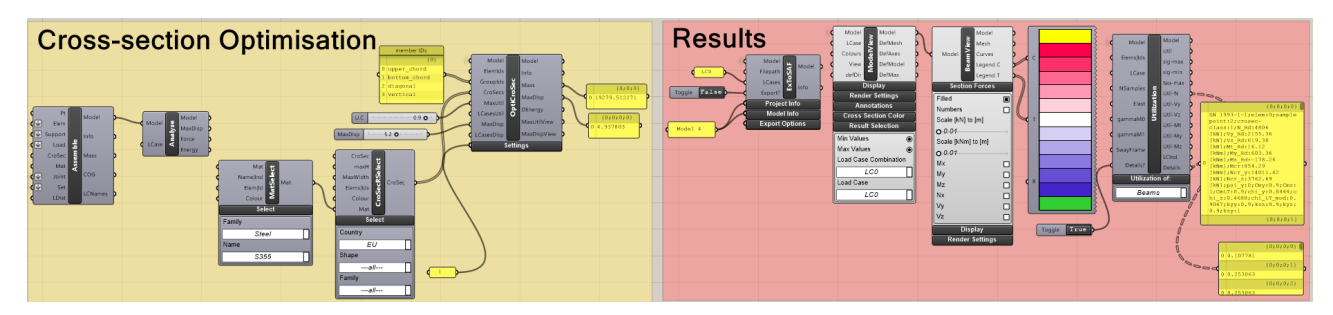


Figure A.18: Cross-section optimisation and results

# Appendix B

## **Standard Truss- Utilisation checks**

## **B.1** Example Calculation

The section properties, reduction factors, and interaction parameters were extracted from Karamba3D's cross-section check panel.

Symbol	Description	Value
crosec-class	-	4
$N_{Rd}$	Plastic axial resistance	$5105.45\mathrm{kN}$
$M_{y,  m Rd}$	Plastic major-axis moment resistance	$1004.40\mathrm{kN}\mathrm{m}$
$M_{z, m Rd}$	Plastic minor-axis moment resistance	$100.77\mathrm{kN}\mathrm{m}$
$N_{{ m cr},y}$	Euler critical load (about y)	$12214.00\mathrm{kN}$
$N_{\mathrm{cr},z}$	Euler critical load (about $z$ )	$449.28\mathrm{kN}$
$M_{ m cr}$	Lateral-torsional critical moment	$277.50\mathrm{kN}\mathrm{m}$
$\psi_{m{y}}$	Moment-gradient factor	1.0
$C_{my}, C_{mz}, C_{mLT}$	Eurocode $C_m$ -factors (uniform moment)	0.9
$\chi_y$	Buckling reduction factor (about $y$ )	0.8578
$\chi_z$	Buckling reduction factor (about $z$ )	0.0729
$\chi_{LT, mod}$	LT-buckling reduction factor	0.2484
$k_{yy}$	Interaction factor for $M_y$	1.0035
$k_{zz}$	Interaction factor for $M_z$	1.0603

Table B.1: Values exported from Karamba®

### Axial buckling about the y-axis

$$\bar{\lambda}_{y} = \sqrt{\frac{N_{pl,Rk}}{N_{cr,y}}} = \sqrt{\frac{5105}{12214}} = 0.65$$

$$\phi = \frac{1}{2} \left[ 1 + \alpha (\bar{\lambda}_{y} - 0.2) + \bar{\lambda}_{y}^{2} \right], \quad \alpha = 0.21 \text{ (curve a)}$$

$$\chi_{y} = \frac{1}{\phi + \sqrt{\phi^{2} - \bar{\lambda}_{y}^{2}}} \approx 0.86$$

### Axial buckling about the z-axis

$$\bar{\lambda}_z = \sqrt{\frac{5105}{449.28}} = 3.37$$

$$\alpha = 0.49 \text{ (curve c)}$$

$$\chi_z \approx 0.073$$

### Lateral torsional buckling of major-axis bending

$$\bar{\lambda}_{LT} = \sqrt{\frac{M_{pl,Rk}}{M_{cr}}} = \sqrt{\frac{1004.4}{277.5}} = 1.90$$

$$\alpha_{LT} = 0.34 \text{ (curve b)}$$

$$\chi_{LT} \approx 0.25$$

**Design actions adopted** Assume the global analysis delivers the following design effects (at the same sample point):

$$N_{\rm Ed} = 1500 \, \rm kN, \quad M_{y,\rm Ed} = 65 \, \rm kN \, m, \quad M_{z,\rm Ed} = 7 \, \rm kN \, m.$$

Shear forces are below half their design resistance, hence no moment–shear interaction is necessary (EC 3, 6.2.8).

Eurocode 3 unity check (clause 6.3.3, Method 1)

$$\eta = \frac{N_{\rm Ed}}{\chi_y N_{pl,\rm Rd}} + k_{yy} \frac{M_{y,\rm Ed}}{\chi_{LT,\rm mod} M_{y,\rm Rd}} + k_{zz} \frac{M_{z,\rm Ed}}{M_{z,\rm Rd}}$$
(B.1)

$$= \frac{1500}{0.8578 \times 5105.45} + 1.0035 \frac{65}{0.2484 \times 1004.4} + 1.0603 \frac{7}{100.77}$$
 (B.2)

$$= 0.343 + 0.362 + 0.106 \tag{B.3}$$

$$= 0.68 < 1.0 \quad (OK)$$
 (B.4)

# **Appendix C**

## **List of Cross-Sections**

The list of cross-sections the cross-section optimizer can choose from is shown below. Only cross-sections with the same family attribute as the initial cross-section can be chosen. Only open sections are shown in the table, optimiser is looking through 3623 cross sections, including Hollow sections, large flats, ropes etc.

IPE	HEAA	HEA	HEB	HEM	HL	HD	HP	I
80	100	100	100	100	920x344	260x54.1	200x43	80
100	120	120	120	120	920x368	260x68.2	200x53	100
120	140	140	140	140	920x390	260x93.0	220x57	120
140	160	160	160	160	920x420	260x114	260x75	140
160	180	180	180	180	920x449	260x142	260x87	160
180	200	200	200	200	920x491	920x491   260x172		180
200	220	220	220	220	920x537	320x74.2	305x88	200
220	240	240	240	240	920x588	260x225	320x88	220
240	260	260	260	260	1000AA	320x97.6	305x95	240
270	280	280	280	280	920x656	320x127	320x103	260
300	300	300	300	300	1000A	320x158	305x110	280
330	320	320	320	320	920x725	260x299	320x117	300
360	340	340	340	340	1000B	320x198	305x126	320
400	360	360	360	360	1000M	360x134	305x149	340
450	400	400	400	400	920x787	320x245	320x147	360
500	450	450	450	450	1000x443	360x147	305x180	380
550	500	500	500	500	1000x483	360x162	305x186	400
600	550	550	550	550	1000x539	360x179	320x184	425
650	600	600	600	600	1000x554	360x196	305x223	450
700	650	650	650	650	1000x591	400x216	360x109	475
800	700	700	700	700	920x970	320x300	400x122	500
900	800	800	800	800	1000x642	400x237	360x133	550
1000	900	900	900	900	920x1077	400x262	400x140	600
					1000x748	400x287	400x158	
					920x1194	400x314	360x152	
					1100A	400x347	400x176	
					1000x883	400x382	360x174	
					920x1269	400x421	360x180	
					920x1377	400x463	400x194	
					1100B	400x509	400x213	
					1100M	400x551	400x231	
					1000x976	400x592		
					1100R	400x634		
						400x677		
						400x744		
						400x818		
						400x900		
						400x990		
						400x1086		
						400x1202		
						400x1299		

Table C.1: List of Cross- Sections

# **Appendix D**

## **Hollowcore Slab Calculation**

For floor layout 1, online tool from VBI is used to check if floor span is feasible. This tool gives a report after doing the necessary checks. The report in Dutch is given in figure D.1. Some important parts are translated to English is shown in table D.1,

Check	Demand	Capacity	Unit	Utilisation
Deflection – immediate (additional)	6	13	mm	0.46
Deflection – long-term (total)	6	26	mm	0.23
Bending moment – Service (SLS)	98.81	112.06	kN⋅m	0.88
Bending moment – Due to camber	53.93	103.80	kN⋅m	0.52
Bending moment – Fire (60 min)	53.93	64.92	kN⋅m	0.83
Bending moment – Characteristic	65.88	103.80	kN⋅m	0.64
Shear force – Service (max)	58.72	100.58	kN	0.59
Shear force – Fire (60 min)	34.03	39.65	kN	0.86
Crack width (bottom fibre)	0.000	0.339	mm	0.00
Compression-layer shear	0.165	0.309	N/mm <sup>2</sup>	0.53

*Table D.1: Hollow-core slab verification (A200, 6400 mm*  $\times$  1200 mm)

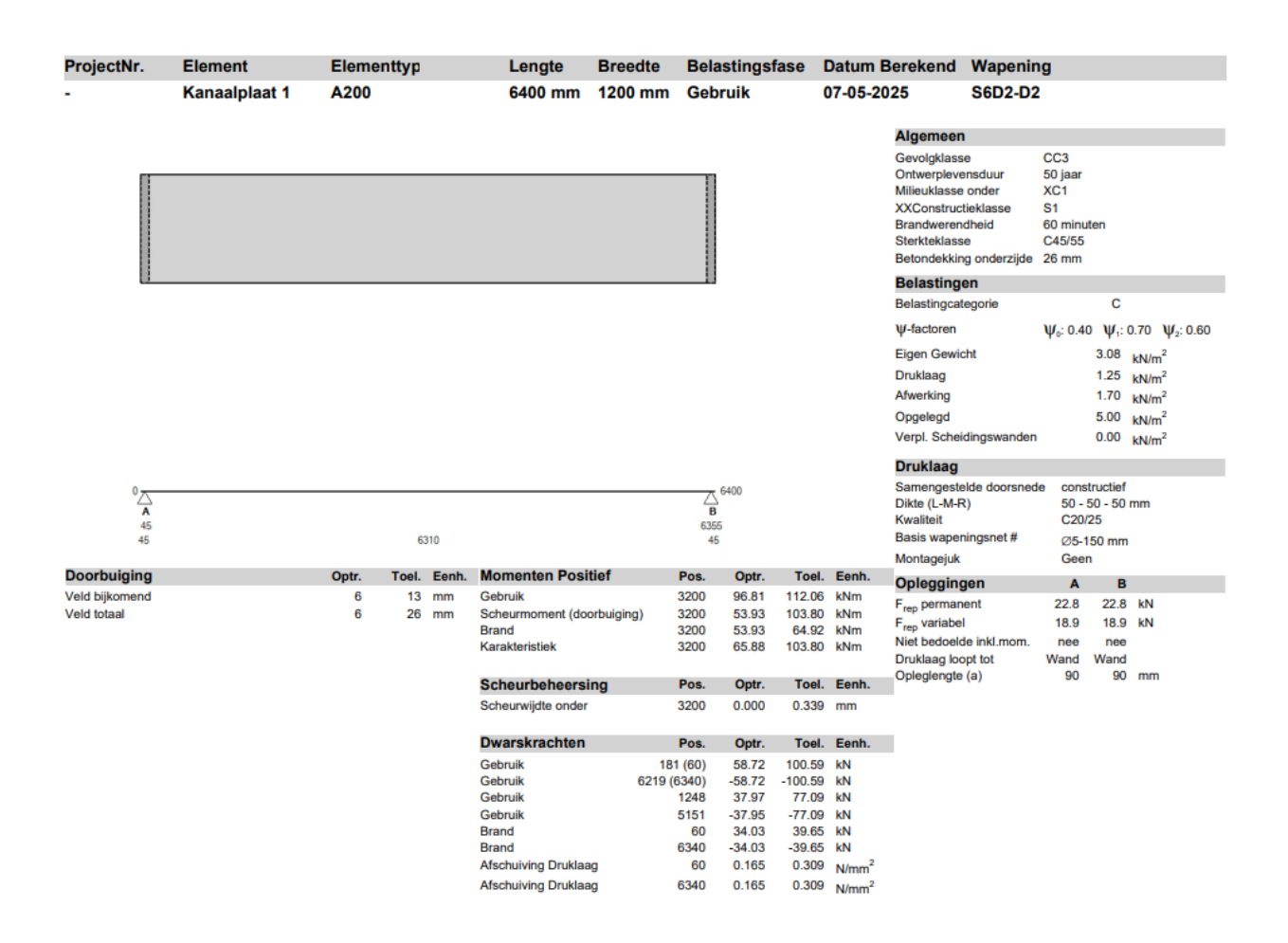


Figure D.1: VBI-1

For floor layout 3, the summary of checks for HC slab is shown in the table D.2. The original report in Dutch is given in figure D.2

Check	Demand	Capacity	Unit	Utilisation
Deflection – immediate (additional)	6	13	mm	0.46
Deflection – long-term (total)	6	29	mm	0.21
Bending moment – Service (SLS)	98.81	112.08	kN⋅m	0.88
Bending moment – Due to camber	53.93	103.80	kN⋅m	0.52
Bending moment – Fire (60 min)	53.93	64.92	kN⋅m	0.83
Bending moment – Characteristic	65.88	103.80	kN⋅m	0.64
Shear force – Service (max)	58.72	100.59	kN	0.59
Shear force – Fire (60 min)	34.03	39.65	kN	0.86
Crack width (bottom fibre)	0.000	0.339	mm	0.00
Compression-layer shear	0.165	0.309	N/mm <sup>2</sup>	0.54

*Table D.2: Verification summary for hollow-core slab layout 3 (A200, 6.40 m*  $\times$  1.20 m)

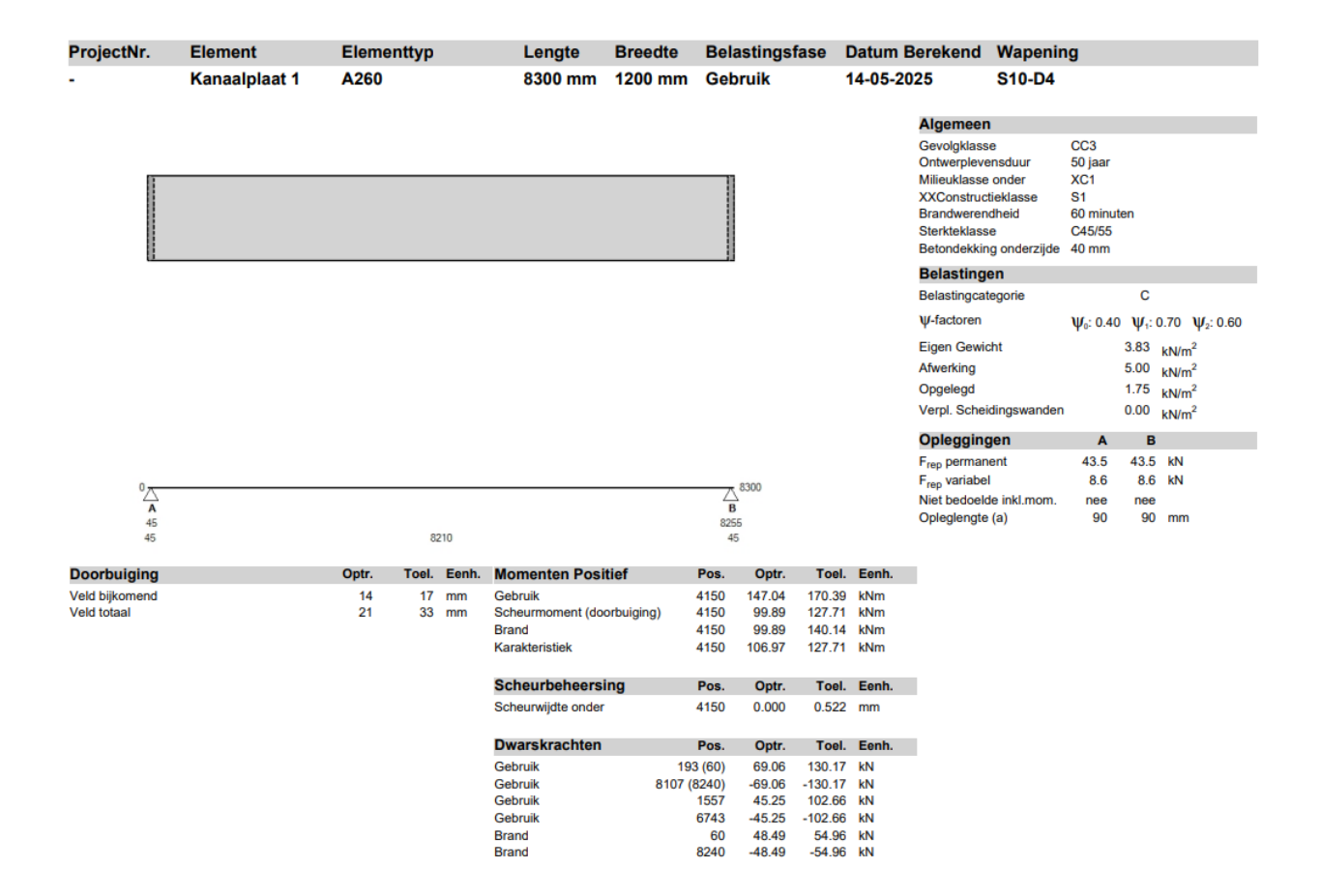


Figure D.2: VBI-3

# **Appendix E**

# **Cost data and Assumptions**

The detailed information from the interviews is included here to keep things transparent and for possible use in future stages of the project.

• Excluded from the model: explicit welding and fabrication terms, detail-specific surcharges and transport.

Welding costs depend on length, thickness and complexity. More complex structures require multiple welding passes, thicker welds or special detailing. A practical welding speed is 350 mm min<sup>-1</sup>. Connections (bolts or plates) are not priced individually at first, because the full amount of work involved (number of bolts and plates) is not known at the design stage. However, with many repeated joints (as in trusses) costs can be rationalised.

There is no fixed price per bolt; instead, a percentage of material cost is used (weight, bolt type, complexity, galvanisation). Extra gusset plates add roughly  $2.5 \in \text{kg}^{-1}$ . Increasing the number of connections from 10 to 20 raises cost by about 40 %; the relationship is not linear. The single largest cost driver remains the weight of steel.

Fillet size	Welding rate (m/h)	Labour cost (€/m)
General (350mm/min)	21	3.4
5mm	7	10.3
6–8mm	2.3	31.3
8–10mm	1.2	60.0

*Table E.1: Welding productivity and labour cost (labour rate* = 72 €/h)

Connection cost is described in Chapter 3 as 3–6% of material cost, where the exact figure depends on joint complexity. Table A.2 records the modifiers suggested by interviewees; they remain valid background data.

Item / Condition	Typical figure
Bolts & plates (fabrication & galvanising)	3–6% of material cost
Extra gusset-plate supply	2.5 € kg <sup>-1</sup>
Truss with diagonal bracing	+50 % labour cost
Doubling connections (10 $\rightarrow$ 20 joints)	+40 % total cost
One simple detail (rule-of-thumb)	150 € each

Table E.2: Connection and complexity cost modifiers

#### **E.1** Cost Estimation Interview Summaries

Interview summary from cost estimator 1 from steel contracting company A is given below.

- 1. What are the direct and indirect costs considered when quoting the total price? The pricing is usually for the main structure. Direct costs- labour, material, steel profiles, engineering, mounting and welding. Indirect costs- administration and supporting staff and general overhead. Indirect costs are factored in through calculated tariffs and are applied per hour or per unit depending on the task. For e.g., welding labour is estimated around 10 hours per ton of steel. Additional work like painting or coating and higher execution class requirements (which demand more testing and or inspection) are also considered.
- 2. Welded or bolted connection cost? Welding costs depend on length, thickness and complexity. More complex structures require multiple welding passes, thicker welds or special detailing. Welding speed estimates 350 mm per minute. Connections (bolts or plates) aren't priced individually at first, because the full amount of work involved (number of bolts and plates) isn't known at the design stage. However, when repeated many times like in trusses it becomes easier to estimate.
- 3. **Different steel profiles sizes and prices** Steel prices vary by size, weight and profile type. Steel prices vary depending on the grade with price differences reaching up to 0.05 euro per kg between grades. For e.g. If you are buying a beam that weights 100 kg and the better steel grade is 0.05 euro more expensive per kilogram, that adds 5 euro to the cost. Because steel prices are fluctuating, they usually get prices from the supplier quotes and they extract specific profiles and calculate the cost based on the weight and type of material. They don't maintain a fixed list or prices because the price from the supplier fluctuates daily or weekly. Prices are typically confirmed shortly before the purchase of project execution. Profiles and materials used in less frequent production runs are pricier due to limited availability.
- 4. **Transportation and logistics cost** Transportation depends on segment sizes, truck types and permits. Road transport for trusses might need segmentation if the sizes exceed standard truck dimensions.
- 5. **Production process and labour cost** Unique connections require manual labour and more engineering effort. This means that standardised components are more efficient but custom designs increase cost and effort. Labour costs are estimated based on the weight and type of work. 10-12 hours per ton for repeated elements. The weld length and size and number of bolts and complexity of joints all contribute.

Interview summary from cost estimator 1 from steel contracting company B is given below.

- 1. What are the direct and indirect costs considered when quoting the total price? Direct costs: Steel purchase, engineering, fabrication, coating/galvanising, transport, site erection and installation. Indirect costs are minimal and include slight (1-5%) profit margin and risk buffer. These are included in hourly rates and depend on annual utilisation.
- 2. Welded or bolted connection cost? Costs are calculated based on welding time and weld size. 5mm: 7m/hr 6-8mm: 2.3m/hr 8-10mm: 1.2m/hr Welding cost is about 72 euro/hr. Prep time is 2 times the welding time but becomes stable for bigger welds. There is no fixed price per bolt. Instead use a percentage of material cost based on weight of the structure, bolt types, complexity and galvanisation. Estimated range: 3-6%. Cost impact on bolt sizes is not separately calculated. It is baked into the percentage estimation. Material+ making cost of steel gusset plates: 2,5/kg. More plates = more welding and composition/welding time, thus higher cost. More cost for detailed geometry because of detailed engineering and special beams. Truss

with diagonal reinforcements can increase labour cost by 50% Cannot calculate the cost of one detail. Cost of one easy detail is 150 euros approx. But not possible to zoom in and calculate in more detail. They provide a complete work price for the entire structure. This estimation includes all steps like engineering and fabrication, they do not separate this. The cost of increasing the number of connections in a truss from 10- 20 is not linear, or not a simple doubling. Instead, the increase is about 40%. so, the cost rises but not proportionally. The biggest cost driver remains the weight of the steel. It is too complex to input all these into software because there is not fixed pricing model that works universally. They rely on experience and overall estimation, especially since you only know the costs at the end of the project.

- 3. **Different steel profiles sizes and prices** S355 from mills: 30 euro /ton more than S235 S355 from stock: 60-80 euro/ton more than S235 Mill orders start from 10 tons with a 6–10-week lead time. Emphasis on steel weight because it has more impact on cost than connections. The heavier the structure the more costly it becomes. It is important to look after the total setup and how things fit and are built together. The standard design for easy trusses includes: rectangular cold formed tubes in specific arrangements like upper, bottom, diagonal and vertical chords. Cost depends heavily on the profile and weight. Price list in not available. But for rectangular tubes cost is 5-10% more than round tubes. In some cases, the price difference can reach up to 30% depending on the profile and the market.
- 4. **Transportation and logistics cost** General permit allows segments up to 3.5m x 23m. Special permits, guidance vehicles etc add cost. Steel transport per km ranges form 2-5 euro/km. Standard truck size is 3.5m x 23m.

# Appendix F

# **Case Study: Interview summary**

Interview summary from the conversation with a structural Engineer about segmentation strategies of truss in different projects is given below.

### F.1 Case study 1: Omnisport Apeldoorn

#### (a) Can you give an overview of the project?

The project is the Omni Sport Apeldoorn, a large indoor cycling arena with a curved roof and trusses spanning over 100 meters. Each truss varied in length, some reaching up to 85 meters.

#### (b) How are such large trusses segmented for transport and assembly?

Such trusses are fabricated in workshops and then cut into smaller, transportable segments. The typical transportable length is between 30 and 40 meters, depending on road limitations and permit types. In the Omni Sport project, each truss was divided into three segments that were bolted together on-site. Transport height also plays a role. While 5-meter-high trusses can be transported vertically, this may require special permits or nighttime transport.

#### (c) What factors determine where the cuts are made in the trusses?

The location of cuts depends on structural logic and practical concerns. Cuts are usually placed to avoid vertical members and are made through chords and diagonals instead. This avoids weakening the structure at high-stress points. Compression areas like the top chord can have simpler connections, while tension areas like the bottom chord need more robust bolted connections, sometimes involving over 30 bolts in a single splice.

#### (d) When do you choose welded connections instead of bolted ones?

Welded connections are often chosen for their cleaner appearance and structural performance, especially in areas under compression. However, welding on construction sites can be unreliable because of environmental factors like temperature and humidity. As a result, bolted connections are usually preferred for on-site work. Many projects use a combination of both, welding in the workshop and bolting on-site.

# (e) Are there any examples where the connection strategy was adapted to suit the project?

Yes, in one case, diagonals sticking out from a truss raised concerns during transport, so

the connection was adapted with a double-bolted joint to prevent damage.

(f) What are some challenges when working with circular hollow sections (CHS)? CHS members are more difficult to bolt than traditional I-beams because of their curved surfaces. While flange plates can be added for bolting, these connections can be bulky and limit the number of bolts. In contrast, I-beams have flat surfaces that make it much easier to use bolted plates. It's also easier to design clean connections in compression than in tension, since tension forces tend to pull connections apart, requiring extra reinforcement.

### F.2 Case Study 2- Adam Tower

Interview summary from conversation with a Structural engineer about the A'DAM Tower project is given below.

#### (a) Can you describe the project and the design challenges involved?

The A'DAM Tower project involved extending an existing high-rise building by adding three new stories on top. The new structure was rotated 45 degrees relative to the existing tower, creating a complex loading situation. The design had to transfer all major loads to just four corner points of the original core structure, since those were the only locations capable of bearing significant additional weight. Due to space constraints and the desire to maintain an open, panoramic "Skydeck" viewing area, traditional bracing systems were ruled out, and a different approach altogether was needed.

#### (b) What structural solution was used for the new upper floors?

The team decided on a Vierendeel truss system. While less efficient when structurally compared to traditional triangulated trusses, this method eliminated the need for diagonal bracing and allowed for open, unobstructed space inside the Skydeck. This was especially important for architectural reasons, since the top floor was designed to function as an observation area with  $360^{\circ}$  views. The design relied on rigid connections at the nodes, which required more material and stronger columns, but offered the visual openness the client and architect wanted.

#### (c) How were lateral loads like wind addressed without traditional bracing?

The Vierendeel structure itself provided some lateral stability, but additional wind bracing was added to make the structure fully non-sway. These braces were integrated into the remaining core wall elements, such as elevator shafts and stair walls, minimizing the visual impact and maintaining architectural freedom. In some cases, the architect even altered the floor layout to accommodate optimal bracing placement.

#### (d) What was the size and segmentation strategy for the trusses?

The trusses were around 30 meters in length and required segmentation for practical assembly. Here, the four main Vierendeel trusses formed the structure, supported by the four main corner columns. Although the spans could technically be transported in one piece, limitations in crane capacity at 74 meters of height made segmentation necessary. Two of the main trusses were fabricated in multiple parts with bolted connections and intermediate support columns. Continuous trusses were also divided based on internal force diagrams to ease transport and reduce on-site hoisting time.

#### (e) What were the erection and hoisting considerations?

Hoisting capacity and scheduling played a key role in the strategy. There was only one

crane in Europe capable of the required lifting height and load, and it had to be reserved two years in advance. To minimize the number of hoisting operations, the steel supplier proposed assembling large sections on the ground, including the composite deck and scaffolding, and hoisting them into place as complete modules. This allowed faster installation and safer working conditions at height.

#### (f) Can you describe the connection details and joint types?

The segmented trusses were connected with a combination of bolted tension and compression joints. For example, the bottom chord connections were in compression, while the top chord connections were in tension. Special plates were added at joint locations to ensure proper alignment and load transfer. Some connections were intentionally placed at areas with low internal force in order to reduce structural stress and simplify assembly.

## F.3 Case study 3: X

#### (a) Can you describe the project?

The project involved a facility, which included a 46-meter-span steel truss with a height of approximately 4 meters. The building required a column-free interior space, meaning the truss had to span the full width between supports. Due to its size and height, the full truss could not be transported to the construction site as one piece and had to be segmented.

#### (b) What was the segmentation and assembly strategy?

The truss was designed to be fabricated in four segments, transported to the site, welded together on the ground, and then hoisted into place as a single, fully welded unit. The cuts were planned near the ends of the truss rather than the center to avoid high internal forces during assembly. It was also mentioned that the exact cut locations were not fixed by the structural designer but were typically proposed by the steel contractor based on practical factors.

#### (c) Were there any complications with regards to cutting and fitting the members?

Yes, some cuts involved diagonals that extended through multiple segments, which introduced challenges in aligning and welding the pieces accurately on site. Cantilevering parts of the truss before final assembly could also result in deflections that complicate alignment.

#### (d) How were decisions made about bolted vs. welded connections?

In this project, all visible connections were required to be welded due to architectural preferences. This ruled out bolted joints even though they might have simplified transport and assembly. It was noted that in other scenarios, engineers may compare different connection options: one favoring the architect, one the contractor, and one the structural engineer and weigh trade-offs like cost, feasibility, and appearance.

#### (e) Why was segmentation necessary in this project?

The primary driver for segmentation was transportation limits. The truss was too long and too tall to be transported vertically or flat. While transporting it diagonally on a truck is theoretically possible, it requires custom supports and limits the number of trusses per truck. The structural engineer emphasized that segmentation was the most practical solution, especially given the number of trusses and the logistics of transporting them to site.

### F.4 Case Study 4: Y

#### (a) Can you describe the project and its structural challenges?

The project involves a very large steel truss, approximately 100 meters long, that must be prefabricated, galvanized, and transported to site. The primary challenge was reconciling the size of the truss with the physical limitations of the galvanizing process and transport. The hot-dip galvanizing bath available was only about 23–25 meters long, making it impossible to dip the full truss in one piece. Additionally, transportation by road posed further limits on segment length and orientation.

#### (b) What was the segmentation and assembly strategy?

To address these constraints, the truss will be cut into several smaller segments. Each segment will be fabricated with a double-column configuration and end plates at both the top and bottom chords to allow for bolted connections. This modular system allows for easier galvanizing and transport while maintaining structural integrity. The current plan is to assemble the segments on-site using bolts, minimizing field welding.

#### (c) Were there any complications related to cutting and fitting the members?

Yes, segmenting such a large structure introduces alignment challenges, particularly at joints where diagonal or vertical members meet the chords. The engineer acknowledged that too many on-site connections can become labor-intensive and reduce quality. Therefore, they are aiming to reduce the total number of field connections wherever possible and keep them consistent to avoid overly complex detailing.

#### (d) How were decisions made about bolted vs. welded connections?

In this case, bolted connections were preferred over welding due to ease of assembly and reduced on-site work. The double-column and end plate system allows for modularity and cleaner joins. Welding would have required more specialized site work and introduced quality control issues, especially given the size and location of the joints.

#### (e) What role do eccentricities and member alignment play in truss detailing?

The team is using a symmetrical detailing strategy to ensure that member centerlines align cleanly at joints, reducing eccentricities and simplifying load transfer. They also emphasized that aligning and assembling connections off-site, wherever possible, improves structural stability during transport and avoids complications from irregular or angled member cuts.

#### (f) Why was segmentation necessary in this project?

Segmentation was driven by two main constraints: the limited size of the galvanizing bath and the transport restrictions of standard trucks. Transporting the full truss in one piece was not feasible due to road size limits and clearance requirements. The current solution involves stacking segments diagonally on trucks to make full use of permitted envelope dimensions while keeping each piece within galvanizing limits.

# Appendix G

# **Box Beam Design**

#### **Bending resistance (ULS)**

Symbol	Value		
$f_y$	$355~\mathrm{Nmm^{-2}}$		
$\gamma_{M0}$	1.0		
$M_{Ed}$	$4.26 \times 10^9 \; \mathrm{N}  \mathrm{mm}$		
$W_{pl,y}$	$1.63\times10^7~\mathrm{mm^3}$		

Table G.1: Design data – bending (ULS)

$$M_{Ed} = \frac{q_{ULS}L^2}{8}, \qquad q_{ULS} = 1.35(37.6 + 4.71) + 1.5(32) = 105.1 \text{ kN m}^{-1}$$
 
$$M_{Rd} = \frac{W_{pl,y}f_y}{\gamma_{M0}} = \frac{1.63 \times 10^7 \times 355}{1.0} = 5.78 \times 10^9 \text{ N mm} = 5.78 \text{ MN m}$$
 
$$\boxed{M_{Ed} = 4.26 \text{ MN m} \leq M_{Rd} = 5.78 \text{ MN m}} \qquad \eta = \frac{4.26}{5.78} \approx 0.74 \text{ (OK)}$$

#### **Shear resistance (ULS)**

Symbol	Value
$f_y$	$355~\mathrm{N}\mathrm{mm}^{-2}$
$\gamma_{M0}$	1.0
$V_{Ed}$	928.8 kN
$A_v$	$2t_w H = 2(20)(880) = 3.52 \times 10^4 \text{ mm}^2$

Table G.2: Design data – shear (ULS)

$$V_{Rd} = \frac{A_v \, f_y}{\sqrt{3} \, \gamma_{M0}} = \frac{3.52 \times 10^4 \times 355}{\sqrt{3}} = 7.21 \times 10^6 \; \text{N} = 7.21 \times 10^3 \; \text{kN} = 7.21 \; \text{MN}$$

$$V_{Ed} = 0.93 \text{ MN } \le V_{Rd} = 7.21 \text{ MN}$$
  $\eta = \frac{0.93}{7.21} \approx 0.13 \text{ (OK)}$ 

#### **Total-load deflection (SLS)**

Symbol	Value
Q	$37.6 + 32 + 4.71 = 74.31 \text{ kN m}^{-1}$
L	18.0 m
E	210 <b>GP</b> a
I	$6.75 \times 10^9 \; \mathrm{mm}^4$

Table G.3: Serviceability data – total load

$$\delta_{\rm act} = \frac{5}{384} \frac{Q \, L^4}{E \, I} = \frac{5}{384} \frac{74.31 \, (18\,000)^4}{210\,000 \times 6.75 \times 10^9} = 71.6 \, \, {\rm mm} \qquad \delta_{\rm allow} = \frac{L}{250} = 72 \, \, {\rm mm}$$
 
$$\boxed{\delta_{\rm act} = 71.6 \, \, {\rm mm} \, < \, \delta_{\rm allow} = 72 \, \, {\rm mm}} \qquad \Longrightarrow \qquad {\rm OK}$$

#### Live-load deflection

$$\delta_{\rm act} = \frac{5}{385} \frac{q \, L^4}{E \, I}, \qquad q = 32 \; \rm kN \; m^{-1}$$
 
$$\delta_{\rm act} = \frac{5}{385} \frac{32 \; (18 \, 000)^4}{210 \, 000 \times 6.75 \times 10^9} = 30.8 \; \rm mm, \qquad \delta_{\rm allow} = \frac{L}{300} = 60 \; \rm mm$$
 
$$\boxed{\delta_{\rm act} = 30.8 \; \rm mm \; < \; \delta_{\rm allow} = 60 \; \rm mm} \qquad \Longrightarrow \qquad \rm OK$$

Weight of the edge beam = 4.39 kN/m

#### **Key section properties (for interior beam)**

Outer size:  $B \times H = 300 \times 880$  mm, web thickness  $t_w = 20$  mm, flange thickness  $t_f = 50$  mm

$$I = \frac{BH^3 - (B - 2t_w)(H - 2t_f)^3}{12} = 6.75 \times 10^9 \text{ mm}^4$$

$$W_{pl,y} = 1.63 \times 10^7 \text{ mm}^3$$

$$A = BH - (B - 2t_w)(H - 2t_f) = 61200 \text{ mm}^2$$

$$w_{\text{beam}} = A\rho q = 4.71 \text{ kN m}^{-1}$$

Moment, shear and deflection checks are verified for the interior beam with section properties as mentioned above and the weight of the interior beam = 4.71 kN/m

# **Appendix H**

# **Detailed Result of Case Study Option 1**

## H.1 Option A

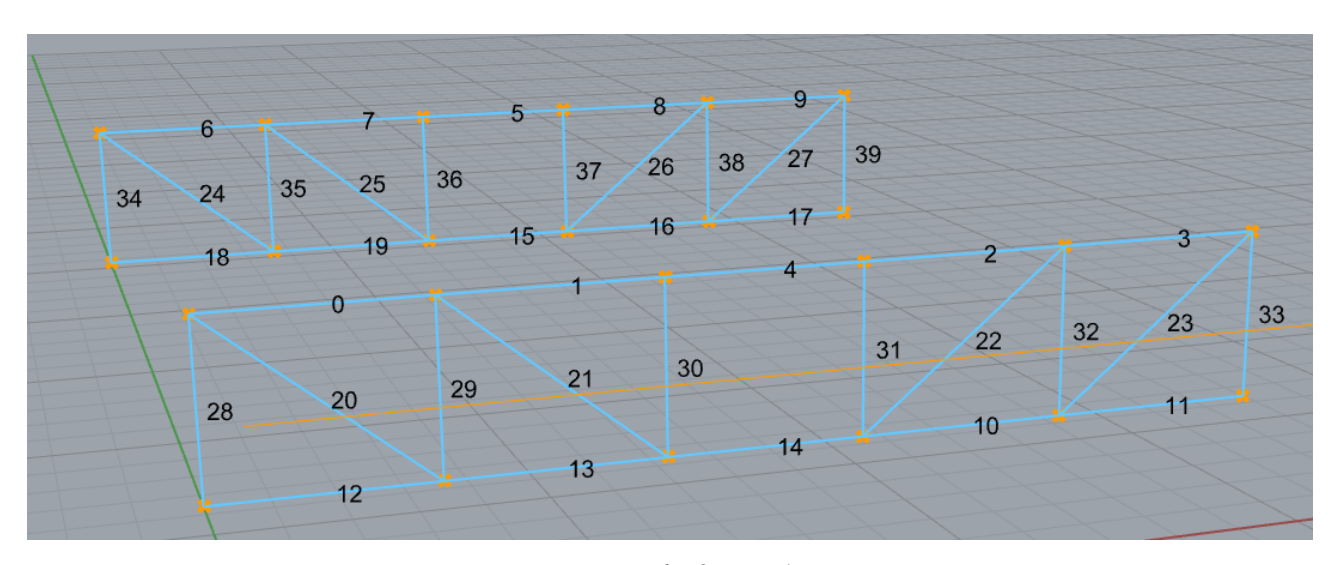


Figure H.1: Option A

### **Utilisaiton Check: Example Calculation for member number 4**

The section properties, reduction factors, and interaction parameters were extracted from Karamba3D's cross-section check panel.

Symbol	Description	Value
crosec-class	-	3
$N_{ m Rd}$	Plastic axial resistance	$2841.38\mathrm{kN}$
$M_{y,\mathrm{Rd}}$	Plastic major-axis moment resistance	$248.13\mathrm{kN}\mathrm{m}$
$M_{z,\mathrm{Rd}}$	Plastic minor-axis moment resistance	$-83.60\mathrm{kN}\mathrm{m}$
$N_{\mathrm{cr},y}$	Euler critical load (about y)	$18736.03\mathrm{kN}$
$N_{{ m cr},z}$	Euler critical load (about z)	$6576.44\mathrm{kN}$
$M_{ m cr}$	Lateral-torsional critical moment	$935.31\mathrm{kN}\mathrm{m}$
$\psi_y$	Moment–gradient factor	0.0204
$C_{my}, C_{mz}, C_{mLT}$	Eurocode $C_m$ -factors (uniform moment)	0.9
$\chi_y$	Buckling reduction factor (about $y$ )	0.9305
$\chi_z$	Buckling reduction factor (about $z$ )	0.7515
$\chi_{LT,  ext{mod}}$	LT-buckling reduction factor	1
$k_{yy}$	Interaction factor for $M_y$	0.933
$k_{zz}$	Interaction factor for $M_z$	0.969

*Table H.1: Values exported from Karamba*®

#### (a) Non-dimensional slenderness

$$\bar{\lambda}_y = \sqrt{\frac{N_{pl,\text{Rk}}}{N_{cr,y}}} = \sqrt{\frac{2841.38}{18736.03}} = 0.389$$
  $\bar{\lambda}_z = \sqrt{\frac{2841.38}{6576.44}} = 0.657,$ 

#### (b) Buckling reduction factors

$$\chi_y = 0.9305$$
 (curve a;  $\alpha = 0.21$ ),  $\chi_z = 0.7515$  (curve c;  $\alpha = 0.49$ ),  $\chi_{LT} = 1.000$  obtained with  $\phi = \frac{1}{2} \left[ 1 + \alpha (\bar{\lambda} - 0.2) + \bar{\lambda}^2 \right]$ ,  $\chi = \frac{1}{\phi + \sqrt{\phi^2 - \bar{\lambda}^2}}$ .

(c) Interaction factors (EC 3 Annex B.3, symmetrical I-section)

$$k_{yy} = 0.933, \qquad k_{zz} = 0.969$$
 with  $k_{yy} = k_{zz} = 1 + \beta \left( \frac{N_{\rm Ed}}{N_{pl,\rm Rd}} - n_0 \right), \; \beta = 0.6, \; n_0 = 0.20.$ 

#### (d) Utilisation equation

$$\begin{split} \eta &= \frac{N_{\rm Ed}}{\chi_y \, N_{pl, \rm Rd}} \, + \, k_{yy} \, \frac{M_{y, \rm Ed}}{\chi_{LT} \, M_{y, pl, \rm Rd}} \, + \, k_{zz} \, \frac{M_{z, \rm Ed}}{\chi_{LT} \, M_{z, pl, \rm Rd}} \\ &= \frac{415.11}{0.9305 \times 2\,841.38} \, + \, 0.933 \times \frac{74.70}{1.00 \times 248.13} \, + \, 0.969 \times \frac{0}{1.00 \times 83.60} \\ &= 0.438 \, \leq \, 1.00 \qquad \checkmark \end{split}$$

Member 4 (upper chord) satisfies the combined axial compression, major-axis bending, and lateral—torsional instability requirements of EN 1993-1-1 with a maximum interaction utilisation of  $\eta_{\rm max}$  = 0.44.

# **Appendix I**

# **Connection Design**

## I.1 Connection on Top chord

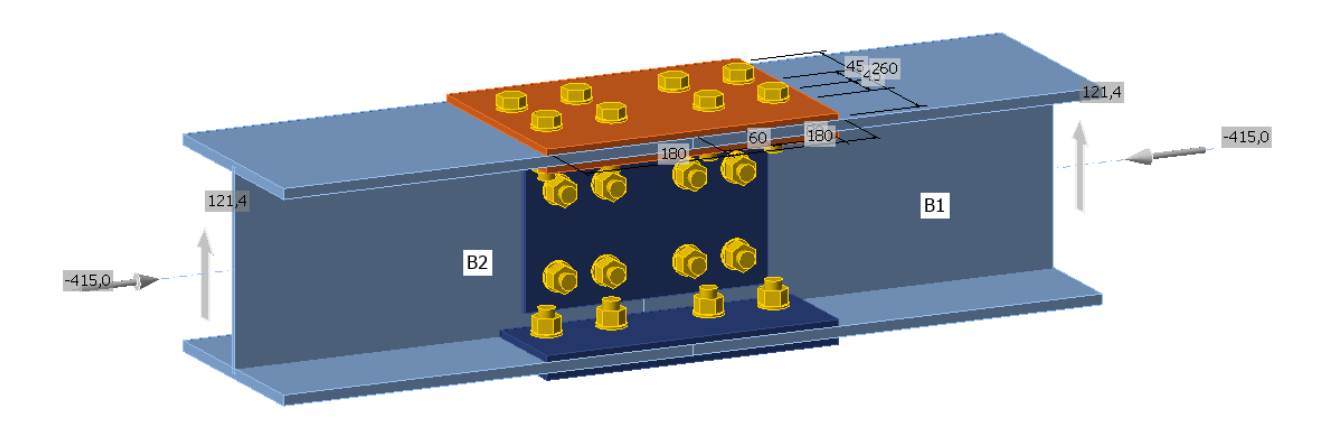


Figure I.1: Connection for splice on top chord

Name	Material		
HEA260	S 355		

Table I.1: Cross-sections present in the splice

Name / Grade	d [mm]	$f_y$ [MPa]	$f_u$ [MPa]	$A_{ m gross}$ [mm $^2$ ]
M20 8.8	20	640	800	314

Table I.2: Bolt data used in the design

Name	N [kN]	$V_y$ [kN]	$V_z$ [kN]	$M_x$ [kNm]	$M_y$ [kNm]	$M_z$ [kNm]
LE1 B1 / End	-415.0	0.0	121.4	0.0	0.0	0.0
LE1 B2 / End	-415.0	0.0	121.4	0.0	0.0	0.0

Table I.3: Member-end forces applied to the splice

#### **Plates**

Name	t <sub>p</sub> [mm]	Loads	σ <sub>Ed</sub> [MPa]	ε <sub>ΡΙ</sub> [%]	σ <sub>c,Ed</sub> [MPa]	Status
B1-bfl 1	12.5	LE1	258.4	0.0	35.6	OK
B1-tfl 1	12.5	LE1	175.3	0.0	35.4	OK
B1-w 1	7.5	LE1	355.1	0.0	35.4	OK
B2-bfl 1	12.5	LE1	173.5	0.0	38.2	OK
B2-tfl 1	12.5	LE1	258.2	0.0	35.5	OK
B2-w 1	7.5	LE1	355.1	0.0	38.2	OK
SPL1a	8.0	LE1	314.0	0.0	35.5	OK
SPL1b	8.0	LE1	326.9	0.0	35.4	OK
SPL1c	8.0	LE1	326.4	0.0	34.8	OK
SPL2a	8.0	LE1	315.5	0.0	35.6	OK
SPL2b	8.0	LE1	326.8	0.0	35.2	OK
SPL2c	8.0	LE1	326.4	0.0	35.4	OK
SPL3a	6.0	LE1	208.2	0.0	12.7	OK
SPL3b	6.0	LE1	208.4	0.0	12.7	OK

Figure I.2: Check for plate

#### Design data

Material	f <sub>y</sub> [MPa]	ε <sub>lim</sub> [%]	
S 355	355.0	5.0	

Figure I.3: Design data

where,

$$\begin{split} & \mathbf{t}_p: \text{ plate thickness} \\ & \sigma_{\mathrm{Ed}}: \text{ equivalent stress} \\ & \varepsilon_{\mathrm{Pl}}: \text{ plastic strain} \\ & \sigma_{c,\mathrm{Ed}}: \text{ contact stress} \\ & f_y: \text{ yield strength} \end{split}$$

 $\varepsilon_{\rm lim}$ : limit of plastic strain

Design yield strength: 
$$f_{yd} = \frac{f_y}{\gamma_{M0}} = \frac{355 \text{ MPa}}{1.00} = 355 \text{ MPa}$$
 (I.1)

Strength check:  $\sigma_{Ed} \leq f_{yd} \Rightarrow \text{plate remains in the elastic range (Status: OK)}$  (I.2)

#### **Bolts**

Shape	Item	Grade	Loads	F <sub>t,Ed</sub> [kN]	F <sub>v,Ed</sub> [kN]	F <sub>b,Rd</sub> [kN]	Ut <sub>t</sub>	Ut <sub>s</sub>	Ut <sub>ts</sub>	Detailing	Status
	B1	M20 8.8 - 1	LE1	22.5	19.2	235.7	16.0	20.4	31.8	ОК	OK
	B2	M20 8.8 - 1	LE1	2.9	19.1	245.0	2.1	20.3	21.8	OK	OK
	В3	M20 8.8 - 1	LE1	22.6	19.2	235.7	16.0	20.4	31.8	ОК	ОК
7 4 4 6	B4	M20 8.8 - 1	LE1	2.9	19.1	245.0	2.0	20.3	21.8	OK	ОК
4 3 7 8	B5	M20 8.8 - 1	LE1	23.4	18.6	235.7	16.6	19.8	31.6	OK	OK
	B6	M20 8.8 - 1	LE1	2.8	19.8	245.0	2.0	21.0	22.4	OK	OK
	B7	M20 8.8 - 1	LE1	23.4	18.6	235.7	16.6	19.8	31.7	ОК	OK
	B8	M20 8.8 - 1	LE1	2.9	19.8	245.0	2.0	21.0	22.5	OK	OK
	B9	M20 8.8 - 1	LE1	23.5	18.6	235.7	16.6	19.8	31.7	ОК	OK
	B10	M20 8.8 - 1	LE1	2.9	19.8	245.0	2.0	21.0	22.5	OK	OK
	B11	M20 8.8 - 1	LE1	23.4	18.6	235.7	16.6	19.8	31.6	OK	OK
109 1314	B12	M20 8.8 - 1	LE1	2.8	19.8	245.0	2.0	21.0	22.4	OK	OK
1211 1516	B13	M20 8.8 - 1	LE1	22.6	19.2	235.7	16.0	20.4	31.8	ОК	ОК
	B14	M20 8.8 - 1	LE1	2.9	19.1	245.0	2.0	20.3	21.8	OK	ОК
	B15	M20 8.8 - 1	LE1	22.7	19.2	235.7	16.1	20.4	31.9	OK	OK
	B16	M20 8.8 - 1	LE1	2.9	19.1	245.0	2.1	20.3	21.8	ОК	OK
	B17	M20 8.8 - 2	LE1	2.9	12.5	69.0	2.0	18.1	14.7	ОК	OK
	B18	M20 8.8 - 2	LE1	1.0	6.6	147.0	0.7	9.0	7.5	OK	ОК
1817 2122	B19	M20 8.8 - 2	LE1	4.6	25.9	147.0	3.2	35.3	29.9	ОК	ОК
	B20	M20 8.8 - 2	LE1	3.0	23.5	147.0	2.1	32.0	26.5	ОК	OK
20 19 23 24	B21	M20 8.8 - 2	LE1	4.6	25.9	147.0	3.2	35.3	29.9	ОК	OK
	B22	M20 8.8 - 2	LE1	3.0	23.5	147.0	2.1	32.0	26.5	ОК	ОК
	B23	M20 8.8 - 2	LE1	2.9	12.5	69.0	2.0	18.1	14.7	ОК	OK
	B24	M20 8.8 - 2	LE1	1.0	6.6	147.0	0.7	9.0	7.5	OK	ОК

#### Design data

Grade	F <sub>t,Rd</sub> [kN]	B <sub>p,Rd</sub> [kN]	F <sub>v,Rd</sub> [kN]	
M20 8.8 - 1	141.1	187.8	94.1	
M20 8.8 - 2	141.1	140.8	94.1	

Figure I.4: Check for Bolt

where,

 $F_{t,Ed}$ : tension force

 $F_{v,\mathrm{Ed}}$ : resultant of bolt shear forces  $V_y$  and  $V_z$  in the shear planes

 $F_{b,Rd}$ : plate bearing resistance (EN 1993-1-8, Table 3.4)

 $\mathbf{U}_t$ : utilisation in tension  $U_s$ : utilisation in shear

 $U_{ts}$ : combined utilisation for tension+shear (EN 1993-1-8, Table 3.4)

#### 1. Tension resistance check (EN 1993-1-8, Tab 3.4)

$$F_{t,Rd} = \frac{k_2 \, f_{ub} \, A_s}{\gamma_{M2}} = \frac{0.90 \, \times 800 \, \mathrm{MPa} \, \times 245 \, \mathrm{mm}^2}{1.25} = 141.1 \, \, \mathrm{kN} \ \, \geq \ \, F_{t,Ed} = 22.5 \, \, \mathrm{kN} \, \Longrightarrow \, \, \mathrm{OK}$$

Where:

- $F_{t,Rd}$ : bolt tension resistance (EN 1993-1-8, Table 3.4)  $k_2 = 0.90$  – factor for non-preloaded bolts
- $f_{ub} = 800 \text{ MPa} \text{ultimate tensile strength of bolt}$
- $A_s = 245 \text{ mm}^2 \text{tensile-stress}$  area of bolt
- $\gamma_{M2} = 1.25$  partial safety factor for bolts in tension

#### 2. Punching (pull-through) resistance check

$$B_{p,Rd} = \frac{0.6 \, d_m \, t_p \, f_u}{\gamma_{M2}} = \frac{0.6 \times 32 \, \text{mm} \times 8 \, \text{mm} \times 490 \, \text{MPa}}{1.25} = 187.8 \, \text{kN} \ \geq \ F_{t,Ed} = 22.5 \, \text{kN} \implies \text{OK}$$

Where:

- $B_{p,Rd}$ : punching shear resistance (EN 1993-1-8, Table 3.4)  $d_m = 32 \text{ mm} - \text{mean across-flats dimension of bolt head/nut}$
- $t_p = 8 \text{ mm} \text{plate thickness under bolt head/nut}$
- $f_u = 490 \text{ MPa} \text{ultimate plate strength}$
- $\gamma_{M2}$  = 1.25 safety factor

#### 3. Shear resistance check

$$F_{v,Rd} = \frac{\beta_p \, \alpha_v \, f_{ub} \, A_s}{\gamma_{M2}} = \frac{1.00 \times 0.60 \times 800 \, \text{MPa} \times 245 \, \text{mm}^2}{1.25} = 94.1 \, \text{kN} \geq F_{v,Ed} = 19.2 \, \text{kN} \implies \text{OK}$$

Where:

- $F_{v,Rd}$ : bolt shear resistance (EN 1993-1-8, Table 3.4) $\beta_p = 1.00$  packing reduction factor
- $\alpha_v = 0.60$  shear-stress reduction factor
- $f_{ub}, A_s, \gamma_{M2}$  as in Check 1

#### 4. Bearing resistance check

$$F_{b,Rd} = \frac{k_1 \, \alpha_b \, dt \, f_u}{\gamma_{M2}} = \frac{2.50 \times 0.96 \times 20 \times 13 \times 490}{1.25} = 235.7 \, \text{kN} \ \geq \ F_{b,Ed} = 37.0 \, \text{kN} \implies \text{OK}$$

Where:

- $k_1 = 2.50 \text{edge/spacing factor} \left( k_1 = \min\{2.8 e_2/d_0 1.7, 1.4 p_2/d_0 1.7, 2.5\} \right)$
- $\alpha_b = 0.96$  end-distance factor  $(\alpha_b = \min\{e_1/(3d_0), p_1/(3d_0) + \frac{1}{4}f_u/f_{ub}, 1\})$
- d = 20 mm nominal bolt diameter
- t = 13 mm plate thickness in bearing
- Remaining symbols as defined above

#### 5. Utilisation in tension

$$U_t = \frac{F_{t,Ed}}{\min(F_{t,Rd}, B_{p,Rd})} = \frac{22.5}{141.1} = 0.16 \le 1.0 \implies \text{OK}$$

#### 6. Utilisation in shear

$$U_s = \max\left(\frac{F_{v,Ed}}{F_{v,Rd}}, \frac{F_{b,Ed}}{F_{b,Rd}}\right) = \max\left(\frac{19.2}{94.1}, \frac{37.0}{235.7}\right) = 0.20 \le 1.0 \implies OK$$

#### 7. Interaction of tension and shear (EN 1993-1-8, Tab 3.4)

$$U_{ts} = \frac{F_{v,Ed}}{F_{v,Rd}} + \frac{F_{t,Ed}}{F_{t,Rd}} = \frac{19.2}{94.1} + \frac{22.5}{141.1} = 0.32 \le 1.0 \implies OK$$

### I.2 Connection on Bottom Chord

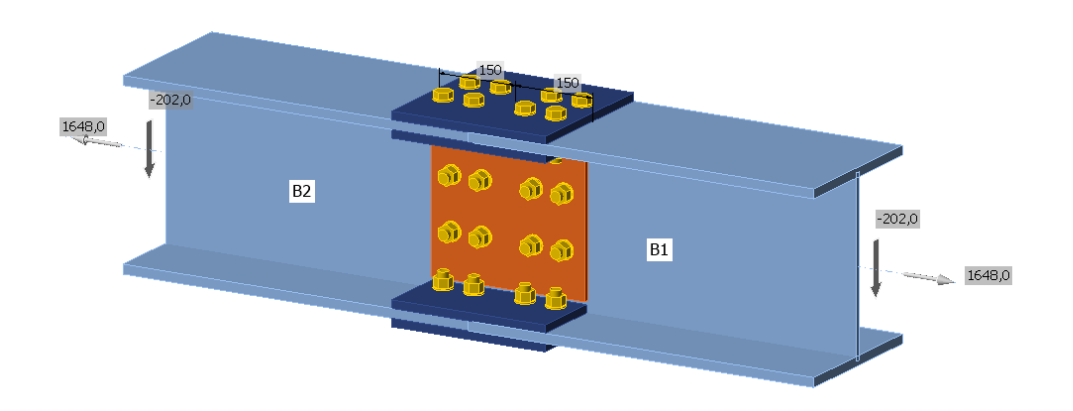


Figure I.5: Splice connection for tension member

Name	Material
HEA360	S 355

Table I.4: Cross-section present in the splice

Name	Diameter [mm]	$f_y$ [MPa]	$f_u$ [MPa]	Gross area [mm <sup>2</sup> ]
M20 8.8	20	640.0	800.0	314

Table I.5: Bolt properties adopted in the design

Name	Member	N [kN]	$V_y$ [kN]	$V_z$ [kN]	$M_x$ [kNm]	$M_y$ [kNm]	$M_z$ [kNm]
LE1	B1 / End	1648.0	0.0	-202.0	0.0	0.0	0.0
LE1	B2 / End	1648.0	0.0	-202.0	0.0	0.0	0.0

*Table I.6: Member-end forces applied to the splice (equilibrium check)* 

#### **Plates**

Name	t <sub>p</sub> [mm]	Loads	σ <sub>Ed</sub> [MPa]	<b>ε</b> ρι [%]	σ <sub>c,Ed</sub> [MPa]	Status
B1-bfl 1	17.5	LE1	355.3	0.1	44.2	OK
B1-tfl 1	17.5	LE1	341.0	0.1	23.4	OK
B1-w 1	10.0	LE1	356.8	0.9	44.2	OK
B2-bfl 1	17.5	LE1	341.1	0.1	23.3	OK
B2-tfl 1	17.5	LE1	355.3	0.1	43.8	OK
B2-w 1	10.0	LE1	356.8	0.9	43.8	OK
SPL1a	15.0	LE1	308.2	0.0	59.1	OK
SPL1b	15.0	LE1	344.2	0.0	38.3	OK
SPL1c	15.0	LE1	343.5	0.0	39.3	ОК
SPL2a	15.0	LE1	309.2	0.0	60.5	OK
SPL2b	15.0	LE1	341.4	0.0	50.5	OK
SPL2c	15.0	LE1	342.1	0.0	50.3	OK
SPL3a	10.0	LE1	288.5	0.0	28.4	OK
SPL3b	10.0	LE1	288.6	0.0	28.4	ОК

Figure I.6: Check for plate

#### Design data

Material	f <sub>y</sub> [MPa]	ε <sub>lim</sub> [%]
S 355	355.0	5.0

Figure I.7: Design data

where,

$$\begin{split} & \mathbf{t}_p: \text{ plate thickness} \\ & \sigma_{\mathrm{Ed}}: \text{ equivalent stress} \\ & \varepsilon_{\mathrm{Pl}}: \text{ plastic strain} \\ & \sigma_{c,\mathrm{Ed}}: \text{ contact stress} \\ & f_y: \text{ yield strength} \end{split}$$

 $\varepsilon_{\rm lim}$  : limit of plastic strain

Design yield strength: 
$$f_{yd} = \frac{f_y}{\gamma_{M0}} = \frac{355 \text{ MPa}}{1.00} = 355 \text{ MPa}$$
 (I.3)

Strength check:  $\sigma_{Ed} \le f_{yd} \implies$  plate remains in the elastic range (Status: OK) (I.4)

#### **Bolts**

Shape	Item	Grade	Loads	F <sub>t,Ed</sub> [kN]	F <sub>v,Ed</sub> [kN]	F <sub>b,Rd</sub> [kN]	Ut <sub>t</sub> [%]	Ut <sub>s</sub> [%]	Ut <sub>ts</sub> [%]	Detailing	Status
	B1	M20 8.8 - 1	LE1	16.1	78.4	259.8	11.4	83.3	91.4	OK	OK
	B2	M20 8.8 - 1	LE1	17.1	76.0	226.1	12.1	80.7	89.4	OK	OK
	B3	M20 8.8 - 1	LE1	15.5	78.3	259.8	11.0	83.3	91.1	OK	OK
<del> </del>	B4	M20 8.8 - 1	LE1	17.1	76.0	226.1	12.1	80.8	89.4	OK	OK
<b>4</b>	B5	M20 8.8 - 1	LE1	12.6	76.9	259.8	9.0	81.8	88.2	OK	OK
	B6	M20 8.8 - 1	LE1	17.6	77.4	226.1	12.5	82.3	91.2	OK	OK
	B7	M20 8.8 - 1	LE1	12.8	76.9	259.8	9.1	81.8	88.2	OK	OK
	B8	M20 8.8 - 1	LE1	17.6	77.4	226.1	12.5	82.3	91.2	OK	OK
	B9	M20 8.8 - 1	LE1	12.2	76.9	259.8	8.7	81.7	87.9	OK	OK
	B10	M20 8.8 - 1	LE1	17.7	77.4	226.1	12.5	82.2	91.2	OK	OK
40.0	B11	M20 8.8 - 1	LE1	12.1	76.9	259.8	8.5	81.7	87.8	OK	OK
104 1314	B12	M20 8.8 - 1	LE1	17.6	77.4	226.1	12.5	82.3	91.2	OK	OK
1 <sup>2</sup> 1 <sup>1</sup> 1 <sup>5</sup> 1 <sup>6</sup>	B13	M20 8.8 - 1	LE1	15.7	78.3	259.8	11.1	83.2	91.2	OK	OK
	B14	M20 8.8 - 1	LE1	17.1	75.9	226.1	12.1	80.7	89.4	OK	OK
	B15	M20 8.8 - 1	LE1	16.1	78.3	259.8	11.4	83.3	91.4	OK	OK
	B16	M20 8.8 - 1	LE1	17.0	75.9	226.1	12.1	80.7	89.3	OK	OK
	B33	M20 8.8 - 2	LE1	3.4	47.8	148.5	2.4	64.3	52.5	OK	OK
	B34	M20 8.8 - 2	LE1	10.8	47.2	129.2	7.6	73.1	55.6	OK	OK
24.22 27.22	B35	M20 8.8 - 2	LE1	4.6	61.4	148.5	3.3	82.8	67.7	OK	OK
34,33 37,38	B36	M20 8.8 - 2	LE1	13.4	59.9	129.2	9.5	92.7	70.4	OK	OK
36 35 39 40	B37	M20 8.8 - 2	LE1	4.5	61.4	148.5	3.2	82.7	67.5	OK	ОК
	B38	M20 8.8 - 2	LE1	13.4	59.9	129.2	9.5	92.8	70.5	OK	ОК
	B39	M20 8.8 - 2	LE1	3.6	47.8	148.5	2.5	64.4	52.6	OK	ОК
	B40	M20 8.8 - 2	LE1	10.8	47.2	129.2	7.6	73.1	55.6	OK	OK

#### Design data

Grade	F <sub>t,Rd</sub> [kN]	B <sub>p,Rd</sub> [kN]	F <sub>v,Rd</sub> [kN]
M20 8.8 - 1	141.1	352.1	94.1
M20 8.8 - 2	141.1	234.7	94.1

Figure I.8: Check for bolts